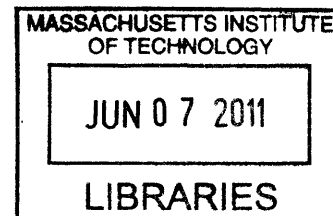


CONTINUED INVESTIGATIONS OF THE CATALYTIC REDUCTION OF N₂ TO NH₃
BY MOLYBDENUM TRIAMIDOAMINE COMPLEXES

Brian S. Hanna

B.S. in Chemistry,
University of Delaware
May 2005



Submitted to the Department of Chemistry
In Partial Fulfillment of the Requirements
for the Degree of

ARCHIVES

DOCTOR OF PHILOSOPHY

at the

MASSACHUSETTS INSTITUTE OF TECHNOLOGY

June 2011

© Massachusetts Institute of Technology, June 2011
All rights reserved.

Signature of Author .

Department of Chemistry
April 25, 2011

Certified by _

Richard R. Schrock
Thesis Supervisor

Accepted by _____

Robert W. Field
Chairman, Departmental Committee on Graduate Students

This doctoral thesis has been examined by a Committee of the Department of Chemistry as follows:

Professor Richard R. Schrock _____

Thesis Supervisor

Professor Christopher Cummins _____

Chairman

Professor Stephen J. Lippard _____

For Meredith, the love of my life.

CONTINUED INVESTIGATIONS OF THE CATALYTIC REDUCTION OF N₂ TO NH₃
BY MOLYBDENUM TRIAMIDOAMINE COMPLEXES

BY

Brian S. Hanna

Submitted to the Department of Chemistry
on April 25, 2011 in Partial Fulfillment of the
Requirements for the Degree of Doctor of Philosophy in Chemistry

ABSTRACT

A study of the effects of employing different solvents and the introduction of dihydrogen during the catalytic reduction of dinitrogen to ammonia with [HIPTN₃N]Mo complexes was completed. During a catalytic reaction, the use of different solvents including fluorobenzene, THF, and toluene did not produce catalytic turnover of ammonia from dinitrogen. The acid source used was [CollH][BAR'₄] which was soluble in each of these solvents and dihydrogen was generated. It was found that dihydrogen acts as a powerful inhibitor of the catalytic reduction of dinitrogen to ammonia.

In hopes of isolating species relevant to the proposed structures of [HIPTN₃N]MoH₂, where an amide arm has become unbound from the metal center, [HIPTN₃N]MoPMe₃ was investigated. [HIPTN₃N]MoPMe₃ can be synthesized cleanly and oxidized to [HIPTN₃N]MoPMe₃[BAR'₄] by treatment with H[(Et₂O)₂][BAR'₄]. An interesting species, [HIPTN₃N]Mo(H)PMe₃ was developed which was unstable *in vacuo*. The J_{PH} value for the molybdenum hydride was 111 Hz, which is higher than a typical M(H)PMe₃ J_{PH} . [HIPTN₃N]W(H)PMe₃ was synthesized in an effort to elucidate the nature of the metal phosphine and metal hydride binding. The J_{PH} was found to be 117 Hz for [HIPTN₃N]W(H)PMe₃. The $J_{WH} = 12.5$ Hz and $J_{WP} = 119$ Hz values for [HIPTN₃N]W(H)PMe₃ suggested that the hydride and phosphine were bound to the tungsten center, and that the phosphine and hydride have some interaction.

New ligand systems based on a C_s symmetric framework were also explored. [(TerPh)HIPT₂N₃N]Mo complexes were synthesized but provided no catalytic reduction of dinitrogen to ammonia. The decomposition of [(TerPh)HIPT₂N₃N]MoN₂H was found to be slower ($t_{1/2} = 15$ hours) than previously investigated C_s symmetric [N₃N] complexes (< 10 minutes). A new electron donating symmetric ligand based on the [HIPTN₃N]Mo was synthesized containing a methoxy group, [*p*MeOHIPTN₃N]Mo. This complex was shown to reduce dinitrogen to ammonia catalytically (6.5 equiv.). Other symmetric species, [DTBATN₃N]Mo and [DTBAN₃N]MoN, were developed and found to be crystalline but not catalytically active in the reduction of dinitrogen to ammonia.

Thesis Supervisor: Richard R. Schrock
Title: Fredrick G. Keyes Professor of Chemistry

Table of Contents

ABSTRACT	3
Table of Figures	8
List of Equations	15
List of Tables	15
List of Abbreviations Used in Text	16
Chapter 1. Introduction	22
Industrial Nitrogen Fixation	22
Natural Nitrogenase Systems	23
Transition Metal Dinitrogen Complexes	25
Dinitrogen Complexes from the Schrock Lab	27
Catalytic Reduction of Dinitrogen to Ammonia at a Well-Defined Metal Center	28
References	34
Chapter 2. Hydrogen and Catalytic Studies of [HIPTN ₃ N]	38
Introduction	38
Results and Discussion	39
Synthesis of [HIPTN ₃ N]MoH ₂	39
Quantification of H ₂ on [HIPTN ₃ N]MoH ₂	42
“Direct Nitride” Synthesis of [HIPTN ₃ N]MoN	45
Variations of Catalytic Reactions With [HIPTN ₃ N]MoN	47
Conclusion	51
Experimental	53
	4

References	57
Chapter 3. Group VI Phosphine Complexes	60
Introduction	60
Results and Discussion	62
Synthesis of Molybdenum Phosphine Complexes	62
Synthesis of [HIPTN ₃ N]MoP(H)PMe ₃	68
Attempted Syntheses of [HIPTN ₃ N]MoPH ₃	71
Attempts to Use Various Mono and Bidentate Phosphines	73
Steric Variations of [N ₃ N] Phosphine Complexes	73
Tungsten Phosphine Complexes	75
Reactivity of Molybdenum and Tungsten Trimethylphosphine Complexes	80
Conclusions	82
Experimental	84
References	89
Chapter 4. Symmetric and C _s symmetric [N ₃ N] complexes	92
Introduction	92
Results and Discussion	93
Synthesis of C _s Symmetric Ligands	93
Synthesis of [HIPT ₂ TerPhN ₃ N]Mo Complexes	95
Symmetric [N ₃ N] Variations	107
Synthesis of H ₃ [<i>p</i> MeOHIPTN ₃ N]	109
Synthesis of [<i>p</i> MeOHIPTN ₃ N] Molybdenum Complexes	110

Synthesis of DTBA and DTBAT Ligands	119
Synthesis of DTABT and [DTABTN ₃ N]Mo	122
Conclusions	126
Experimental	128
References	144
Appendix A. Investigation of Triamidophosphine Ligands	143
Introduction	143
Results and Discussion	143
TRAP	147
TRAP Chalcogenides	149
Silylated TRAP	150
Propyl Phosphine Ligands	154
Tris(2-carboxyethyl)phosphine TCEP	154
DCC Coupling of TCEP with HIPT	155
Experimentals	157
References	160
Appendix B. Alterations of the Catalytic Apparatus	163
Introduction	163
Changes to the Magnetic Drive	164
Mechanically Driven Apparatus	165
High Pressure Apparatus	167
References	169

Table of Figures

Figure 1.1: FeMoco.....	24
Figure 1.2: Allen and Senoff Complex	25
Figure 1.3: Hidai Complex	25
Figure 1.4: Tungsten Complex Developed by Chatt	26
Figure 1.5: Various Modes of N ₂ binding.....	26
Figure 1.6: [HIPTN ₃ N]MoX.....	28
Figure 1.7: Yandulov Schrock Cycle.....	30
Figure 1.8: Schematic of Catalytic Reactor	31
Figure 1.9: C _s Symmetric ligand, [(TRIP)HIPT ₂ N ₃ N]MoX.....	32
Figure 1.10: Catalyst That Reduces Dinitrogen to Ammonia.....	33
Figure 2.1: Proposed Equilibrium of [HIPTN ₃ N]MoH ₂	39
Figure 2.2: Synthesis of [HIPTN ₃ N]MoH ₂	40
Figure 2.3: Proposed Mechanism for H/D Scrambling	41
Figure 2.4: Liberation of H ₂ From [HIPTN ₃ N]MoH ₂ by CO.	43
Figure 2.5: “Direct Nitride” Synthesis of [HIPTN ₃ N]MoN	47
Figure 3.1: [N ₃ N _F]Re Complexes	60
Figure 3.2: Generic Synthesis of [N ₃ N _F](H)PR ₃ [BAR' ₄].....	61
Figure 3.3: Synthesis of [HIPTN ₃ N]MoPMe ₃	63
Figure 3.4: Alternate Synthesis of [HIPTN ₃ N]MoPMe ₃	63
Figure 3.5: Synthesis of [HIPTN ₃ N]MoPMe ₃ [BAR' ₄]	64
Figure 3.6: Synthesis of [HIPTN ₃ N]MoPMe ₃ [BPh ₄]	65

Figure 3.7: Thermal ellipsoid representation [HIPTN ₃ N]MoPMe ₃ [BPh ₄]. Isopropyl groups and hydrogen atoms omitted for clarity. Selected bond distances (Å) and angles (°): Mo(1)-N(1) = 1.946(7), Mo(1)-N(4) = 2.205(7), Mo(1)-P(1) = 2.569(3). Mo(1)- N(1)-C _{ipso} = 131.3(6), N(1)-Mo(1)-N(4) = 80.1(3).....	66
Figure 3.8: Cyclic Voltammogram of 2mM [HIPTN ₃ N]MoPMe ₃ in 0.1 M [TBA]BAr' ₄ /PhF. WE: Pt; Scan rate: 200 mV/s vs. Fc/Fc ⁺	68
Figure 3.9: Synthesis of [HIPTN ₃ N]Mo(H)PMe ₃	69
Figure 3.10: Alternate Synthesis of [HIPTN ₃ N]Mo(H)PMe ₃	71
Figure 3.11: Attempted Syntheses of [HIPTN ₃ N]MoPH ₃	72
Figure 3.12: Synthesis of [HIPTN ₃ N]MoPMe ₃ [BPh ₄]	75
Figure 3.13: Cyclic voltammogram of 2mM [HIPTN ₃ N]MoPMe ₃ in 0.1 M [TBA]BAr' ₄ /PhF. WE: Pt; scan rate: 200 mV/s vs. Fc/Fc ⁺	77
Figure 3.14: Synthesis of [HIPTN ₃ N]WPMe ₃	78
Figure 3.15: Synthesis of [HIPTN ₃ N]W(H)PMe ₃	79
Figure 3.16: Selected Regions of ¹ H and ³¹ P NMR Spectra for [HIPTN ₃ N]W(H)PMe ₃	80
Figure 3.17: Oxidation of [HIPTN ₃ N]MoPMe ₃ with H(Et ₂ O) ₂ BAr' ₄	81
Figure 3.18: Oxidation of [HIPTN ₃ N]MoNH ₃ with [H(Et ₂ O) ₂][BAr' ₄]	82
Figure 4.1: Synthesis of H ₃ [(TerPh)HIPT ₂ N ₃ N].....	94
Figure 4.2: Synthesis of [(TerPh)HIPT ₂ N ₃ N]MoCl.....	95
Figure 4.3: Synthesis of [(TerPh)HIPT ₂ N ₃ N]MoN	97
Figure 4.4: Alternative Nitride Synthesis of [(TerPh)HIPT ₂ N ₃ N]MoN	97
Figure 4.5: Synthesis of [(TerPh)HIPT ₂ N ₃ N]MoNH[BAr' ₄].....	98
Figure 4.6: Synthesis of [(TerPh)HIPT ₂ N ₃ N]MoNH ₃ [BAr' ₄]	99

Figure 4.7: Synthesis of [(TerPh)HIPT ₂ N ₃ N]MoN ₂ Na(THF) _x	100
Figure 4.8: Synthesis of [(TerPh)HIPT ₂ N ₃ N]MoN ₂ K	101
Figure 4.9: Synthesis of [(TerPh)HIPT ₂ N ₃ N]MoN ₂	102
Figure 4.10: [(TerPh)HIPT ₂ N ₃ N]MoN ₂ H.....	104
Figure 4.11: (2,6-(TRIP) ₂ phenol); HIPTOH.....	107
Figure 4.12: Synthetic Routes to 3,5-(TRIP) ₂ -4-anisolebromide.....	108
Figure 4.13: Synthesis of H ₃ [<i>p</i> MeOHIPTN ₃ N]	109
Figure 4.14: Synthesis of [<i>p</i> MeOHIPTN ₃ N]MoCl	110
Figure 4.15: Synthesis of [<i>p</i> MeOHIPTN ₃ N]MoN ₂ Na(THF) _x	111
Figure 4.16: Synthesis of [<i>p</i> MeOHIPTN ₃ N]MoN ₂	112
Figure 4.17: Clean Synthesis of [<i>p</i> MeOHIPTN ₃ N]MoN ₂	113
Figure 4.18: Synthesis of [<i>p</i> MeOHIPTN ₃ N]MoN	114
Figure 4.19: X-ray Crystal Structure of [<i>p</i> OMeHIPTN ₃ N]MoN Thermal ellipsoid representation [<i>p</i> MeOHIPTN ₃ N]MoN. Isopropyl groups and hydrogen atoms omitted for clarity. Selected bond distances (Å) and angles (°): Mo(1)-N(5) = 1.650(4), Mo(1)- N(4) = 2.433(4). Mo(1)- N(1)-C _{ipso} = 126.17, N _{amide} -Mo(1)-N(4) = 77.00	115
Figure 4.20: Synthesis of [<i>p</i> MeOHIPTN ₃ N]MoNH ₃ [BAr' ₄]	117
Figure 4.21: Area of N ₂ peak observed by IR Spectroscopy; ln(1-(Area/Area _{inf})/ vs. time ...	118
Figure 4.22: Synthesis of H ₃ [DTBAN ₃ N]	120
Figure 4.23: Synthesis of [DTBAN ₃ N]MoN	121
Figure 4.24: Synthesis of DTBATBr	123
Figure 4.25: Synthesis of H ₃ [DTBATN ₃ N].....	123
Figure 4.26: Synthesis of [DTBATN ₃ N]MoN.....	124

Figure 4.27: Synthesis of [DTBATN ₃ N]MoCl.....	125
Figure 4.28: Synthesis of [DTBATN ₃ N]MoN ₂ K.....	125
Figure A.1: TRAP or [N ₃ P] Ligand	143
Figure A.2: 2,2',2''-nitrilotriacetic acid.....	144
Figure A.3: Synthesis of HIPTNH ₂ done by Nathan Smythe.....	144
Figure A.4: General Palladium Cross-coupling Reactions for Synthesis of HIPTNH ₂	144
Figure A.5: DCC Coupling Mechanism	145
Figure A.6: Synthesis of H ₃ [HIPT(N ₃ N) _{amide}]	146
Figure A.7: Possible Tautomers of H ₃ [HIPT(N ₃ N) _{amide}]	147
Figure A.8:TRAP·3HCl	148
Figure A.9: Deprotonation of TRAP·3HCl.....	150
Figure A.10: Synthesis of TRAP-sulfide.....	150
Figure A.11: H ₃ [(TMS) ₃ N ₃ P].....	150
Figure A.12: Attempted Synthesis of Functionlized [N ₃ P].	153
Figure A.13: Synthesis of H ₃ [HIPTN ₃ P(propyl-amide)].....	155
Figure B.1: Top View of Magnetic Drive.....	164
Figure B.2: Side View of Magnetic Drive.....	164
Figure B.3: New Exterior Magnet Drive	165
Figure B.4: Original Exterior Magnet Belt Drive.....	165
Figure B.5: Mechanically Driven Apparatus.....	166
Figure B.6: Plug for Mechanically Driven Apparatus	167
Figure B.7: High Pressure Glass Apparatus.....	168
Figure 1.1: FeMoco.....	24

Figure 1.2: Allen and Senoff Complex	25
Figure 1.3: Hidai Complex	25
Figure 1.4: Tungsten Complex Developed by Chatt	26
Figure 1.5: Various Modes of N ₂ binding.....	26
Figure 1.6: [HIPTN ₃ N]MoX.....	28
Figure 1.7: Yandulov Schrock Cycle.....	30
Figure 1.8: Schematic of Catalytic Reactor	31
Figure 1.9: C _s Symmetric ligand, [(TRIP)HIPT ₂ N ₃ N]MoX.....	32
Figure 1.10: Catalyst That Reduces Dinitrogen to Ammonia.....	33
Figure 2.1: Proposed Equilibrium of [HIPTN ₃ N]MoH ₂	39
Figure 2.2: Synthesis of [HIPTN ₃ N]MoH ₂	40
Figure 2.3: Proposed Mechanism for H/D Scrambling	41
Figure 2.4: Liberation of H ₂ From [HIPTN ₃ N]MoH ₂ by CO.	43
Figure 2.5: “Direct Nitride” Synthesis of [HIPTN ₃ N]MoN	47
Figure 3.1: [N ₃ N _F]Re Complexes	60
Figure 3.2: Generic Synthesis of [N ₃ N _F](H)PR ₃ [BAR' ₄].....	61
Figure 3.3: Synthesis of [HIPTN ₃ N]MoPMe ₃	63
Figure 3.4: Alternate Synthesis of [HIPTN ₃ N]MoPMe ₃	63
Figure 3.5: Synthesis of [HIPTN ₃ N]MoPMe ₃ [BAR' ₄]	64
Figure 3.6: Synthesis of [HIPTN ₃ N]MoPMe ₃ [BPh ₄]	65
Figure 3.7: Thermal ellipsoid representation [HIPTN ₃ N]MoPMe ₃ [BPh ₄]. Isopropyl groups and hydrogen atoms omitted for clarity. Selected bond distances (Å) and angles (°):	

Mo(1)-N(1) = 1.946(7), Mo(1)-N(4) = 2.205(7), Mo(1)-P(1) = 2.569(3). Mo(1)- N(1)- C _{ipso} = 131.3(6), N(1)-Mo(1)-N(4) = 80.1(3).....	66
Figure 3.8: Cyclic Voltammogram of 2mM [HIPTN ₃ N]MoPMe ₃ in 0.1 M [TBA]BAr' ₄ /PhF. WE: Pt; Scan rate: 200 mV/s vs. Fc/Fc ⁺	68
Figure 3.9: Synthesis of [HIPTN ₃ N]Mo(H)PMe ₃	69
Figure 3.10: Alternate Synthesis of [HIPTN ₃ N]Mo(H)PMe ₃	71
Figure 3.11: Attempted Syntheses of [HIPTN ₃ N]MoPH ₃	72
Figure 3.12: Synthesis of [HIPTN ₃ N]MoPMe ₃ [BPh ₄]	75
Figure 3.13: Cyclic voltammogram of 2mM [HIPTN ₃ N]MoPMe ₃ in 0.1 M [TBA]BAr' ₄ /PhF. WE: Pt; scan rate: 200 mV/s vs. Fc/Fc ⁺	77
Figure 3.14: Synthesis of [HIPTN ₃ N]WPMe ₃	78
Figure 3.15: Synthesis of [HIPTN ₃ N]W(H)PMe ₃	79
Figure 3.16: Selected Regions of ¹ H and ³¹ P NMR Spectra for [HIPTN ₃ N]W(H)PMe ₃	80
Figure 3.17: Oxidation of [HIPTN ₃ N]MoPMe ₃ with H(Et ₂ O) ₂ BAr' ₄	81
Figure 3.18: Oxidation of [HIPTN ₃ N]MoNH ₃ with [H(Et ₂ O) ₂][BAr' ₄]	82
Figure 4.1: Synthesis of H ₃ [(TerPh)HIPT ₂ N ₃ N].....	94
Figure 4.2: Synthesis of [(TerPh)HIPT ₂ N ₃ N]MoCl.....	95
Figure 4.3: Synthesis of [(TerPh)HIPT ₂ N ₃ N]MoN	97
Figure 4.4: Alternative Nitride Synthesis of [(TerPh)HIPT ₂ N ₃ N]MoN	97
Figure 4.5: Synthesis of [(TerPh)HIPT ₂ N ₃ N]MoNH[BAr' ₄].....	98
Figure 4.6: Synthesis of [(TerPh)HIPT ₂ N ₃ N]MoNH ₃ [BAr' ₄]	99
Figure 4.7: Synthesis of [(TerPh)HIPT ₂ N ₃ N]MoN ₂ Na(THF) _x	100
Figure 4.8: Synthesis of [(TerPh)HIPT ₂ N ₃ N]MoN ₂ K	101

Figure 4.9: Synthesis of [(TerPh)HIPT ₂ N ₃ N]MoN ₂	102
Figure 4.10: [(TerPh)HIPT ₂ N ₃ N]MoN ₂ H.....	104
Figure 4.11: (2,6-(TRIP) ₂ phenol); HIPTOH.....	107
Figure 4.12: Synthetic Routes to 3,5-(TRIP)2-4-anisolebromide.....	108
Figure 4.13: Synthesis of H ₃ [<i>p</i> MeOHIPTN ₃ N]	109
Figure 4.14: Synthesis of [<i>p</i> MeOHIPTN ₃ N]MoCl	110
Figure 4.15: Synthesis of [<i>p</i> MeOHIPTN ₃ N]MoN ₂ Na(THF) _x	111
Figure 4.16: Synthesis of [<i>p</i> MeOHIPTN ₃ N]MoN ₂	112
Figure 4.17: Clean Synthesis of [<i>p</i> MeOHIPTN ₃ N]MoN ₂	113
Figure 4.18: Synthesis of [<i>p</i> MeOHIPTN ₃ N]MoN	114
Figure 4.19: X-ray Crystal Structure of [<i>p</i> OMeHIPTN ₃ N]MoN Thermal ellipsoid representation [<i>p</i> MeOHIPTN ₃ N]MoN. Isopropyl groups and hydrogen atoms omitted for clarity. Selected bond distances (Å) and angles (°): Mo(1)-N(5) = 1.650(4), Mo(1)- N(4) = 2.433(4). Mo(1)- N(1)-C _{ipso} = 126.17, N _{amide} -Mo(1)-N(4) = 77.00	115
Figure 4.20: Synthesis of [<i>p</i> MeOHIPTN ₃ N]MoNH ₃ [BAr' ₄]	117
Figure 4.21: Area of N ₂ peak observed by IR Spectrscopy; ln(1-(Area/Area _{inf})/ vs. time ...	118
Figure 4.22: Synthesis of H ₃ [DTBAN ₃ N]	120
Figure 4.23: Synthesis of [DTBAN ₃ N]MoN	121
Figure 4.24: Synthesis of DTBATBr	123
Figure 4.25: Synthesis of H ₃ [DTBATN ₃ N].....	123
Figure 4.26: Synthesis of [DTBATN ₃ N]MoN.....	124
Figure 4.27: Synthesis of [DTBATN ₃ N]MoCl.....	125
Figure 4.28: Synthesis of [DTBATN ₃ N]MoN ₂ K.....	125

List of Equations

Equation 1.1: Reduction of Dinitrogen.....	23
Equation 1.2: Reduction of Dinitrogen by Nitrogenase Enzymes.....	23

List of Tables

Table 2.1: Catalytic Reactions with Various Solvent.....	48
Table 2.2: Catalytic Reaction Results with Alterations.....	51
Table 3.1: Selected Bond Lengths (Å) and Angles (°) for [HIPTN ₃ N]MoPMe ₃ [BPh ₄] Compared to [HIPTN ₃ N]MoNH ₃ [BAR' ₄].....	67
Table 4.1: Selected Bond Lengths (Å) and Angles (°) for [pMeOHIPTN ₃ N]MoN compared to [HIPTN ₃ N]MoN.....	116
Table 4.2: Half Life of Ammonia for Dinitrogen Exchange.....	119
Table 4.3: Summary of Catalytic Reactions.....	126
Table C.1: Crystal Data and Structure Refinement for [pMeOHIPTN ₃ N]MoN.....	172
Table C.2: Selected Bond Length (Å) and Angles (°) for [pMeOHIPTN ₃ N]MoN.....	173
Table C.3: Crystal Data and Structure Refinement for [HIPTN ₃ N]MoPMe ₃ [BPh ₄].....	174
Table C.4: Selected Bond Length (Å) and Angles (°) for [HIPTN ₃ N]MoPMe ₃ [BPh ₄].....	175

List of Abbreviations Used in Text

Å	Angstrom
Ar	Aryl
Anal.	Analysis
Atm	Atmosphere(s)
BAr' ₄	Tetra-bis(trifluoromethyl)phenyl borate
BINAP	2,2'-bis(diphenylphosphino)-1,1'-binaphthyl
BPh ₄	Tetraphenyl borate, B[C ₆ H ₅] ⁻
br	Broad
Bu	Butyl
°C	Degrees Celcius
Calcd.	Calculated
C _{ipso}	Ipsso Carbon in an Aryl Group
cm ⁻¹	Wavenumbers, Reciprocal Centimeters
Collidine	2,4,6-Trimethylpyridine
[CollH]	2,4,6-Trimethylpyridinium
Cp [*]	Pentamethylcyclopentadienyl
CV	Cyclic Volatammetry

d	Doublet
δ	Chemical Shift
dba	Dibenzylideneacetone
DCC	Dicyclohexylcarbodiimide
DCU	Dicyclohexylurea
dd	Doublet of Doublets
DTBA	DiTertButylAnisole, 1,3-di-tert-butyl-2-methoxybenzene
DTBAT	DiTertButylAnisoleTerphenyl 3,3",5,5"-tetra-tert-butyl- 4,4"-dimethoxy-1,1':3',1"-terphenyl
EI	Electron Impact (Mass Spectrometry)
eq., equiv.	Equivalent
Et	Ethyl
Et ₂ O	Diethyl Ether
ESI	Electron Spray Ionization (Mass Spectrometry)
η_x	Hapticity of a Ligand Bound to a Metal Through x Atoms
h	Hour(s)
Hz	Hertz
HRMS	High Resolution Mass Spectrometry
HIPT	HexaIsoPropyl Terphenyl
Fc/Fc ⁺	Ferrocene/Ferrocinium $\text{Fe}(\eta^5\text{-C}_5\text{H}_5)_2/\text{Fe}(\eta^5\text{-C}_5\text{H}_5)_2^+$

g	Gram(s)
iPr	Isopropyl (-CH(CH ₃) ₂)
IR	Infrared
<i>J</i> _{xy}	Coupling constant between atom x and atom y
kcal	Kilocalorie
L	Liter
LL	Luer Lock
Lutidine	2,6-dimethylpyridine
[LutH]	2,6-dimethylpyridinium
μ	Magnetic Moment
M	Molar
m	multiplet
MALDI-TOF	Matrix Assisted LASER Desorption Ionization Time of Flight
Me	Methyl
mg	Milligram(s)
MHz	Megahertz
Min	Minute(s)
mL	Milliliter(s)
mM	Millimolar
mmol	Millimole(s)
μmol	Micromolar

mV/s	Millivolts per Second
ν	Frequency
N_{α}	Nitrogen Directly Bound to the Metal
N_{β}	Nitrogen Two Bonds from the Metal
$[N_3N]$	$[N(CH_2CH_2NH)]^{3-}$
$[N_3N]_{amide}$	$[N(CH_2C(O)NH)_3]^{3-}$
$[N_3P]$	$[P(CH_2CH_2NH)]^{3-}$
NMR	Nuclear Magnetic Resonance
NPT	National Pipe Thread
Oac	Acetate, ($[-CO_2CH_3]^-$)
Otf	Triflate, trifluoromethanesulfonate, ($-O_3SCF_3]^-$)
Ph	Phenyl
ppm	Parts Per Million
PSI	Pounds per Square Inch
q	Quartet
RT	Room Temperature
S	Electron Spin
s	Singlet
sept	Septet
T	Temperature
t	Triplet
tBu	Tertiary butyl ($-C(CH_3)_3$)

TCEP	3,3',3''-phosphinetriyltripropanoic acid
TCMP	Tricarboxylicmethylene phosphine
	2,2',2''-phosphinetriyltriacetic acid
TerPh	1,1':3',1''-terphenyl
THF	Tetrahydrofuran
TMS	Trimethylsilyl
TMS ₂ O	1,1,1,3,3,3-hexamethyldisiloxane
TRAP	2,2',2''-phosphinetriyltriethanamine, P((CH ₂ CH ₂ NH ₂) ₃)
TREN	N ¹ ,N ¹ -bis(2-aminoethyl)ethane-1,2-diamine, N(CH ₂ CH ₂ NH ₂) ₃
UV-Vis	Ultraviolet-Visible
V	Volts

Chapter 1

Introduction

Chapter 1. Introduction

The fixation of atmospheric dinitrogen to ammonia is vital for life. Atmospheric dinitrogen can not be directly incorporated into amino acids so it is ‘fixed’ into a usable form either naturally or industrially. Nature uses nitrogenase enzymes of microbes to synthesize usable forms of nitrogen for incorporation into plant life. The introduction of the Haber-Bosch process has coincided with a large worldwide population increase. The increase in available nutrients, through the application of synthetic fertilizers has increased crop yields and played an important role in the population boom during the 20th century.¹

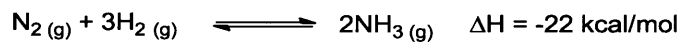
Industrial Nitrogen Fixation

Industrially, ammonia is produced mainly for use in fertilizers, though its use in explosives was an important driving factor for the development of industrial synthetic routes. Worldwide, ammonia is generated on a massive scale ($> 168 \times 10^6$ tons/year)² using the Haber-Bosch process. This process is energy intensive, requiring 150–350 atmospheres of N_2 and H_2 pressure at temperatures of 300–550 °C. A large amount of the global energy supply, 1–2% each year, is consumed not only from the harsh conditions required for the ammonia synthesis but also the synthesis of H_2 .² H_2 is obtained primarily from natural gas or coal through steam reformation and the water gas shift process, which are both energy intensive processes.¹

Despite the fact that dinitrogen reduction to ammonia (Equation 1.1) is exothermic ($\Delta H = -22$ kcal/mol),² there is a large activation barrier due to the strong nitrogen-nitrogen triple bond (BDE = 226 kcal/mol).³ High temperatures are required to overcome this large

activation barrier. The reaction is entropically unfavorable, so the equilibrium constant is shifted by using high pressures. In the industrial process only an 18–22% yield of ammonia is realized during each pass of N₂ and H₂ over the catalyst.¹ The yield can be increased as unreacted N₂ and H₂ are repeatedly fed back through the system.

Equation 1.1: Reduction of Dinitrogen

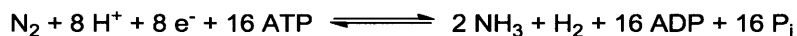


As currently performed the Haber-Bosch process utilizes a heterogeneous iron catalyst which is often doped with ruthenium, though many catalysts have been shown to work to some degree.¹ The reaction mechanism for the reduction of dinitrogen to ammonia at the iron surface is not well known. It is believed that N₂ is adsorbed onto the iron surface, where the reaction occurs.

Natural Nitrogenase Systems

Dinitrogen is reduced to ammonia in nature at ambient pressure and temperature using various nitrogenase enzymes (Equation 1.2). Nitrogenase enzymes in microbes reduce dinitrogen in approximately 10⁸ tons per year by the route shown in Equation 1.2.⁴

Equation 1.2: Reduction of Dinitrogen by Nitrogenase Enzymes



The most common and most efficient known nitrogenase is FeMoco (Figure 1.1),⁵ though FeV,⁶ FeW,⁷ and Fe only⁸ nitrogenases have also been isolated. FeMoco can be isolated from *Azotobacter vinlandii*⁹ among other proteins and has been studied in efforts to elucidate mechanistic details.¹⁰

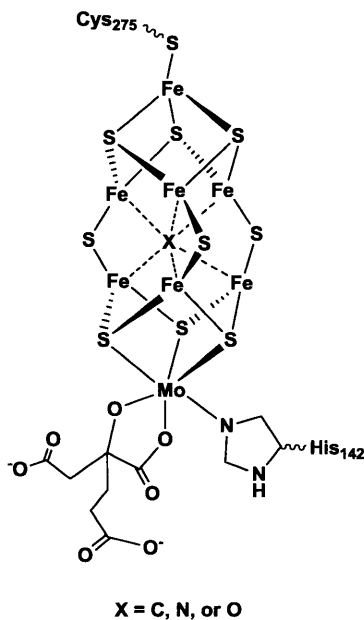


Figure 1.1: FeMoco

The first X-ray structure of FeMoco was published in 1992.¹¹ A higher resolution structure was obtained suggesting the presence of an atom between the Fe-S clusters which is believed to be N, O, or C (Figure 1.1).¹² Evidence from the Hoffmann Lab, based on ENDOR studies, suggests the unknown atom is neither nitrogen nor carbon.¹³

During the catalytic reduction of dinitrogen to ammonia by FeMoco, at least one equivalent of hydrogen is generated per equivalent of nitrogen that is reduced. The highest reported ratio of ammonia to hydrogen production during the reduction of dinitrogen in

nitrogenase is 2:1.⁹ With respect to electrons efficiency of the enzyme is diminished by generation of H₂ during dinitrogen reduction.

Transition Metal Dinitrogen Complexes

Since the isolation of the first nitrogenase enzyme in 1960,¹⁴ and the discovery of the first transition metal dinitrogen complex by Allen and Senoff in 1965 (Figure 1.2),¹⁵ the idea of reducing dinitrogen under mild conditions has received great attention. In 1969, Hidai reported the first molybdenum dinitrogen complex (Figure 1.3).¹⁶

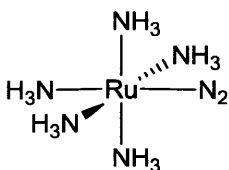


Figure 1.2: Allen and Senoff Complex

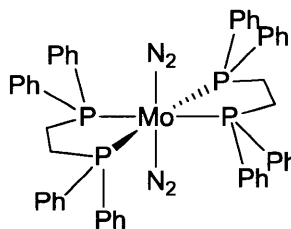


Figure 1.3: Hidai Complex

Chatt later showed that ammonia could be produced from a W(0) center $W(N_2)_2[P(Me_2Ph)_4]$ (Figure 1.4) in near stoichiometric yield, 1.9 equivalents of ammonia per tungsten.¹⁷ The reaction conditions employed were harsh, requiring strong acids and a small amount of hydrazine was produced. In 1970, Shilov demonstrated it was possible to catalytically reduce dinitrogen to hydrazine which disproportionates to ammonia with a 10:1 ratio of hydrazine to ammonia.¹⁸

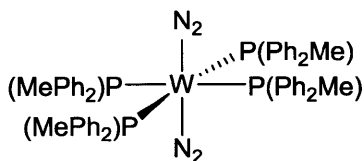


Figure 1.4: Tungsten Complex Developed by Chatt

Many other dinitrogen containing complexes have been reported. Dinitrogen can be bound in a variety of ways. End-on bound dinitrogen complexes, end-on bridging, side-on bridging, side-on-end-on bound complexes have all been reported and a sample of each is shown below.

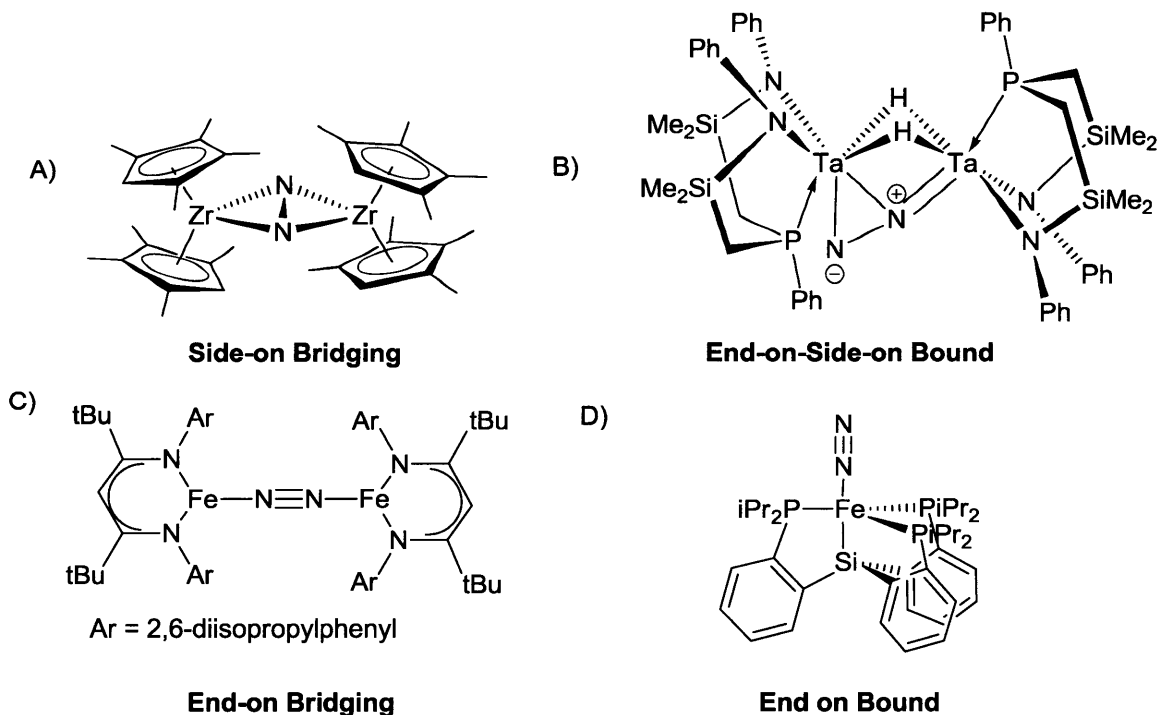


Figure 1.5: Various Modes of N₂ binding

Complex A (Figure 1.5), $[(\eta^5\text{-C}_5\text{Me}_4\text{H})_2\text{Zr}]_2(\mu_2, \eta^2, \eta^2\text{-N}_2)$, reported by Chirik was observed to add two equivalents of H_2 across the Zr-N bonds to form a bridging $(\mu_2, \eta^2, \eta^2\text{-N}_2\text{H}_2)$ zirconium hydride species, $[(\eta^5\text{-C}_5\text{Me}_4\text{H})_2\text{ZrH}]_2(\mu_2, \eta^2, \eta^2\text{-N}_2\text{H}_2)$. $[(\eta^5\text{-C}_5\text{Me}_4\text{H})_2\text{ZrH}]_2(\mu_2, \eta^2, \eta^2\text{-N}_2\text{H}_2)$ was then heated at 85 °C under an atmosphere of H_2 and found to release a sub-stoichiometric amount of ammonia (10-15%).¹⁹ Complex B (Figure 1.5) is a unique complex developed by Fryzuk which contains a nitrogen unit that is simultaneously side-on and end-on bound to tantalum.²⁰ Complex C (Figure 1.5) is an example of a low valent iron complex, which was developed by Holland in hopes of elucidating mechanistic details of the nitrogenase enzyme.²¹ Complex D (Figure 1.5), $\text{Si}(o\text{-C}_6\text{H}_4\text{PiPr}_2)_3\text{FeN}_2$, is an iron complex developed in the Peters lab.²² $\text{Si}(o\text{-C}_6\text{H}_4\text{PiPr}_2)_3\text{FeN}_2$ has been shown to have the ability to bind dinitrogen and ammonia. $\text{Si}(o\text{-C}_6\text{H}_4\text{PiPr}_2)_3\text{FeNH}_3$ has been shown to form $\text{Si}(o\text{-C}_6\text{H}_4\text{PiPr}_2)\text{FeN}_2$ under an N_2 atmosphere.

Dinitrogen Complexes from the Schrock Lab

Triamidoamine ligands, $\text{R}[\text{N}_3\text{N}]$ ($\text{N}_3\text{N} = [(\text{NHC}_2\text{H}_4)_3\text{N}]^{3-}$, TREN; $\text{R} = \text{Ar}, \text{Si}(\text{Ph}_n\text{Me}_{3-n}), \text{C}_6\text{F}_5$), were synthesized in the Schrock lab and $[\text{N}_3\text{N}]$ based metal complexes that readily bind dinitrogen end-on were developed.²³ With the introduction of palladium catalyzed C-N couplings,^{24,25} a large library of $[\text{ArN}_3\text{N}]$ ligands could be synthesized. Many of these metal complexes containing $[\text{ArN}_3\text{N}]$ ligands were shown to dimerize irreversibly.²³ In 2001, it was shown that using 3,5-di-substituted terphenyls, $[\text{N}_3\text{N}]$ ligands could be synthesized that were sterically large enough to prevent dimerization.²⁵ Many of these aryl substituents were

synthesized and complexes relating to proposed intermediates in the Chatt cycle¹⁷ were synthesized.

Catalytic Reduction of Dinitrogen to Ammonia at a Well-Defined Metal Center

A new terphenyl, HIPT (HIPT = 2,4,6,2'',4'',6''-hexaisopropyl-1,1',3,3'-terphenyl, HexaIsoPropylTerphenyl), was synthesized by Dmitry Yandulov and was found that [HIPTN₃N]MoX (X = N, NH₃, N₂) (Figure 1.6) catalytically reduced dinitrogen in the presence of a reductant and an acid source.^{26,27} At present a maximum of four turnovers or eight equivalents of ammonia are produced by the system.

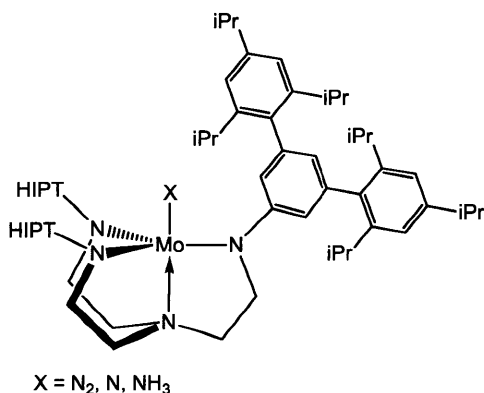


Figure 1.6: [HIPTN₃N]MoX

The HIPT ligand employed provides a sterically protected pocket that allows for the reduction of dinitrogen to ammonia without decomposition of key intermediates. One example of the unique steric protection afforded by the HIPT ligand is the isolation of [HIPTN₃N]MoN₂H. No other transition metal N₂H complex had been structurally characterized up to this point.²⁸ [HIPTN₃N]Mo also allows for the binding of both dinitrogen

and ammonia, and the exchange between the two occurs on a reasonable time scale ($t_{1/2} = 110$ minutes) under an N_2 atmosphere. The ability for dinitrogen to displace ammonia was critical for the catalytic activity of the system.

The catalytic reduction of dinitrogen to ammonia was believed to proceed through a Chatt-like cycle (Figure 1.7) by stepwise addition of protons and electrons. A number of complexes in this proposed mechanistic cycle have been synthesized and characterized (Figure 1.7).²⁸ Two additional intermediates, $[HIPTN_3N]MoNNH_2$ and $[MoNH_2]^+$, have been observed in solution but were not isolated. For the Yandulov-Schrock cycle it was believed that initial protonation of dinitrogen takes place through a PCET (proton-coupled electron transfer) because Cp_2^*Cr is not strong enough to reduce the bound dinitrogen ligand.²⁸ Other steps in the cycle may also involve a PCET reaction however definitive mechanistic details are not available.²⁹

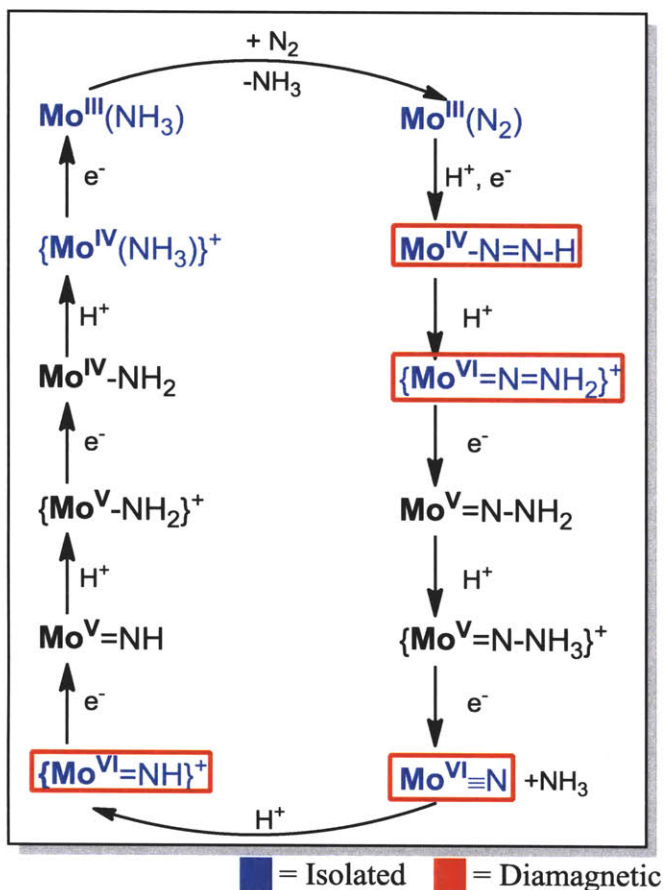


Figure 1.7: Yandulov Schrock Cycle.

Catalytic reduction of dinitrogen to ammonia utilizing $[\text{HIPTN}_3\text{N}]\text{Mo}$ was optimized through the use of a glass reactor (Figure 1.8) which allowed for the slow addition (over 6 hours) of a reducing agent to a flask containing the catalyst and acid source.²⁶ Cp_2^*Cr and $[\text{LutH}][\text{BAR}'_4]$ (Lut = 2,6-dimethylpyridine; $[\text{BAR}'_4]^- = [\text{B}[3,5-(\text{CF}_3)_2\text{C}_6\text{H}_3]_4]^-$)³⁰ or $[\text{CollH}][\text{BAR}'_4]$ (Coll = 2,4,6-trimethylpyridine)³¹ were found to produce optimum results when heptane was employed as the solvent. Heptane was critical for the catalytic success of this reaction because the acid source was sparingly soluble in heptane.

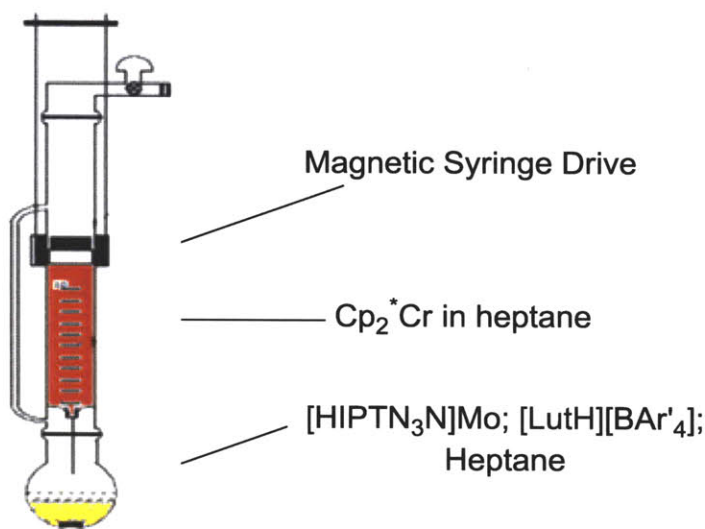


Figure 1.8: Schematic of Catalytic Reactor

As for nitrogenase enzymes, H_2 is generated during the course of the reaction with $[HIPTN_3N]Mo$. H_2 has been shown to be an inhibitor of both the natural systems,³² as well as $[HIPTN_3N]Mo$ ³³ and may be a limiting factor of the catalytic activity of the system.

Multiple variations of the $[HIPTN_3N]$ ligand system have been tried to improve the turnover number or elucidate the mechanism of the catalytic reduction of dinitrogen to ammonia.³⁴ Symmetric variations such as $[HTBTN_3N]Mo$ (HTBT = HexaTertButylTerphenyl = 2,4,6,2'',4'',6''-hexatert-butyl-1,1':3',1''-terphenyl) and $[HMTN_3N]Mo$ (HMT = HexaMethylTerphenyl = 2,4,6,2'',4'',6''-hexamethyl-1,1':3',1''-terphenyl) have been synthesized.³⁴ HTBT was shown to be too sterically encumbering to allow for the dinitrogen for ammonia exchange ($t_{1/2} > 6000$ minutes), and HMT was assumed to not be sterically protecting enough to protect key intermediates.³⁴

$[p\text{BrHIPTN}_3\text{N}]\text{Mo}$ ($p\text{BrHIPT}$ = 2'-bromo-2,4,6,2'',4'',6''-hexaisopropyl-1,1':3',1''-terphenyl) was shown to be catalytic, producing 7.1 equivalents of dinitrogen from ammonia. The reason this system was catalytic, was because the steric nature of the ligand was left mostly unaltered while the electronics of the system were slightly affected.³⁴

Large changes to the steric nature of the $[\text{N}_3\text{N}]$ system did not produce a complex which reduced dinitrogen to ammonia, so smaller changes were examined. A library of C_s symmetric complexes were synthesized where a single amine arm was changed from its original HIPT ligand. With a lone exception, $[(\text{TRIP})\text{HIPT}_2\text{N}_3\text{N}]\text{Mo}$ (Figure 1.9) which generated 2.5 equivalents of ammonia per metal center, these systems did not catalytically reduce dinitrogen to ammonia.³⁵

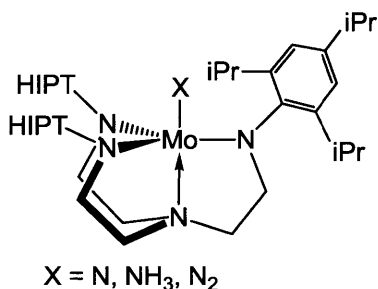
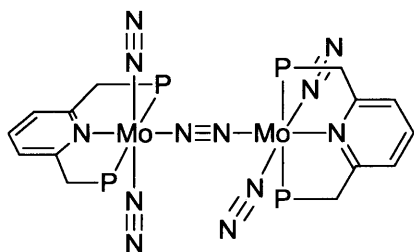


Figure 1.9: C_s Symmetric ligand, $[(\text{TRIP})\text{HIPT}_2\text{N}_3\text{N}]\text{MoX}$

Attempts to employ other elements, chromium,^{36a} tungsten,³⁷ and vanadium^{36b} with the $[\text{HIPTN}_3\text{N}]$ framework, did not produce complexes that catalytically reduce dinitrogen to ammonia. $[\text{HIPTN}_3\text{N}]\text{W}$ failed to catalytically reduce dinitrogen to ammonia presumably because the ammonia species, $[\text{HIPTN}_3\text{N}]\text{WNH}_3$, was not stable on a catalytically reasonable time scale. Cyclic voltammetry performed on $[\text{HIPTN}_3\text{N}]\text{WNH}_3[\text{BAR}'_4]$ showed that the reduction was not reversible at a scan rate of 500 mV/s, however it became quasi-reversible

as the scan rate was increased to 2.0 V/s.³⁷ Chromium and vanadium catalysts also proved ineffective and a variety of reasons were proposed.³⁶

Recently it was reported that the reduction of dinitrogen to ammonia was achieved using a PNP (PNP = 2,6-bis(di-*t*-butylphosphinomethyl)pyridine supporting ligand with molybdenum (Figure 1.10).³⁸ The complex, $[\text{Mo}(\text{N}_2)_2(\text{PNP})]_2(\mu\text{-N}_2)$, shown in Figure 1.10 reduces dinitrogen using Cp_2Co , and $[\text{LutH}][\text{OTf}]$. A maximum of 23.2 equivalents of ammonia per dinuclear complex was achieved after a reaction time of 20 hours. While many mechanistic details are unknown for $[\text{Mo}(\text{N}_2)_2(\text{PNP})]_2(\mu\text{-N}_2)$, it does produce twelve equivalents of ammonia per metal center or six turnovers of N_2 .



P = PtBu_2

Figure 1.10: Catalyst That Reduces Dinitrogen to Ammonia

While the amount of ammonia able to be generated at a single (or two) metal center(s) is increasing, the use of metallocene reducing agents and exotic acid sources ($[\text{LutH}][\text{OTf}]$ or $[\text{CollH}][\text{BAR}'_4]$) precludes the systems' ability to compete with the Haber-Bosch process. The Haber-Bosch process, while energy intensive, is efficient and cheap.

References

1. Smil, V. *Enriching the Earth: Fritz Haber, Carl Bosch, and the Transformation of World Food Production*; MIT Press: Cambridge, MA, 2004.
2. Ammonia. *Ullmann's Encyclopedia of Industrial Chemistry* [Online] Wiley, Posted December 15, 2006. <http://onlinelibrary.wiley.com/doi/10.1002/14356007.a02143.pub2/pdf>. (Accessed Mar. 19, 2007).
3. *CRC Handbook of Chemistry and Physics, 73rd ed.* Lide, D.R., Ed.; CRC Press: Boca Raton, FL, 1993; Chapter 9, p 132.
4. Eady, R. R. *Chem. Rev.* **1996**, *96*, 3013.
5. Smith, B. E.; Durrant, M. C.; Fairhurst, S. A.; Gormal, C. A.; Gronberg, K. L. C.; Henderson, R. A.; Ibrahim, S. K.; Le Gall, T.; Pickett, C. J. *Coord. Chem. Rev.* **1999**, *185*, 669.
6. Robson, R. L.; Eady, R. R.; Richardson, T. H.; Miller, R. W.; Hawkins, M.; Postgate, J. *R. Nature* **1986**, *322*, 388.
7. Siemann, S.; Schneider, K.; Oley, M.; Müller, A. *Biochemistry* **2003**, *42*, 3846.
8. Chisnell, J. R.; Premakumar, R.; Bishop, P. E. *J. Bacteriol.* **1988**, *170*, 27.
9. Shah, V. K.; Brill, W. J. *Proc. Natl. Acad. Sci. U. S. A.* **1977**, *74*, 3249.
10. Eady, R. R. *Chem. Rev.* **1996**, *96*, 3013.
11. Kim, J.; Rees, D. C. *Science* **1992**, *257*, 1677.
12. Einsle, O.; Tezcan, A.; Andrade, S. L. A.; Schmid, B.; Yoshida, M.; Howard, J. B.; Rees, D. C. *Science* **2002**, *297*, 1696.

-
13. Lukoyanov, D.; Pelmenschikov, V.; Maeser, N.; Laryukhin, M.; Yang, T. C.; Noodleman, L.; Dean, D. R.; Case, D. A.; Seefeldt, L. C.; Hoffman, B. M. *Inorg. Chem.* **2007**, *46*, 11437.
 14. Carnahan, J. E.; Mortenson, L. E.; Mower, H. F.; Castle, J. E. *Biochim. Biophys. Acta* **1960**, *44*, 520.
 15. Allen, A. D.; Senoff, C. V. *Chem. Commun.* **1965**, 621.
 16. (a) Hidai M.; Tominari K.; Uchida Y.; Misono A. *Chem. Commun.* **1969**, 814. (b) Hidai M.; Tominari K.; Uchida Y.; Misono, A. *Chem. Commun.* **1969**, 1392.
 17. Chatt, J.; Dilworth, J. R.; Richards, R. L. *Chem. Rev.* **1978**, *78*, 589.
 18. Shilov, A. E., *Russ. Chem. Bull. Int. Ed.* **2003**, *52*, 2555.
 19. Pool, J. A.; Lobkovsky, E.; Chirik, P. J. *Nature* **2004**, *427*, 527.
 20. Fryzuk, M. D.; Johnson, S. A.; Rettig, S. J. *J. Am. Chem. Soc.* **1998**, *120*, 11024.
 21. a) Smith, J. M.; Lachicotte, R. J.; Pittard, K. A.; Cundari, T. R.; Lukat-Rodgers, G.; Rodgers, K. R.; Holland, P. L. *J. Am. Chem. Soc.* **2001**, *123*, 9222. b) Smith, J. M.; Sadique, A. R.; Cundari, T. R.; Rodgers, K. R.; Lukat-Rodgers, G.; Lachicotte, R. J.; Flaschenriem, C. J.; Vela, J.; Holland, P. L. *J. Am. Chem. Soc.* **2006**, *128*, 756.
 22. Mankad, N. P.; Whited, M. T.; Peters, J. C. *Angew. Chem. Int. Ed.* **2007**, *46*, 5768.
 23. Schrock, R. R. *Acc. Chem. Res.* **1997**, *30*, 9.
 24. a) Hartwig, J. F. *Nature* **2008**, *455*, 314. b) Surry, D. S.; Buchwald, S. L. *Angew. Chem., Int. Ed.* **2008**, *47*, 6338. Cacchi, S.; Fabrizi, G.; Goggiamani, A.; Licandro E. *Org. Lett.* **2005**, *7*, 1497.

-
25. a) Greco, G. E.; Schrock, R. R. *Inorg. Chem.* **2001**, *40*, 3850. b) Greco, G. E.; Schrock, R. R. *Inorg. Chem.* **2001**, *40*, 3861.
26. Yandulov, D. V.; Schrock, R. R. *Science* **2003**, *301*, 76.
27. Yandulov, D. V.; Schrock, R. R. *J. Am. Chem. Soc.* **2002**, *124*, 6252.
28. Yandulov, D. V.; Schrock, R.R. *Inorg. Chem.* **2005**, *44*, 1103.
29. Munisamy T.; Schrock, R. R. Manuscript in Preparation.
30. Brookhart, M; Grant, B.; Volpe, A. F. Jr. *Organometallics* **1992**, *11*, 3920.
31. Weare, W. W. Synthetic and Mechanistic Study of Catalytic Dinitrogen Reduction. Ph.D. Thesis, Massachusetts Institute of Technology, Cambridge, MA, 2006.
32. Guth, J. H.; Burris, R. H. *Biochemistry* **1983**, *22*, 5111.
33. Hetterscheid, D. G. H.; Hanna, B. S.; Schrock, R. R. *Inorg. Chem.* **2009**, *48*, 8569.
34. Ritleng, V.; Yandulov, D. V.; Weare, W. W.; Schrock, R. R.; Hock, A. S.; Davis, W. M. *J. Am. Chem. Soc.* **2004**, *126*, 6150.
35. Weare, W. W.; Schrock, R. R.; Hock, A. S.; Müller P. *Inorg. Chem.* **2006**, *45*, 9185.
36. a) Smythe, N. C.; Schrock, R.R.; Müller, P.; Weare, W. W. *Inorg. Chem.* **2006**, *45*, 7111. b) Smythe, N. C.; Schrock, R.R.; Müller, P.; Weare, W. W. *Inorg. Chem.* **2006**, *45*, 9197.
37. Yandulov, D. V.; Schrock, R. R. *Can. J. Chem.* **2005**, *83*, 34.
38. Arashiba, K.; Miyake, Y.; Nishibayashi, Y. *J. Nat. Chem.* **2011**, *3*, 120.

Chapter 2

Hydrogen and Catalytic Studies of [HIPTN₃N]

Chapter 2. Hydrogen and Catalytic Studies of [HIPTN₃N]

Introduction

After the discovery of catalytic reduction of dinitrogen to ammonia by a single molybdenum center,¹ different steric and electronic variations of HIPTN₃N (HIPT = 2,4,6,2'',4'',6''-hexaisopropyl-1,1':3',1''-terphenyl, [(RNCH₂CH₂N)₃]³⁻ = TREN = N₃N) were explored in hopes of improving catalytic activity.² Since these ligand variations were not successful in increasing the quantity of dinitrogen that was reduced by our system^{2,3,4} attention was turned to further investigation of [HIPTN₃N]Mo complexes. The [HIPTN₃N] system has been well studied with respect to the reactivity and properties of catalytic intermediates.^{5,6} Complexes of [HIPTN₃N]MoX (X = C₂H₄, CO, C₂H₂) were also investigated.⁷ The [HIPTN₃N]Mo(C₂H₂) complex was of interest since acetylene has been shown to be reduced to ethylene by the natural nitrogenase enzymes, and is commonly used to determine the activities of samples of nitrogenase.⁸

H₂ is another important product in the natural system, FeMoco nitrogenase,⁹ and H₂ production is observed during the catalytic reduction of dinitrogen in both the natural and [HIPTN₃N]Mo systems. During the catalytic reduction of dinitrogen to ammonia by FeMoco, one equivalent of hydrogen is typically generated per equivalent of dinitrogen that is reduced. The best reported conversion of 2:1 ammonia to H₂ was achieved at N₂ pressure of 50 atmospheres.⁹ Efficiency of the catalyst with respect to electrons is diminished by generation of H₂ during dinitrogen reduction. The [HIPTN₃N]Mo system is typically compared with the natural system with regards to its efficiency and with respect to electrons or reducing agent. In the [HIPTN₃N]Mo system our best reductions are 65% efficient with

respect to the reducing agent (Cp₂Cr*) under one atmosphere of N₂. Successful catalytic reaction of N₂ at pressures above two atmospheres has not been achieved because the glassware will not hold the greater pressure. Since H₂ is generated in both nitrogenase and [HIPTN₃N]Mo, and H₂ has been shown to be an inhibitor of the natural system,¹⁰ we wished to explore the interaction of H₂ with [HIPTN₃N]Mo. Dennis Hettterscheid began exploring reactions between [HIPTN₃N]MoX (X = N₂, NH₃) and H₂ and found that he could synthesize and isolate [HIPTN₃N]MoH₂.¹¹ [HIPTN₃N]MoH₂ was believed to exist in equilibrium between three proposed structures (Figure 2.1).

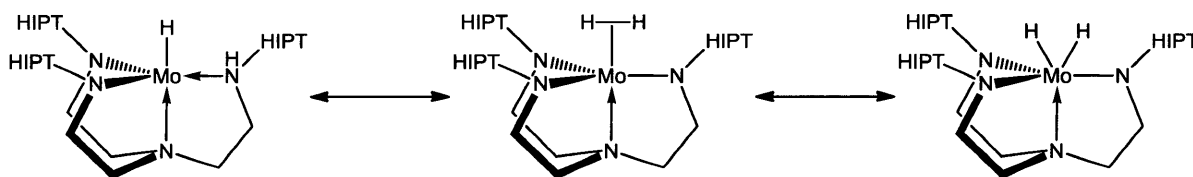


Figure 2.1: Proposed Equilibrium of [HIPTN₃N]MoH₂

Results and Discussion

Synthesis of [HIPTN₃N]MoH₂

[HIPTN₃N]MoH₂ can be synthesized by published methods through addition of H₂ to [HIPTN₃N]MoN₂ in toluene heated to 70 °C for 48 hours.¹¹ It can also be synthesized from [HIPTN₃N]MoN₂ in toluene at room temperature by extending the reaction time to 72 hours. An alternative method of synthesizing [HIPTN₃N]MoH₂ by introducing an atmosphere of H₂ to a solid sample of [HIPTN₃N]MoN₂ requires a seven day reaction time.¹¹ The benefit of this synthetic method is that recrystallization is not required; however a seven day reaction

time is impractical when a fresh sample must be prepared for accurate analysis. The compound is unstable therefore samples were not stored for more than 24 hours.

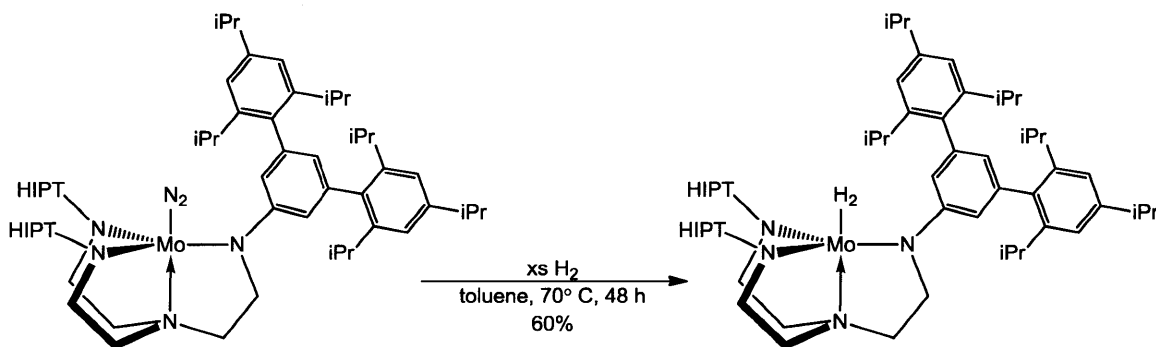


Figure 2.2: Synthesis of [HIPTN₃N]MoH₂.

When [HIPTN₃N]MoH₂ was used as the starting material for a catalytic reaction, ammonia was generated in 52% yield relative to equivalents of reducing agent.¹¹ A 52% yield is only slightly less than the 60-65% yield found for other [HIPTN₃N]MoX (X = NH₃[BAR'₄], N₂, N³⁻) precursors.¹¹

Another interesting property of [HIPTN₃N]MoH₂ was the scrambling of H₂ and D₂ to give HD. The statistical average 1:2:1 of H₂:HD:D₂ was achieved in two hours.¹¹ This scrambling was also observed for another TREN based system,¹² [N₃N_F]ReH₂, as well as in the natural system.^{8,13} The mechanism of this H/D scrambling is unknown but a possible mechanism of H/D scrambling for [HIPTN₃N]MoH₂ (Figure 2.3) was also proposed for [N₃N_F]ReH₂.¹² The H₂ of [HIPTN₃N]MoH₂ was heterolytic cleaved to form one of the proposed equilibrium structures of [HIPTN₃N]MoH₂ (A, Figure 2.3). Formation of a protonated amide arm and a metal hydride allows for a molecule of D₂ to oxidatively add to

molybdenum and form a trihydride (B, Figure 2.3). The trihydride can then reversibly release HD (C, Figure 2.3) resulting in the scrambling of H/D. There is precedent for the existence of a trihydride with the HIPTN₃N ligand system, i.e., [HIPTN₃N]WH₃ is a known compound.¹⁴ The existence of [HIPTN₃N]WH₃ suggests the HIPTN₃N ligand framework can support a trihydride so a molybdenum trihydride intermediate is reasonable.

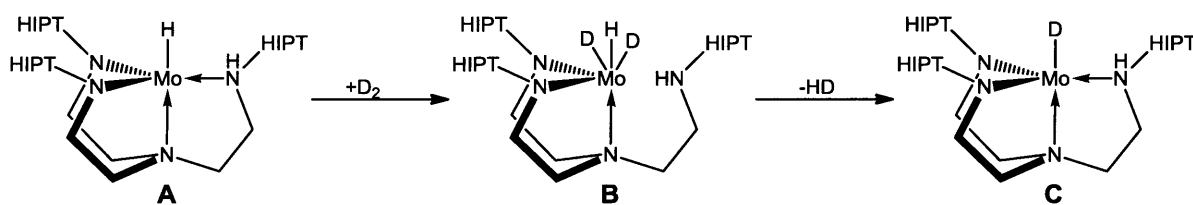


Figure 2.3: Proposed Mechanism for H/D Scrambling

It would seem unlikely that a tetrahydride is formed by addition of H₂ to the Mo(IV) dihydride. Based on the electronics of the [HIPTN₃N]Mo center, not enough electrons would be available for the binding of a fourth hydride. While there are examples of molybdenum tetrahydrides in the literature, they tend to involve electron rich molybdenum metal centers.¹⁵ No examples of tetrahydrides exist for a TREN based ligand of any transition metal.

If H/D scrambling is taking place through a trihydride intermediate the bound H₂ must be heterolytically split prior to reversible oxidative addition of a second equivalent of H₂. While no Mo-H or N-H stretches are observed for [HIPTN₃N]MoH₂ by IR spectroscopy, evidence of heterolytic splitting has come from ENDOR (ENDOR = Electron Nuclear Double Resonance) spectroscopy studies done in collaboration with the Hoffmann group. The existence of a Mo(III) hydride was supported by the observation of ENDOR spectroscopy

resonances that were not consistent with the Mo(IV) [HIPTN₃N]MoH. When [HIPTN₃N]MoH is cryoreduced at 77 K by γ -radiation to {[HIPTN₃N]MoH}⁻, resonances observed by ENDOR spectroscopy for Mo(III) hydride match those observed for [HIPTN₃N]MoH₂. The Mo(III) hydride observed by ENDOR spectroscopy is proposed to be part of the equilibrium of [HIPTN₃N]MoH₂ between the various possible ground state structures.

Throughout the ENDOR spectroscopy studies performed by Hoffmann's group, as well as the studies performed in our group using ¹H NMR and IR spectroscopy, no spectroscopic evidence of the amine bound proton was found. This lack of spectroscopic evidence led to the investigation of [HIPTN₃N]Mo phosphine complexes. These phosphine complexes were initially explored in an attempt to trap an amine arm of the ligand off of molybdenum and are discussed in detail in Chapter 3.

Quantification of H₂ on [HIPTN₃N]MoH₂

No satisfactory elemental analysis or X-ray structure of [HIPTN₃N]MoH₂ could be obtained. Analyzing for two additional protons on a molecule with 145 protons would also be difficult, so the quantification of H₂ bound to the molybdenum center was explored. Gas chromatography (GC) was performed on a molecular sieve column at 150 °C using N₂ as the carrier gas. Quantification of the molybdenum bound H₂ by GC is performed by treating solid [HIPTN₃N]MoH₂ with excess CO and quantifying the amount of hydrogen that is displaced (Figure 2.4). A sample of [HIPTN₃N]MoH₂, prepared by published methods,¹¹ yielded less than one equivalent of H₂ as measured by GC. Multiple attempts to measure the

hydrogen from isolated [HIPTN₃N]MoH₂ gave one quarter to one third of the expected equivalents of H₂. These samples of [HIPTN₃N]MoH₂ were isolated by removing solvent under vacuum, and crude [HIPTN₃N]MoH₂ was crystallized from pentane. The isolated product was then dried *in vacuo* (10 mtorr) for 24 hours to remove residual solvent.

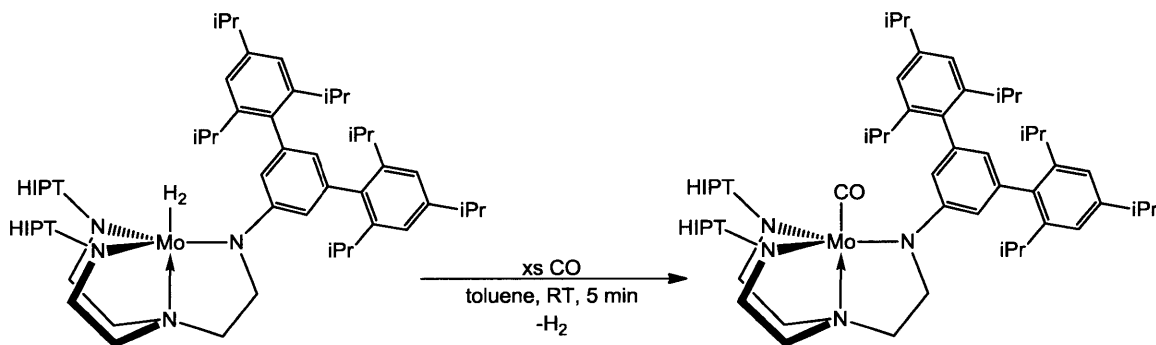


Figure 2.4: Liberation of H₂ From [HIPTN₃N]MoH₂ by CO.

Production of sub-stoichiometric amounts of hydrogen could result from incomplete conversion of [HIPTN₃N]MoH₂ to [HIPTN₃N]MoCO. A solution of [HIPTN₃N]MoH₂ in toluene (10 mM) was prepared and similar results were obtained by GC. Another option considered, was a hydride insertion into CO to form formaldehyde, similar to that observed for ethylene.¹³ Since CO may complicate the quantification of H₂, another strong Lewis base, PMe₃ was tried. Using PMe₃ to displace H₂ was found to produce similar results to those of CO, with one-quarter to one-third of an equivalent of H₂ released. When a sample of MoH₂ was isolated by crystallization, without drying the sample for 24 hours, nearly half an equivalent of H₂ was detected by GC. When [HIPTN₃N]MoH₂ was isolated on a frit and

vacuum was applied for several minutes to remove filtrate, two-thirds of an equivalent of H₂ was measured by GC.

Using 0.7 mL of a C₆D₆ stock solution with an internal standard (TMS₂O) about 73% of the sample is shown to be [HIPTN₃N]MoH₂ by integration of the 2' proton of HIPT by ¹H NMR spectroscopy. The [HIPTN₃N]MoH₂ sample was placed under vacuum (10 mtorr) on a Schlenk line for 24 hours, after which 0.7 mL of the stock solution of C₆D₆ and TMS₂O was added under an argon atmosphere to prevent N₂ contamination. A ¹H NMR spectrum taken after the sample was under vacuum for 24 hours showed that the sample of [HIPTN₃N]MoH₂ contained roughly one third of the original concentration of [HIPTN₃N]MoH₂. One third of an equivalent of H₂, initially observed by GC was consistent with the results observed by ¹H NMR spectroscopy. After a sample of [HIPTN₃N]MoH₂ was under vacuum for 72 hours the ¹H NMR resonances relating to [HIPTN₃N]MoH₂ are barely distinguishable from the baseline. These ¹H NMR spectrum show that the molybdenum-bound hydrogen on [HIPTN₃N]MoH₂ was labile and re-introduction of hydrogen to the [HIPTN₃N]MoH₂ sample decomposed *in vacuo* does not result in regeneration of [HIPTN₃N]MoH₂. Other substrates (PMe₃ and CO) were added to the decomposition product of [HIPTN₃N]MoH₂ and were found not to react with decomposed [HIPTN₃N]MoH₂. When H₂ was removed *in vacuo* the complex irreversibly decomposed to an unidentified paramagnetic substance.

Samples of [HIPTN₃N]MoN₂ and [HIPTN₃N]MoNH₃ were prepared by published methods, placed under vacuum for a week, and monitored by ¹H NMR spectroscopy as described for the [HIPTN₃N]MoH₂ species. These samples showed no degradation as

measured by ¹H NMR spectroscopy. [HIPTN₃N]MoN₂ was also monitored by IR spectroscopy which showed the ν_{NN} stretch at 1990 cm⁻¹.⁵

Since [HIPTN₃N]MoH₂ was sensitive to the partial pressure of H₂, N₂ and vacuum were avoided during the syntheses and analysis of samples of [HIPTN₃N]MoH₂. The syntheses and decomposition of [HIPTN₃N]MoH₂ were done *in situ*. Three samples of [HIPTN₃N]MoH₂ were synthesized concurrently in 25 mL and 50 mL Schlenk flasks. Each sample of known concentration (15-30 mM in toluene) was placed under one atmosphere of hydrogen for 72 hours at room temperature and the atmosphere was refreshed every 24 hours. After 3 days, the *in situ* generated sample of [HIPTN₃N]MoH₂ was flushed with a flow of nitrogen gas for 15 minutes. A control study was performed and no H₂ was detected by GC after a 15 minute N₂ purge of flasks, similar to those used for the quantification studies. H₂, dissolved in toluene, was accounted for during calibration. The exchange of N₂ for H₂ was assumed to be negligible on this time scale (minutes) since the N₂ for H₂ exchange takes hours.¹¹ CO was injected into the Schlenk flask containing the [HIPTN₃N]MoH₂ sample with a syringe to decompose the complex, as described. An average of > 90% of the expected hydrogen was quantified by GC for the three samples (0.93 ± 0.2). This showed that each [HIPTN₃N]MoH₂ complex contains one equivalent of H₂.

“Direct Nitride” Synthesis of [HIPTN₃N]MoN

In an effort to synthesize molybdenum nitride complexes quickly for use in catalytic experiments, a new method for the synthesis of a molybdenum nitride was explored. The synthesis of M(NMe₂)(tpa) (M = Ti, Zr; tpa = tris(pyrrolyl- α -methyl)amine) by Odom

utilized zirconium or titanium tetrakisdimethylamine to metallate the ligands through protonolysis.¹⁶ In our lab zirconium, hafnium, and molybdenum have been used to synthesize metal complexes of various ligand systems that were difficult to synthesize by other methods.^{17,18}

Since [HIPTN₃N]MoN is a common starting point for our catalytic reactions, we chose to use NMo(NMe₂)₃¹⁹ for our protonolysis reactions rather than molybdenum tetrakisdimethylamide. When one equivalent of NMo(NMe₂)₃ was added to a pentane solution of H₃[HIPTN₃N] (30 mM) at room temperature no reaction was observed by ¹H NMR spectroscopy. If the solution was heated to 50 °C for 12 hours [HIPTN₃N]MoN was observed by ¹H NMR spectroscopy, but about 50% of H₃[HIPTN₃N] remained unreacted. The reaction was monitored easily by ¹H NMR spectroscopy because the 2' proton of HIPT exhibited a characteristic shift from δ 6.54 ppm for the ligand to δ 7.94 ppm for [HIPTN₃N]MoN. After 2 hours the progress of the reaction from free ligand to [HIPTN₃N]MoN stopped and NMo(NMe₂)₃ was no longer observable by ¹H NMR spectroscopy. Isolation of the reaction mixture by filtration through Celite yielded a yellow solution that contains a 1:1 mixture of nitride to ligand. When two equivalents of NMo(NMe₂)₃ was used (Figure 2.5) with one equivalent of H₃[HIPTN₃N] in toluene at 50 °C the reaction proceeded to completion with full consumption of ligand in twelve hours, with an 84% isolated yield of [HIPTN₃N]MoN. The need for two equivalents of NMo(NMe₂)₃ was believed to be due to the thermal decomposition of NMo(NMe₂)₃ since the reaction must be heated due to the steric hindrance of the bulky HIPTN₃N ligand. In

reactions discussed in Chapter 4, less sterically demanding ligands were used, eliminating the requirement for heating, the reactions proceeded stoichiometrically:

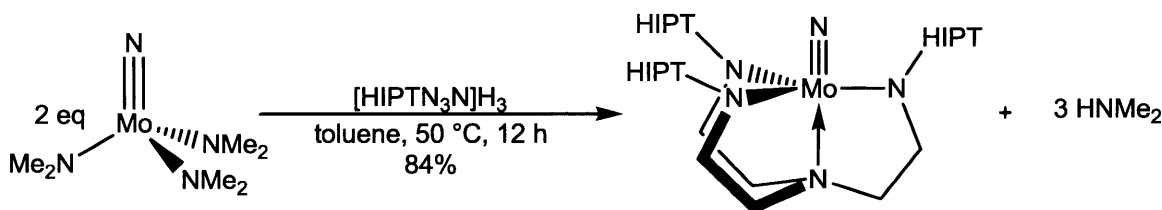


Figure 2.5: “Direct Nitride” Synthesis of [HIPTN₃N]MoN

Variations of Catalytic Reactions With [HIPTN₃N]MoN

If our goal of achieving the electro-catalytic reduction of dinitrogen to ammonia is to be realized, a solvent with a higher dielectric constant than *n*-heptane (1.92)²⁰ will be needed to provide efficient electrochemical reduction. Common solvents used in electrochemistry such as acetonitrile and water are incompatible with our catalyst and therefore can not be used. Other solvents such as dichloromethane (9.1),²⁰ fluorobenzene (6.4),²⁰ and THF (7.58)²⁰ have been used in the past for cyclic voltammetry studies in our group. Since these are the most likely to perform the best in the electro-catalytic reduction of dinitrogen to ammonia it is important to understand how these solvents perform under standard catalytic conditions with the glassware setup described in the literature.¹

Fluorobenzene is the most commonly used solvent for electrochemistry in our lab due to its limited reactivity and moderate dielectric constant. When fluorobenzene was employed the acid source used ([CollH][BAR'₄]) completely dissolved. [HIPTN₃N]MoN was used as the starting catalyst and was readily protonated by the acid source (48 fold excess). The color of the [HIPTN₃N]MoN/[CollH][BAR'₄] solution in the receiving flask turned from yellow to

red prior to the addition of any reducing agent. This does not occur in heptane. The red color that was observed suggests the formation of [HIPTN₃N]MoNH[BAr'₄] which is red and is a characterized species. After the reaction was complete the work-up of ammonia was completed an average of 1.4 equivalents of ammonia (Table 2.1) were detected by the indophenol method as published.¹ This is significantly less than the 7.3 equivalents of ammonia (Table 2.1) the reaction yielded under standard conditions, using heptane as the solvent. One equivalent of ammonia was expected starting from [HIPTN₃N]MoN and slightly more than one equivalent of ammonia was observed when fluorobenzene was used. The complex does not catalyze the reduction of dinitrogen to ammonia under these conditions. The same procedure was repeated for both THF and toluene yielding 0.2 equivalents and 0.8 equivalents of ammonia respectively (Table 2.1). The reason for the failure of THF to yield a single equivalent of ammonia from the nitride is unclear; the reaction was repeated with freshly distilled solvent and produced the same result. In cases where the system fails to be catalytic, the equivalents of reducing agent were accounted for by quantifying the H₂ in the headspace and accounted for ~90% of the electrons.

Table 2.1: Catalytic Reactions with Various Solvent

Solvent	Avg. Eq. of NH₃
Heptane	7.3
Fluorobenzene	1.4
THF	0.2
Toluene	0.8

It has been shown that the solubility of [CollH][BAR'₄] in the solvent is critical for the catalytic activity of the system, and that the solubility of the acid source in heptane is the reason it is used for catalytic reactions. Now that other solvents have been tested, it is clear that if the acid source was completely solubilized, the majority of the reducing agent was used to generate H₂. If the electrochemical reduction of dinitrogen to ammonia is to be achieved with the present system, a new acid source that is insoluble in fluorobenzene will need to be employed.

It was shown that catalytic reactions can be performed outside of a nitrogen filled glove box.¹ Performing a catalytic reaction outside of a glove box allows for variations, such as heating or cooling the reaction to be achieved easier than inside of the glove box. Through a modification of the collection flask, a gas or liquid can also be introduced. Walter Weare showed that the atmosphere above the catalytic reactions can be sampled with a microsyringe.³ A microsyringe needle can be inserted through a rubber septum on the side arm of the modified flask, kept sealed when not in use with a 0-4 Teflon[®] stop-cock, alleviating concerns of leakage. Typically a catalytic reaction is completed inside the glove box. The apparatus is then removed for manipulation and analysis.

We decided to introduce H₂ to the apparatus, prior to the start of the reaction and outside of the glovebox, to compare the inhibition of H₂ in the [HIPTN₃N]Mo system to the natural system. A control experiment was performed in which 4 mL of N₂ was injected into the apparatus outside the glove box. This reaction yielded 6.4 equivalents of ammonia from [HIPTN₃N]MoN, less than the reported yield. The yield of ammonia is highly dependent on the purity of the reagents used during a catalytic reaction. When Cp₂*Cr was sublimed

immediately prior to its use in a catalytic reaction, the yield of ammonia is close to the reported yields (7.3 equivalents versus 8 equivalents.). Subsequent catalytic reactions give a decreasing yield of ammonia by roughly an equivalent over the course of several weeks. When Cp₂Cr* is resublimed the full yield of ammonia returns.

Two sets of reactions were run with both 4.5 mL and 9.0 mL of H₂ injected into the apparatus. For these reactions only 0.9 equivalents of ammonia were produced (Table 2.2), consistent with no catalytic turnover starting from [HIPTN₃N]MoN. During a catalytic reaction [HIPTN₃N]MoNH₃ is formed and the ammonia is displaced by N₂. If hydrogen is present at high enough concentrations, then the displacement of ammonia for hydrogen is competitive with N₂, and the cycle is not repeated. It was shown that the displacement of ammonia for hydrogen occurred in minutes, while the exchange of N₂ and ammonia has a half life of 120 minutes.⁵

Since H₂ was shown to inhibit catalytic turnover and was generated under standard catalytic reaction conditions, ways to remove H₂ throughout the catalytic reaction were explored. Throughout a catalytic reaction, a flow of nitrogen gas was introduced to the apparatus through a side arm above the reaction mixture and released through a trap connected to the top of the apparatus by a 28/15 ball joint. The trap was immersed in liquid nitrogen to freeze out any ammonia that was generated during the reaction. Unfortunately, the volume of solvent was slowly reduced and the reaction did not proceed in the typical fashion, yielding only two equivalents of ammonia rather than the normal 7-8 equivalents expected (Table 2.2).

Since the ammonia must be retained throughout the catalytic reaction to be quantified and the solvent appears to be vacuum transferred to the cold trap along with the ammonia, another method was explored using Pd/C with tertbutylethylene to trap out H₂. Unfortunately Pd/C dried *in vacuo* at 230 °C for 48 hours facilitates the decomposition of [Mo]N. After ten minutes the solution turns from yellow to green and MoN is no longer observed by ¹H NMR spectroscopy. For this reason it was believed Pd/C would not be a suitable partner for a catalytic reaction.

Table 2.2: Catalytic Reaction Results with Alterations

Changes to Catalytic Conditions	Avg. Eq. of NH ₃ Quantified
Addition of H ₂ (4.5 mL)	0.87
Addition of H ₂ (9.0 mL)	0.89
Constant Flow of N ₂	1.97

Conclusion

H₂ is formed in both the natural FeMoco nitrogenase enzyme as well as [HIPTN₃N]Mo systems. Complexes of [HIPTN₃N]MoH₂ were synthesized by a variety of methods. Unfortunately [HIPTN₃N]MoH₂ was unstable *in vacuo* and the bound hydrogen could not be directly observed by X-ray diffraction studies, ¹H NMR, or IR spectroscopy. We were able to quantify the amount of hydrogen in the sample of [HIPTN₃N]MoH₂ and propose three reasonable structures believed to be in equilibrium (Figure 2.1).¹¹ Evidence for the presence of a heterolytically split [HIPTN₃N]MoH₂ species has come from collaboration with the Hoffmann group, who found evidence for a Mo(III) hydride using ENDOR spectroscopy.

H₂ has been shown to be a powerful inhibitor of the catalytic activity of [HIPTN₃N]Mo. It is believed that when H₂ is present in a high enough concentration, the exchange of dinitrogen for ammonia is too slow to compete with the exchange of H₂ for ammonia and the reaction does not produce any ammonia from N₂. H₂ inhibition is a parallel between the [HIPTN₃N]Mo system and the FeMoco. Attempts to remove H₂ from the catalytic apparatus during reactions to facilitate a higher yield of ammonia, have not been successful.

Using a synthetic route directly to [HIPTN₃N]MoN from H₃[HIPTN₃N] has allowed rapid synthesis of [HIPTN₃N]MoN. This route is also higher yielding with respect to ligand, which is important for difficult to synthesize ligands.

We were interested in using a solvent with a much higher dielectric constant than heptane for the catalytic reduction of dinitrogen to ammonia. Unfortunately, we did not find a suitable solvent. The reason these reactions were unsuccessful was believed to be due to the increased solubility of [CollH][BAR'₄] in the solvent used.

Experimental

General. Air and moisture sensitive compounds were manipulated utilizing standard Schlenk and dry box techniques under a dinitrogen or argon atmosphere. All glassware was oven and/or flame dried prior to use. Pentane, diethyl ether, toluene, and benzene were purged with dinitrogen and passed through activated alumina columns. Benzene was additionally passed through a column containing copper catalyst to remove oxygen. THF, heptane and tetramethylsilane were dried over Na/benzophenone, freeze-pump-thawed three times, and vacuum transferred. All dried and deoxygenated solvents were stored in a dinitrogen-filled glove box over molecular sieves or in Teflon[®] sealed glass solvent bombs. Molecular sieves (4 Å) and Celite were activated at 230 °C *in vacuo* over several days. [HIPTN₃N]MoN,¹ [HIPTN₃N]MoH₂,¹¹ NMo(NMe₃)¹⁹ were synthesized by published methods. All Mo and W complexes were stored under dinitrogen or argon at -35 °C. ¹H, ¹³C, and ¹⁹F ³¹P NMR spectra were recorded on a Varian Mercury 300 and Varian Inova 500 spectrometers. ¹H and ¹³C NMR spectra are referenced to the residual protons in solvent for ¹H or solvent in ¹³C relative to tetramethylsilane (δ 0 ppm). ¹⁹F NMR spectra were referenced externally to fluorobenzene (δ -113.15 ppm upfield of CFC₁₃). ³¹P NMR spectra were referenced externally to H₃PO₄ (δ 0 ppm). Elemental analyses were performed by Midwest Microlabs, Indianapolis, Indiana, U.S.A.

Quantitation of Hydrogen in [HIPTN₃N]MoH₂. A Schlenk flask of known volume was loaded with [HIPTN₃N]MoN₂ (30 mg, 0.02 mmol) in 1.0 mL of toluene. The flask was then sealed with a rubber septum. A separate 500 mL Schlenk flask was filled with H₂ and cooled in liquid N₂ for 20 min. The Schlenk flask containing the [HIPTN₃N]MoN₂ solution was

freeze/pump/thaw degassed and connected to the Schlenk bomb containing H₂ still immersed in liquid N₂. The two were allowed to equilibrate for 10 min. This procedure was repeated after 24 and 48 h. By ¹H NMR the resonances corresponding to MoN₂ are no longer visible within 48 h. After 72 h the sample of [HIPTN₃N]MoH₂ was frozen in liquid N₂ and purged with a flow of N₂ gas for 10 min. The solution was then removed from liquid N₂ and allowed to warm under a flow of N₂ gas for an additional 10 min. The sample was then sealed and 2.0 mL of CO was injected to form [HIPTN₃N]MoCO, and hydrogen was measured in the atmosphere after 5 min. Four GC measurements employing 20 μL samples yielded an average of 0.95 (0.05 equiv of H₂ per metal center. A run employing 36 mg of [HIPTN₃N]MoH₂ gave an average (four measurements) of 0.86 (0.08 equiv of H₂, while a third employing 61 mg of [HIPTN₃N]MoH₂ gave an average of 0.93 (0.02 equiv of H₂ (five measurements).

General Gas Chromatography. An HP 6890 Series GC equipped with a 50 m x 0.530 mm, 25 μm, HP MoleSieve column and a TCD (Thermal Conductivity Detector) was used for the detection and quantification of H₂. An injection temperature of 150° C, an oven temperature of 200° C, and a detector temperature of 250° C were used with a flow rate of carrier gas, N₂, at 8 psi or 5 mL/min. Under these conditions with samples volumes of 20 μL, H₂ was detected at 1.12 minutes. The sample volumes were corrected for partial pressure of toluene and the volume of CO added.

Synthesis of [HIPTN₃N]MoN using NMo(NMe₂)₃. In a 50 mL Schlenk bomb, of NMo(NMe₂)₃ (86 mg, 0.36 mmol) was added to H₃[HIPTN₃N] (300 mg, 0.19 mmol) in 10 mL of toluene. The reaction was stirred at 50 °C and turns dark yellow. After 12 hours the

reaction was cooled and toluene removed under high vacuum. The remaining solid was extracted in pentane and filtered through Celite to yield a bright yellow solution. The solution volume was reduced *in vacuo* until a yellow solid began to precipitate. The solution was then cooled to -35 °C and the solid product was collected on a glass frit, yield 268 mg (84%, 0.11 mmol). Characterization data is as published.¹

General Procedures for Reductions of Dinitrogen in the Presence of Dihydrogen. A catalytic apparatus was set up in the glovebox according to previously published methods¹ using a receiving flask fitted with a side arm containing a 0-4 Teflon[®] plug, and a rubber septum for gas sampling or addition. The apparatus was then taken from the glovebox and connected to a Schlenk line where the internal pressure was equilibrated to atmospheric under an N₂ flow. The apparatus was then removed from the line and attached to the syringe drive. A pressure-Lok[®] syringe is flushed three times and filled with H₂ drawn from a flask under a constant H₂ purge. The syringe was locked and brought to the catalytic apparatus where it was opened and H₂ slowly driven out until the desired volume was reached. In a continuous motion the syringe was injected into the septum being careful not to overpressurize the side arm. The plug was then opened, and the desired volume of H₂ was injected into the system and mixed by pumping the syringe three times. The system was then allowed to equilibrate for 10 min, and the Teflon[®] stopper was then closed. After 10 min the syringe drive was started, and the run completed as previously described.¹ Analysis of ammonia was also done by the previously reported indophenol method.¹

Catalytic Reduction of Dinitrogen Employing the Modified Reactor. The catalytic apparatus described above had a total volume of 82.0 mL. To a receiving flask containing

[HIPTN₃N]MoN (9.0 mg, 5.31 μ mol) and [CollH][BAr'₄] (321 mg, 0.33 mmol) 1.0 mL of heptane was added. The syringe barrel was then loaded with Cp₂Cr* (81 mg 0.25 mmol) in 9.1 mL of heptane. With the apparatus having a remaining headspace of 72.9 mL, 4.5 mL (0.200 mmol) of N₂ was added to the system as described above. Addition of 4.5 mL of N₂ increases the internal pressure of the apparatus by 6.3%. Upon completion of the catalytic run and indophenol analysis 6.4 equiv of ammonia were obtained relative to molybdenum.

Catalytic Reduction of Dinitrogen in the Presence of Dihydrogen. To a catalytic reaction as described above 4.5 mL (0.200 mmol) of H₂ were added. Addition of 4.5 mL (0.200 mmol) of H₂ increased the internal pressure of the apparatus by 6.3%, and H₂ accounted for 6.3% of the N₂/H₂ mixture, or 32 equiv of H₂ versus Mo. Upon completion of the catalytic run and indophenol analysis an average of 0.87 equiv of ammonia were obtained relative to molybdenum, or none from dinitrogen.

In a second run 9.0 mL (0.400 mmol) of H₂ were added. The internal pressure increased by 12.3% and H₂ to give a N₂/H₂ mixture in which 11.6% consisted of dihydrogen, or 65 equiv of H₂ versus Mo. Upon completion and analysis of the catalytic run 0.89 equiv of ammonia were obtained relative to molybdenum, or 0 from dinitrogen.

References

1. Yandulov, D. V.; Schrock, R. R. *Science* **2003**, *301*, 76.
2. Ritleng, V.; Yandulov, D. V.; Weare, W. W.; Schrock, R. R.; Hock, A. S.; Davis, W. M. *J. Am. Chem. Soc.* **2004**, *126*, 6150.
3. Weare, W. W.; Schrock, R. R.; Hock, A. S.; Müller P. *Inorg. Chem.* **2006**, *45*, 9185.
4. Reithofer, M. R.; Schrock, R. R.; Müller P. *Inorg. Chem.* **2010**, *132*, 8349.
5. Yandulov, D. V.; Schrock, R. R.; *Inorg. Chem.* **2005**, *44*, 1103.
6. Yandulov, D. V.; Schrock, R. R.; *J. Am. Chem. Soc.* **2002**, *124*, 6252.
7. Byrnes, M. J.; Dai, X.; Schrock, R. R.; Hock, A. S.; Müller, P. *Organometallics* **2005**, *24*, 4437.
8. Burgess, B. K.; Lowe, D. J. *Chem. Rev.* **1996**, *96*, 2983.
9. Simpson, F. B.; Burris, R. H. *Science* **1984**, *224*, 1095.
10. Guth, J. H.; Burris, R. H; *Biochemistry* **1983**, *22*, 5111.
11. Hetterscheid, D. G. H.; Hanna, B. S.; Schrock, R. R. *Inorg. Chem.* **2009**, *48*, 8569.
12. Reid, S. M.; Neuner B.; Schrock, R. R.; Davis W. M. *Organometallics* **1998**, *17*, 4077.
13. Liang, J.; Burris, R. *J. Bacteriol.* **1989**, *171*, 3176.
14. Yandulov, D. V.; Schrock, R. R. *Can. J. Chem.* **2005**, *83*, 34.
15. a) Guggenberger, L. J. *Inorg. Chem.* **1973**, *12*, 2295. b) Cloke, F. G. N.; Gibson, V. C. Green, M. L. H. *J. Chem. Soc., Dalton Trans.* **1988**, 2227. c) Baya, M.;

-
- Houghton, J.; Daran, J. C.; Poli, R.; Male, L.; Albinati, A.; Gutman, M. *Chem. Eur. J.* **2007**, *13*, 5347.
- 16 Shi, Y.; Cao, C.; Odom, A. L. *Inorg. Chem.* **2004**, *43*, 275.
17. Wampler, K. M.; Schrock, R. R. *Inorg. Chem.* **2007**, *46*, 8463.
18. Chin, J. *Syntheses and Studies of Molybdenum and Tungsten Complexes for Dinitrogen Reduction*. Ph.D. Thesis, Massachusetts Institute of Technology, Cambridge, MA, 2010.
19. Johnson, M. J. A.; Lee, M. P.; Odom, A. L.; Davis, W. M.; Cummins, C. C. *Angew. Chem., Intl. Ed.* **1997**, *36*, 87.
20. *CRC Handbook of Chemistry and Physics, 73rd ed.* Lide, D.R., Ed.; CRC Press: Boca Raton, FL, 1993; Chapter 8, p 49.

Chapter 3

Group VI Phosphine Complexes

Chapter 3. Group VI Phosphine Complexes

Introduction

The use of phosphine ligands for dinitrogen chemistry has a rich history.¹ Phosphine ligands have been used to prepare molybdenum(0) and tungsten(0) dinitrogen complexes.^{2,3,4,5} Many of these low oxidation state complexes were used in early attempts to catalytically reduce dinitrogen^{2,6} but are not relevant to the chemistry that will be discussed in this chapter. Only a handful of phosphorus-containing molybdenum complexes that contain multiple amide groups have been reported.^{7,8} Within this subset are several molybdenum phosphide and rhenium phosphine complexes that contain $[N_3N]$ ($[N_3N] = [(RNCH_2CH_2N)_3]^{3-}$, TREN).^{9,10}

Several rhenium phosphine complexes (Figure 3.1) have been synthesized. These rhenium complexes also exhibited the same hydrogen H/D scrambling seen for $[HIPTN_3N]MoH_2$ ¹¹ in the presence of H_2 and D_2 .¹⁰ An interesting aspect of this rhenium chemistry was that a $[N_3N_F]Re(O)Cl$ complex ($N_3N_F = [(C_6F_5NCH_2CH_2)_3N]^{3-}$) (Figure 3.1) was isolated as an arm off complex.

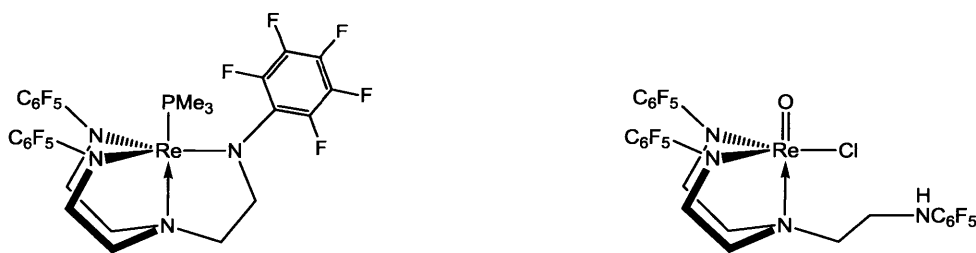


Figure 3.1: $[N_3N_F]Re$ Complexes

Similarities between $[\text{HIPTN}_3\text{N}]\text{MoH}_2$ and $[\text{N}_3\text{N}_\text{F}]\text{ReH}_2$ with respect to H/D scrambling sparked interest in exploring work analogous to the $[\text{N}_3\text{N}_\text{F}]\text{Re}$ complexes. Work done with $[\text{N}_3\text{N}_\text{F}]\text{Re}$ also yielded complexes where a phosphine and hydride were coordinated to the ligand at the same time.¹⁰ These complexes were synthesized by protonation of $[\text{N}_3\text{N}_\text{F}]\text{RePMe}_3$ (

Figure 3.2) with $\text{H}(\text{Et}_2\text{O})_2\text{BAR}'_4$ ($[\text{BAR}'_4]^- = [\text{B}[3,5-(\text{CF}_3)_2\text{C}_6\text{H}_3]_4]^-$)¹² to yield $[\text{N}_3\text{N}_\text{F}]\text{Re}(\text{H})\text{PR}_3[\text{BAR}'_4]$ (

Figure 3.2). The resulting cationic complex contained a hydride that was observed by ^1H NMR spectroscopy.

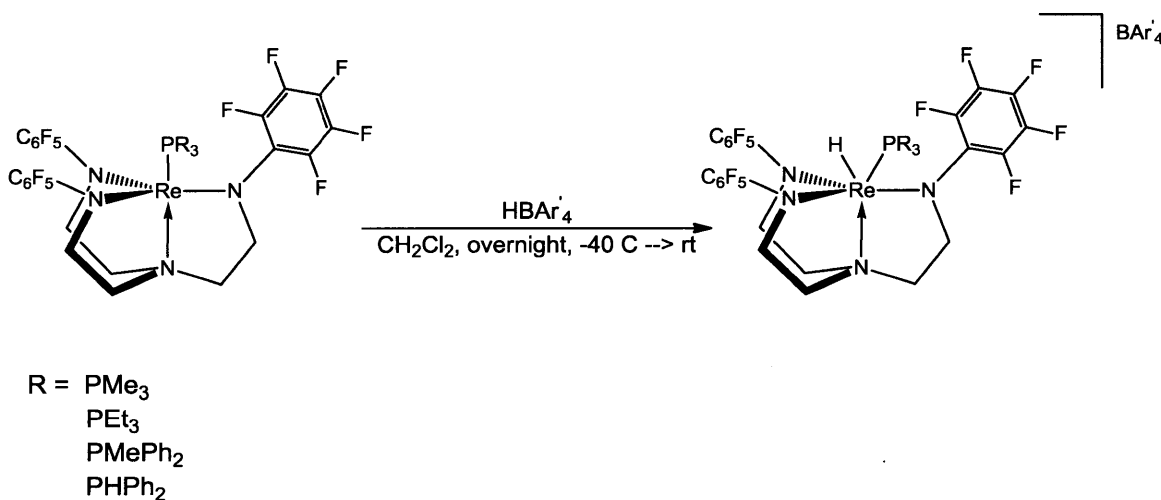


Figure 3.2: Generic Synthesis of $[\text{N}_3\text{N}_\text{F}](\text{H})\text{PR}_3[\text{BAR}'_4]$

As discussed in Chapter 2 (Figure 2.3), it was believed that $[\text{HIPTN}_3\text{N}]\text{MoH}_2$ exists in equilibrium with a species in which H_2 was heterolytically split to yield an amine and a molybdenum hydride. Through coordination of a strong σ -donor, such as a phosphine, it

may be possible to displace the amine produced from the heterolytic cleavage of H_2 . In the $[N_3N_F]Re(H)PR_3$ examples, an amine arm of the $[N_3N_F]$ ligand was not permanently displaced from the metal.¹⁰ It was proposed that steric crowding in the HIPT ligand would promote dissociation of the amine arm to yield $[HIPTN_3N_{armoff}]Mo(H)PR_3$. Therefore, reactions between phosphines and $[HIPTN_3N]Mo$ species were explored.

Results and Discussion

Synthesis of Molybdenum Phosphine Complexes

$[HIPTN_3N]MoPMe_3$ (Figure 3.3) was synthesized from $[HIPTN_3N]MoNH_3[BAr'_4]$ by addition of KC_8 in the presence of excess PMe_3 .¹³ $[HIPTN_3N]MoPMe_3$ was isolated as a red solid in 55% yield after recrystallization from pentane.¹¹ $[HIPTN_3N]MoPMe_3$ was paramagnetic with $S = \frac{1}{2}$ as measured by the Evans method.¹⁴ The 1H NMR spectrum of $[HIPTN_3N]MoPMe_3$ displayed resonances assigned to the N_3N backbone protons ($NH_2CH_2CH_2N$) at δ 15.8 ppm and -25.9 ppm. The ^{31}P NMR spectrum contained a resonance for PMe_3 at δ 19.2 ppm. A 1H NMR resonance for the protons in the 2',4' positions of the internal aryl ring are observed at δ -7.3 ppm.

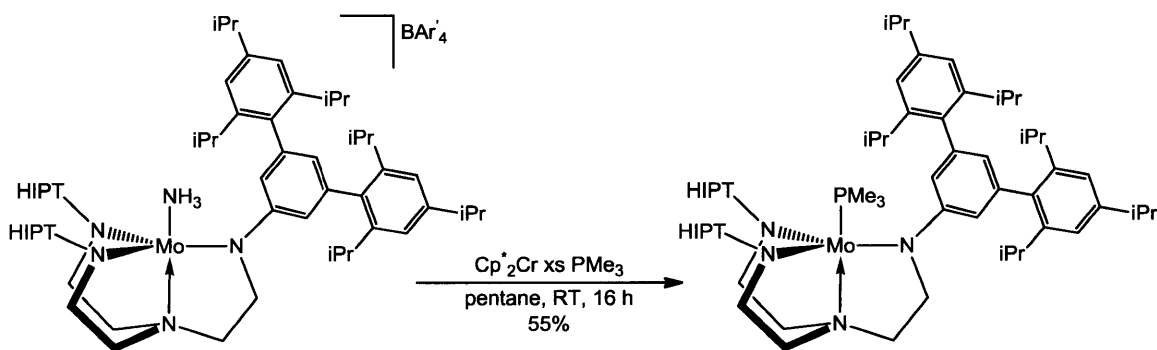


Figure 3.3: Synthesis of [HIPTN₃N]MoPMe₃.¹¹

Alternatively [HIPTN₃N]MoPMe₃ can be synthesized by treating [HIPTN₃N]MoN₂ (Figure 3.4) with PMe₃. The reaction between PMe₃ and [HIPTN₃N]MoN₂ was slower than that between PMe₃ and [HIPTN₃N]MoNH₃. Displacement of ammonia in [HIPTN₃N]MoNH₃ by PMe₃ proceeded to completion within an hour, whereas the reaction between PMe₃ and [HIPTN₃N]MoN₂ required 16 hours. [HIPTN₃N]MoPMe₃ was isolated in 52% yield after recrystallization from pentane.

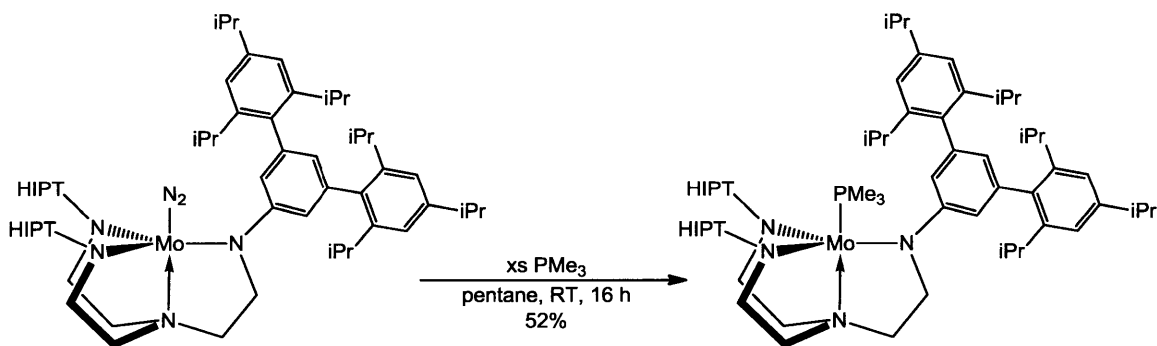


Figure 3.4: Alternate Synthesis of [HIPTN₃N]MoPMe₃

[HIPTN₃N]MoPMe₃[BAR'₄] (Figure 3.5) was prepared by oxidation of [HIPTN₃N]MoPMe₃ by Fc[BAR'₄] (Fc = ferrocene = Fe(η⁵-C₅H₅)₂), but samples of

$[\text{HIPTN}_3\text{N}]\text{MoPMe}_3[\text{BAr}'_4]$ prepared in this way were always contaminated with ferrocene. $[\text{HIPTN}_3\text{N}]\text{MoNH}_3[\text{BAr}'_4]$ or $[\text{HIPTN}_3\text{N}]\text{MoN}_2$ must be synthesized and isolated. It would be beneficial to synthesize a phosphine complex directly from $[\text{HIPTN}_3\text{N}]\text{MoCl}$, thereby eliminating additional synthetic steps.

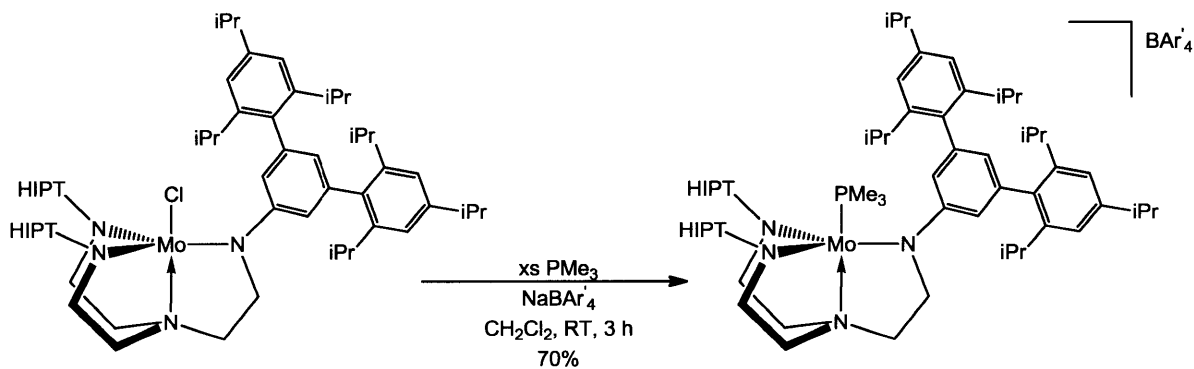


Figure 3.5: Synthesis of $[\text{HIPTN}_3\text{N}]\text{MoPMe}_3[\text{BAr}'_4]$

When NaBAr'_4 was allowed to react with a methylene chloride solution of $[\text{HIPTN}_3\text{N}]\text{MoCl}$ in the presence of excess PMe_3 , $[\text{HIPTN}_3\text{N}]\text{MoPMe}_3[\text{BAr}'_4]$ was obtained in 70% yield. The reaction is complete after three hours, according to ^1H NMR spectroscopy. As with $[\text{HIPTN}_3\text{N}]\text{MoNH}_3[\text{BAr}'_4]$, $[\text{HIPTN}_3\text{N}]\text{MoPMe}_3[\text{BAr}'_4]$ is a high spin Mo(IV) complex with $S = 1$ according to the Evans method. A sharp resonance was observed in the ^1H NMR spectrum at $\delta -10.3$ ppm, corresponding to the methyl protons of PMe_3 . Two additional broad resonances at $\delta -17$ and -96 ppm correspond to the backbone protons. The resonance for $\text{P}(\text{CH}_3)_3$ shifts significantly upfield from $\delta 19.2$ ppm for $[\text{HIPTN}_3\text{N}]\text{MoPMe}_3$ to -10.3 ppm for $[\text{HIPTN}_3\text{N}]\text{MoPMe}_3[\text{BAr}'_4]$. Since the $\text{P}(\text{CH}_3)_3$ resonances were sharp compared to the other resonances for paramagnetic species, the formation of $[\text{HIPTN}_3\text{N}]\text{MoPMe}_3[\text{BAr}'_4]$ was easily monitored by ^1H NMR spectroscopy. A

color change from deep red to bright green provided a basis for monitoring the reaction. Thin plates of $[\text{HIPTN}_3\text{N}]\text{MoPMe}_3[\text{BAR}'_4]$ can be grown from a saturated pentane solution but unfortunately, the plates are not suitable for X-ray diffraction studies. A red impurity was also present after the reaction and was carried through after multiple crystallizations; it was not identified and prevented the appropriate measured percentages of elements during an elemental analysis.

In an attempt to avoid impurities present in $[\text{HIPTN}_3\text{N}]\text{MoPMe}_3[\text{BAR}'_4]$ samples, a $[\text{BPh}_4]^-$ salt was prepared. Under the same reaction conditions described in Figure 3.5, $[\text{HIPTN}_3\text{N}]\text{MoPMe}_3[\text{BPh}_4]$ obtained in 56% yield. $[\text{HIPTN}_3\text{N}]\text{MoPMe}_3[\text{BPh}_4]$ was less soluble in pentane than the $[\text{HIPTN}_3\text{N}]\text{MoPMe}_3[\text{BAR}'_4]$ analogue, which aided in its isolation. $[\text{HIPTN}_3\text{N}]\text{MoPMe}_3[\text{BPh}_4]$ can be crystallized from pentane and obtained in pure form.

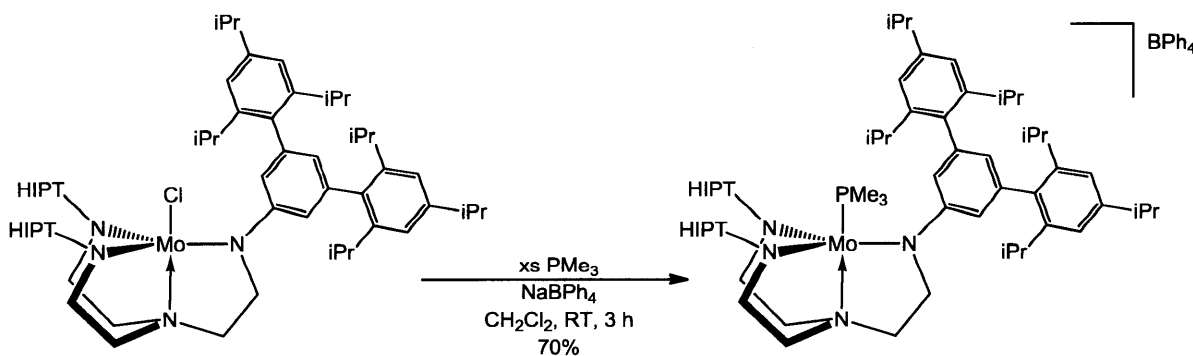


Figure 3.6: Synthesis of $[\text{HIPTN}_3\text{N}]\text{MoPMe}_3[\text{BPh}_4]$

The ^1H NMR spectrum of $[\text{HIPTN}_3\text{N}]\text{MoPMe}_3[\text{BPh}_4]$ taken in C_6D_6 was similar to that of $[\text{HIPTN}_3\text{N}]\text{MoPMe}_3[\text{BAR}'_4]$, except the PMe_3 methyl resonance in $[\text{HIPTN}_3\text{N}]\text{MoPMe}_3[\text{BPh}_4]$ appeared at δ -9.1 ppm compared to δ -10.2 ppm in

[HIPTN₃N]MoPMe₃[BAr'₄]. The methylene resonances in the ligand backbone in [HIPTN₃N]MoPMe₃[BAr'₄] appeared at δ -17 and -96 ppm in the ¹H NMR spectrum; they were observed at δ -19 and -99 ppm for [HIPTN₃N]MoPMe₃[BPh₄].

Crystals of [HIPTN₃N]MoPMe₃[BPh₄] suitable for X-ray diffraction were obtained by layering a diethyl ether solution with pentane (Figure 3.7). Crystals of [HIPTN₃N]MoPMe₃[BPh₄] grow in the P2₁/n space group with four independent molecules ($Z = 4$) in the unit cell. Crystallographic data tables are shown in appendix C.

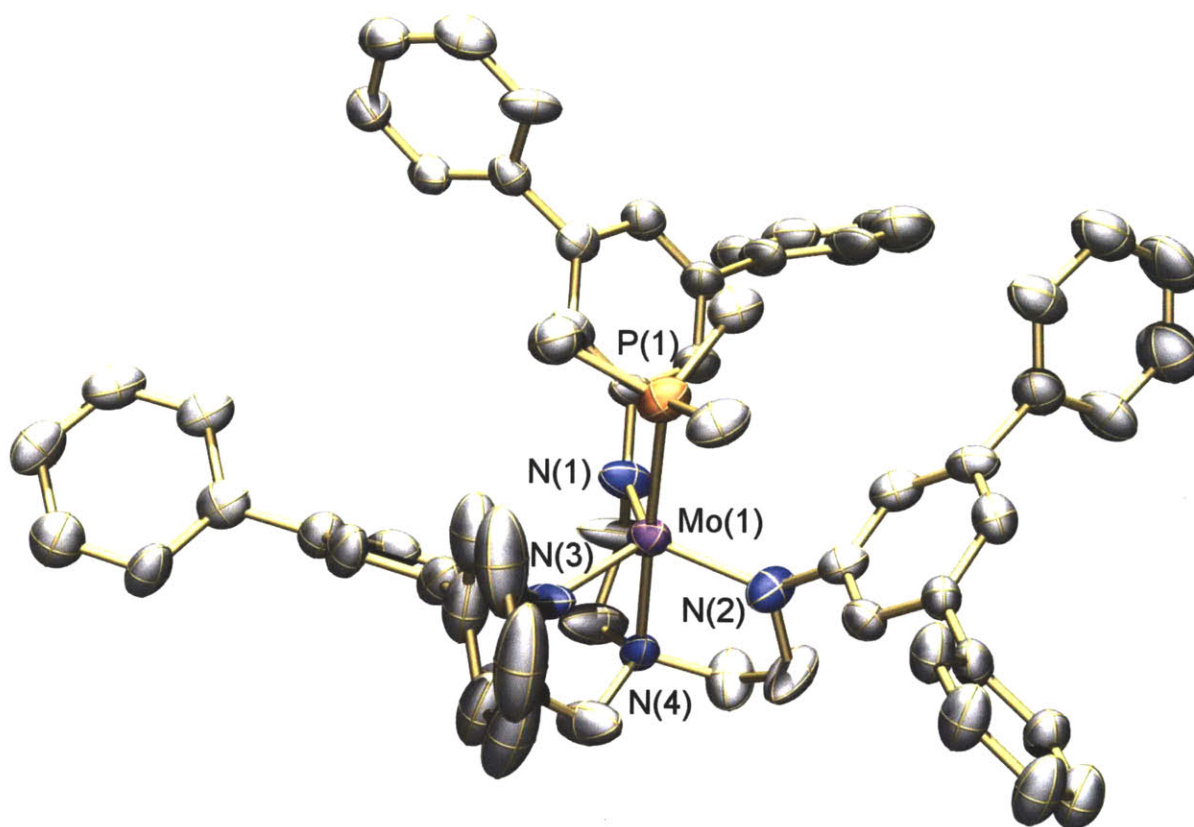


Figure 3.7: Thermal ellipsoid representation [HIPTN₃N]MoPMe₃[BPh₄]. Isopropyl groups and hydrogen atoms omitted for clarity. Selected bond distances (Å) and angles (°): Mo(1)-N(1) = 1.946(7), Mo(1)-N(4) = 2.205(7), Mo(1)-P(1) = 2.569(3). Mo(1)-N(1)-C_{ipso} = 131.3(6), N(1)-Mo(1)-N(4) = 80.1(3).

The phosphorus is bound to the molybdenum center with a molybdenum phosphorus distance of 2.569(3) Å, which is slightly longer than a typical molybdenum phosphine distance.^{5,15,16} The average molybdenum-amide distances in [HIPTN₃N]MoPMe₃[BPh₄] are similar (1.953 Å) to those for the analogous Mo(IV) [HIPTN₃N]MoNH₃[BAR'₄] (1.948 Å).¹³ The Mo-N(4) distance in [HIPTN₃N]MoPMe₃[BPh₄] is ~0.05 Å longer than the Mo-N(4) distance in [HIPTN₃N]MoNH₃[BAR'₄] (2.147(9) Å).¹³

Table 3.1: Selected Bond Lengths (Å) and Angles (°) for [HIPTN₃N]MoPMe₃[BPh₄] Compared to [HIPTN₃N]MoNH₃[BAR'₄]

Selected Bonds (Å) and Angles (°)	[HIPTN ₃ N]MoPMe ₃ [BPh ₄]	[HIPTN ₃ N]MoNH ₃ [BAR' ₄]
Mo-N _{amide} (avg.)	1.988	1.948
Mo-N _{amine}	2.433(4)	2.147(9)
Mo-P(1)	2.569(3)	-----
Mo-N _{ammonia}	-----	2.236(10)
N _{amine} -Mo-N _{amide} (avg.)	79.8	98.8
Mo-N _{amide} -C _{ipso} (avg.)	129.4	128.1

A cyclic voltammogram of [HIPTN₃N]MoPMe₃ (Figure 3.8) shows that [HIPTN₃N]MoPMe₃/[HIPTN₃N]MoPMe₃⁺ has a reversible redox couple at -1.51 V versus Ferrocene/Ferrocinium (Fc/Fc⁺). This is compared to [HIPTN₃N]MoNH₃⁺/[HIPTN₃N]MoNH₃ which has a reversible redox couple at -1.63 V versus Fc⁺/Fc. Both [HIPTN₃N]MoPMe₃[BAR'₄] and [HIPTN₃N]MoPMe₃[BPh₄] can be reduced chemically with Cp₂Cr* or KC₈, as well as various other reducing agents to [HIPTN₃N]MoPMe₃. Reducing either [HIPTN₃N]MoPMe₃[BAR'₄] or [HIPTN₃N]MoPMe₃[BPh₄] with KC₈ yielded

[HIPTN₃N]MoPMe₃ cleanly in 70% yield as a red solid. Excess KC₈ was easily filtered off before isolating product. The molybdenum cations are stable and can be synthesized in good yields on multi-gram scales. This method does not require the isolation of other intermediate complexes which are more difficult to make consistently on larger scales in good yields.

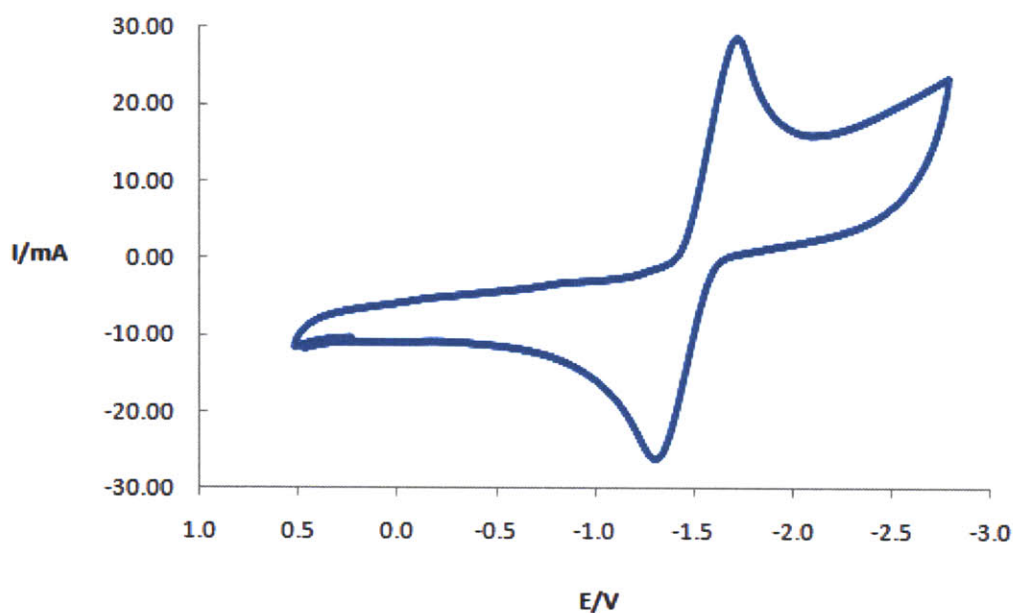


Figure 3.8: Cyclic Voltammogram of 2mM [HIPTN₃N]MoPMe₃ in 0.1 M [TBA]BAR'₄/PhF. WE: Pt; Scan rate: 200 mV/s vs. Fc/Fc⁺

Synthesis of [HIPTN₃N]MoP(H)PMe₃

Reactions between [HIPTN₃N]MoH and PMe₃ were explored. [HIPTN₃N]MoH (Figure 3.9) reacts with PMe₃ rapidly to give purple, crystalline [HIPTN₃N]Mo(H)PMe₃ (Figure 3.9), which was obtained by crystallization from pentane. [HIPTN₃N]Mo(H)PMe₃ is a diamagnetic low spin Mo(IV) complex. The ¹H NMR spectrum contains an interesting hydride resonance that appears at δ -1.19 ppm and has a J_{PH} of 111 Hz. This coupling

constant is unusually high for a non-PH bond.¹⁰ Several rhenium phosphine complexes have J_{PH} values in the 54–64 Hz range,¹⁰ but the most closely analogous complex, $[\text{N}_3\text{N}_\text{F}]\text{Re}(\text{H})\text{PMe}_3[\text{BAR}'_4]$, only has a J_{PH} of 7 Hz.¹⁰ Other molybdenum PMe_3 hydride complexes such as $[\text{Cp}_2^*\text{Mo}(\text{PMe}_3)_3\text{H}_2]\text{BF}_4$ exhibit a J_{PH} around 45 to 65 Hz.¹⁷ In $[\text{Cp}_2^*\text{Mo}(\text{PMe}_3)_3\text{H}_2]\text{BF}_4$ the coupling between the phosphorus and hydrides is not as significant (45–65 Hz) as $[\text{HIPTN}_3\text{N}]\text{Mo}(\text{H})\text{PMe}_3$ (111 Hz) suggesting the higher J_{PH} value results from a bonding interaction between the phosphorus and hydride.

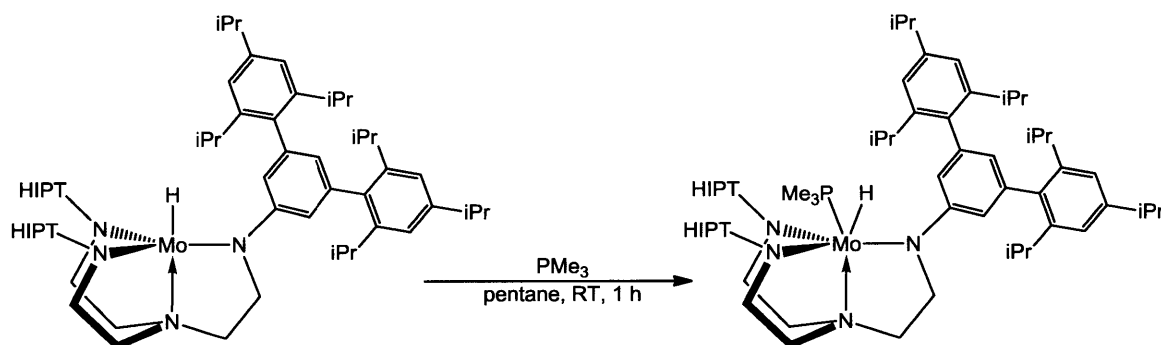


Figure 3.9: Synthesis of $[\text{HIPTN}_3\text{N}]\text{Mo}(\text{H})\text{PMe}_3$

While $[\text{HIPTN}_3\text{N}]\text{MoPMe}_3$ and $[\text{HIPTN}_3\text{N}]\text{MoPMe}_3[\text{BAR}'_4]$ are stable under pressure as low as 10 mtorr, $[\text{HIPTN}_3\text{N}]\text{Mo}(\text{H})\text{PMe}_3$ decomposes to an unidentified paramagnetic compound under vacuum. Addition of PMe_3 to the unidentified complex, did not reform $[\text{HIPTN}_3\text{N}]\text{Mo}(\text{H})\text{PMe}_3$, so decomposition appears to be irreversible. Samples of $[\text{HIPTN}_3\text{N}]\text{Mo}(\text{H})\text{PMe}_3$ were formed *in situ* from $[\text{HIPTN}_3\text{N}]\text{MoH}$, and then vacuum applied through a trap cooled with liquid nitrogen. The trap was a modified air-free bubbler which has been fitted with one female and one male 15/28 ball joints on either side which can be closed with 0-4 Teflon[®] plugs.¹⁸ The isolated volatiles were then transferred into a flask

containing an HCl/Et₂O solution. This mixture was stirred at room temperature for 30 minutes then dried *in vacuo* to give a white solid. When the solids were dissolved in D₂O, nearly an equivalent of PMe₃HCl was observed by both ¹H NMR and ³¹P NMR spectroscopy. (³¹P NMR (D₂O) triplet at δ -2.1 ppm [HPMe₃][Cl] ¹H NMR (D₂O) doublet δ 1.86 ppm [HPMe₃][Cl])

This is an interesting finding because, though [HIPTN₃N]MoH₂ was shown to lose H₂ *in vacuo* as discussed in Chapter 2, it was far slower than the loss of PMe₃ from [HIPTN₃N]Mo(H)PMe₃. The loss of H₂ from [HIPTN₃N]MoH₂ was incomplete after 72 hours but the loss of PMe₃ from [HIPTN₃N]Mo(H)PMe₃ was complete within two hours. This decomposition was never reported for any of the rhenium complexes discussed above,¹⁰ nor is N₂, NH₃, or PMe₃ loss observed from [HIPTN₃N]MoN₂, [HIPTN₃N]MoNH₃ or [HIPTN₃N]MoPMe₃.

It was thought that [HIPTN₃N]Mo(H)PMe₃ could be synthesized from [HIPTN₃N]MoPMe₃[BAr'₄] through addition of a hydride source. In the case of [HIPTN₃N]MoNH₃[BAr'₄] a hydride displaces the ammonia; [HIPTN₃N]Mo(H)NH₃ is not observed. PMe₃ in [HIPTN₃N]MoPMe₃ was bound more strongly to molybdenum than the ammonia in [HIPTN₃N]MoNH₃, as exhibited by the fact that [HIPTN₃N]MoPMe₃ was synthesized from [HIPTN₃N]MoN₂ even under one atmosphere of nitrogen.

Unfortunately, addition of NaHBEt₃ or LiHBEt₃ to [HIPTN₃N]MoPMe₃[BAr'₄] at room temperature yielded [HIPTN₃N]MoPMe₃ as the major product, with [HIPTN₃N]Mo(H)PMe₃ being formed as the minor product. When a solution of LiHBEt₃ (100 μL in 10 mL of -30 °C THF), was added drop-wise via a syringe to a cold solution of [HIPTN₃N]MoPMe₃[BPh₄], a

mixture of both $[\text{HIPTN}_3\text{N}]\text{Mo}(\text{H})\text{PMe}_3$ and $[\text{HIPTN}_3\text{N}]\text{MoPMe}_3$ (Figure 3.10) was formed, but the major product was $[\text{HIPTN}_3\text{N}]\text{Mo}(\text{H})\text{PMe}_3$. Other alkali hydrides such as NaBH_4 , KH , and NaH also reduced the complex, though the $[\text{HIPTN}_3\text{N}]\text{M}(\text{H})\text{PMe}_3$ complex was not found in these cases. Addition of a hydride source to $[\text{HIPTN}_3\text{N}]\text{MoPMe}_3$ was not a viable route for the clean synthesis of $[\text{HIPTN}_3\text{N}]\text{Mo}(\text{H})\text{PMe}_3$.

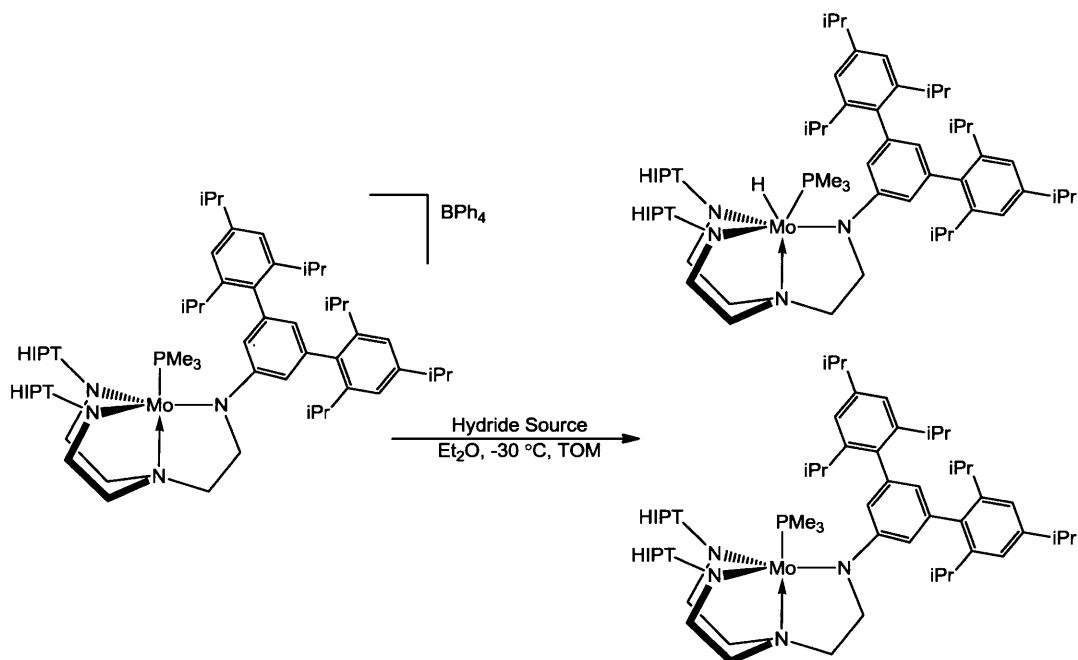


Figure 3.10: Alternate Synthesis of $[\text{HIPTN}_3\text{N}]\text{Mo}(\text{H})\text{PMe}_3$

Attempted Syntheses of $[\text{HIPTN}_3\text{N}]\text{MoPH}_3$

If $[\text{HIPTN}_3\text{N}]\text{MoPH}_3$ was prepared, it could be compared to known $[\text{HIPTN}_3\text{N}]\text{MoNH}_3$. While molybdenum PMe_3 complexes are known,^{5,15,19} no molybdenum PH_3 complexes have been structurally characterized. Only a handful of group V and group VI^{20,21,22,23} PH_3 complexes are reported in the literature, along with one iron example.²⁴

Reactions analogous to those employed for the synthesis of $[\text{HIPTN}_3\text{N}]\text{MoPMe}_3[\text{BAr}'_4]$ (Figure 3.5) and $[\text{HIPTN}_3\text{N}]\text{MoPMe}_3$ (Figure 3.4) were tried. The first reaction in Figure 3.11 involved addition of PH_3 to a cold solution of $[\text{HIPTN}_3\text{N}]\text{MoCl}$ in CH_2Cl_2 containing one equivalent of NaBAr'_4 . The solution appeared to change color initially, but upon warming of the solution, the color disappeared and an intractable black precipitate formed. Only free ligand was observed by ^1H NMR spectroscopy. When this same reaction was performed in CD_2Cl_2 the decomposition was complete, before a ^1H NMR spectrum could be obtained. The reaction also failed when NaBPh_4 was employed (Figure 3.11).

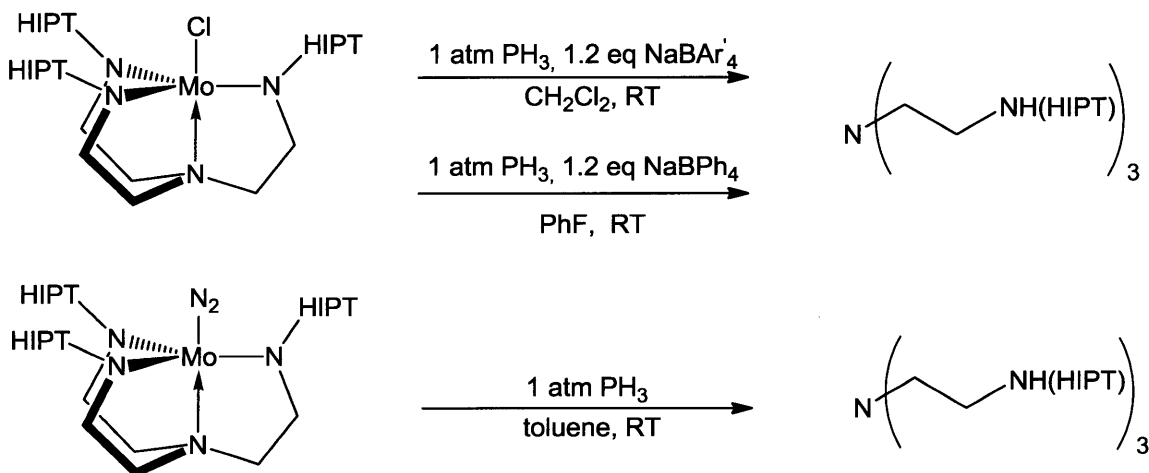


Figure 3.11: Attempted Syntheses of $[\text{HIPTN}_3\text{N}]\text{MoPH}_3$

Attempts to displace N_2 with PH_3 again produced only free ligand. Formation of free ligand suggests that coordinated PH_3 was acidic and a proton migrated to an amide nitrogen. A ^{31}P NMR spectrum of a reaction in solution showed no phosphorus resonance, which suggests that the phosphorus was in the black precipitate.

Attempts to Use Various Mono and Bidentate Phosphines

To gauge the steric limitations of the system, and in hopes of using a steric effect to force an amide arm off of the ligand, a variety of triamidoamine complexes and phosphines were tried. While molybdenum phosphine TREN complexes have been synthesized for monodentate phosphine ligands,¹⁰ none are known for bidentate phosphine ligands.

Attempts to use a bidentate phosphine, where the stronger σ -donor might take the place of an amine arm that results from the heterolytic cleavage of H_2 in $[HIPTN_3N]MoH_2$ were unsuccessful. Numerous bidentate phosphines of with various electronics properties and backbone lengths were tried such as dmpe, dppe, dppm and, dppp (dmpe = 1,2-bis(dimethylphosphino)ethane, dppe = 1,2-bis(diphenylphosphino)ethane, dppm = 1,2-bis(diphenylphosphino)methane, dppp = 1,2-bis(diphenylphosphino)propane) by the same methods discussed earlier for the synthesis of $[HIPTN_3N]MoPMe_3$ or $[HIPTN_3N]MoPMe_3[Bar'_4]$. None of the backbone lengths, steric, or electronic variations provided conditions under which a bidentate phosphine complex was isolated or observed by 1H NMR spectroscopy. No complex in which the bis-phosphine was bound in a monodentate fashion was isolated from these reactions.

Steric Variations of $[N_3N]$ Phosphine Complexes

The bisphosphines used may be too sterically encumbering to efficiently bind and force the release of an amine arm from molybdenum in $[HIPTN_3N]MoH_2$. For this reason, smaller ligand frameworks were examined such as the C_s symmetric complexes $[(3,5-bis-CF_3)HIPT_2N_3N]MoCl^{25}$ and $[(TerPh)HIPT_2N_3N]MoCl$. For both of these complexes, when

PMe_3 was added to a CH_2Cl_2 solution containing NaBAR'_4 , the solution turned red and appeared to form the $[\text{L}]\text{MoPMe}_3[\text{BAR}'_4]$ ($\text{L} = (3,5\text{-bis-CF}_3)\text{HIPT}_2$ or $[(\text{TerPh})\text{HIPT}_2\text{N}_3\text{N}]$) complex as observed by ^1H and ^{19}F NMR spectroscopy. ^1H NMR spectrum resonances appear for PMe_3 and the backbone protons ($\text{NCH}_2\text{CH}_2\text{N}$) in both cases, with resonances similar to those observed for $[\text{HIPTN}_3\text{N}]\text{MoPMe}_3[\text{BAR}'_4]$. These complexes did not readily crystallize from pentane, heptane, or tetramethylsilane. The use of NaBPh_4 instead of NaBAR'_4 did not aid in their isolation. No suitable elemental analysis was ever obtained for these complexes. Furthermore, no bis-phosphine complexes with these C_s symmetric frameworks were isolated despite the reduced steric hinderance of the ligands.

Attempts to synthesize the much more sterically demanding $[\text{HTBTN}_3\text{N}]\text{MoPMe}_3$ ($\text{HTBT} = \text{HexaTertButylTerphenyl}$) complex was unsuccessful. The HTBT ligand²⁶ is presumably too sterically demanding to allow PMe_3 to bind to molybdenum.

$[\text{HIPTN}_3\text{N}]\text{MoCl}$ was reacted with other commercially available phosphines PMe_2Ph , PPhH_2 , and PPh_2Me in the presence of NaBAR'_4 . Due in part to the high boiling points of PMe_2Ph and PPh_2Me , clean product was not obtained, since it could not be separated from un-reacted phosphine. The reactions of $[\text{HIPTN}_3\text{N}]\text{MoCl}$ with phosphines are typically run in a significant excess of 5–6 equivalents or more to achieve a reasonable reaction rate.^{10,11} PMe_2Ph and PPhH_2 do appear to react with $[\text{HIPTN}_3\text{N}]\text{MoCl}$ as observed by a color change from orange to deep red. The crude ^1H and ^{19}F NMR spectra suggested the presence of a new compound as the paramagnetic resonances are similar to those found for $[\text{HIPTN}_3\text{N}]\text{MoPMe}_3[\text{BAR}'_4]$. No clean material was obtained from these reactions.

Tungsten Phosphine Complexes

[HIPTN₃N] tungsten complexes were synthesized in a similar manner to those of molybdenum described above. Since the nature of the coordination of PMe₃ and hydride in [HIPTN₃N]Mo(H)PMe₃ was unknown it may be possible to use ¹⁸³W satellites to determine the nature of the interactions.

[HIPTN₃N]WPMe₃BPh₄ (Figure 3.12) was synthesized by reacting [HIPTN₃N]WCl²⁷ with NaBPh₄ and an excess of PMe₃ in fluorobenzene. When the reaction was run in CH₂Cl₂ the desired product was not observed. Upon isolation from pentane a pink solid was obtained in 87% yield. The magnetic susceptibility of the pink solid was measured by the Evans Method and was consistent with S = 1.¹⁴

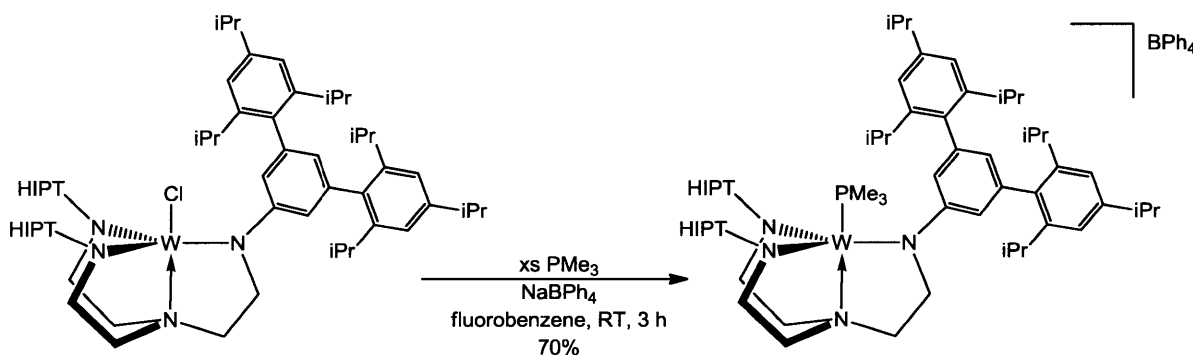


Figure 3.12: Synthesis of [HIPTN₃N]MoPMe₃[BPh₄]

Similar to [HIPTN₃N]MoPMe₃[BPh₄], [HIPTN₃N]WPMe₃[BPh₄] was sparingly soluble in pentane and the clean product was precipitated by cooling a hot pentane solution of [HIPTN₃N]WPMe₃[BPh₄]. Attempts to grow X-ray quality crystals in the same manner as described for [HIPTN₃N]MoPMe₃[BPh₄] were unsuccessful. The ¹H NMR spectrum of

[HIPTN₃N]WPM₃[BPh₄] contained four resonances. The resonance at δ 14.7 ppm corresponds to PMe₃, and three upfield resonances at δ -6.6 ppm, -30 ppm, and -69 ppm correspond to the backbone, methylene, and 4',6'-aryl resonances.

A cyclic voltamogram of [HIPTN₃N]WPM₃[BPh₄] was observed in fluorobenzene (Figure 3.13). The [HIPTN₃N]WPM₃/[HIPTN₃N]WPM₃⁺ redox couple was observed at -1.57 V versus ferrocene/ferrocinium, compared to the [HIPTN₃N]MoPMe₃/[HIPTN₃N]MoPMe₃⁺ redox couple which was found at -1.51 V versus ferrocene/ferrocinium. [HIPTN₃N]WNH₃⁺ was reduced irreversibly to [HIPTN₃N]WNH₃ at -2.06 V. The lack of reversibility presumably arises from the instability of [HIPTN₃N]W(NH₃).²⁷ In contrast {[HIPTN₃N]WPM₃}⁺ was a stable isolable product. A second oxidation of [HIPTN₃N]WPM₃[BPh₄] to [HIPTN₃N]WPM₃²⁺ at 0.25 V is not reversible.

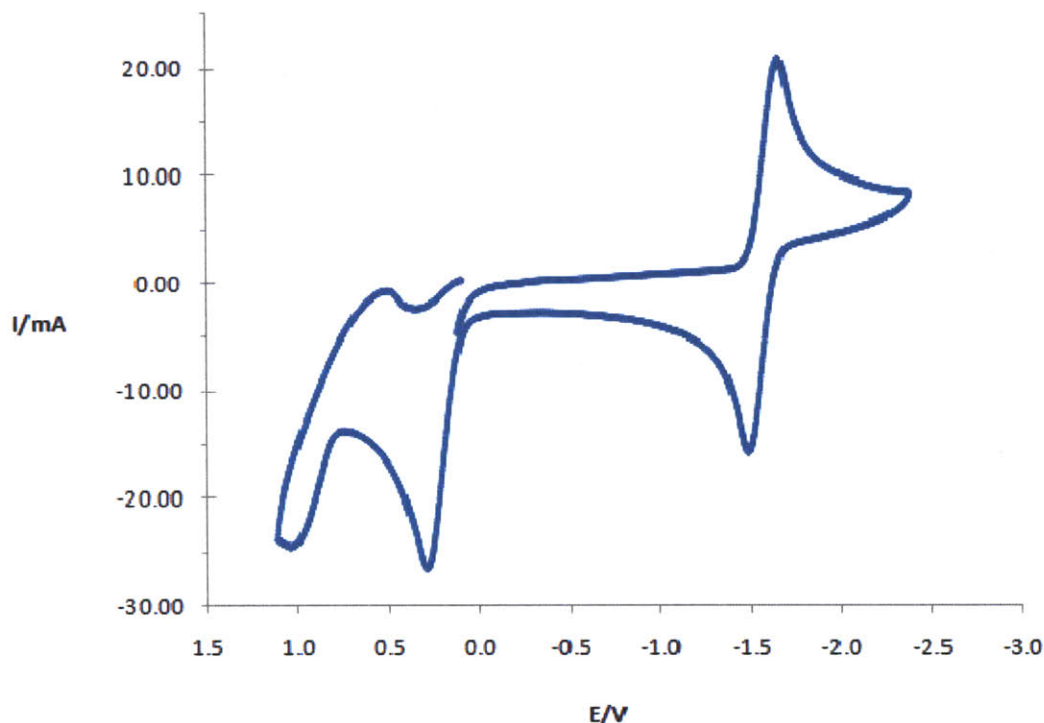


Figure 3.13: Cyclic voltammogram of 2mM [HIPTN₃N]MoPMe₃ in 0.1 M [TBA]BAR'₄/PhF. WE: Pt; scan rate: 200 mV/s vs. Fc/Fc⁺.

[HIPTN₃N]WN₂ (22 mM) did not react with an excess of PMe₃ (0.10 M) in toluene at 22 °C after two days. The N₂ is bound more strongly to tungsten²⁷ in [HIPTN₃N]WN₂, $\nu_{\text{NN}} = 1888 \text{ cm}^{-1}$ than to molybdenum in [HIPTN₃N]MoN₂, $\nu_{\text{NN}} = 1990 \text{ cm}^{-1}$.

[HIPTN₃N]WPMe₃ [BPh₄]^{*} could be reduced with both KC₈ and Cp₂Cr to yield [HIPTN₃N]WPMe₃ (Figure 3.14). Resonances observed by ¹H NMR spectroscopy were found at δ 19 ppm corresponding to the methyl groups of PMe₃, and δ -2 ppm and -50 ppm for the backbone methylene protons with the resonance corresponding to the *para* position of the aryl ring (2') relative to the metal at δ -27 ppm. When [HIPTN₃N]WPMe₃[BPh₄]^{*} was

treated with half an equivalent of Cp_2^*Cr both sets of resonances for $[\text{HIPTN}_3\text{N}]\text{WPM}_3[\text{BPh}_4]$ and $[\text{HIPTN}_3\text{N}]\text{WPM}_3$ was observed by ^1H NMR spectroscopy.

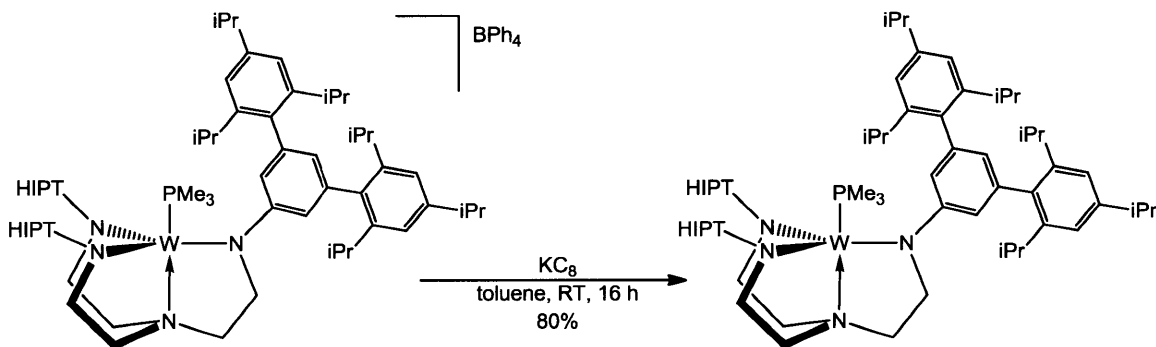


Figure 3.14: Synthesis of $[\text{HIPTN}_3\text{N}]\text{WPM}_3$

$[\text{HIPTN}_3\text{N}]\text{W}(\text{H})\text{PMe}_3$ (Figure 3.15) was synthesized from $[\text{HIPTN}_3\text{N}]\text{WPM}_3[\text{BPh}_4]$ through addition of a dilute THF solution of LiHBET_3 to a cold THF solution of $[\text{HIPTN}_3\text{N}]\text{WPM}_3[\text{BPh}_4]$, the same method employed to prepare $[\text{HIPTN}_3\text{N}]\text{Mo}(\text{H})\text{PMe}_3$ (Figure 3.9). Unfortunately, samples of $[\text{HIPTN}_3\text{N}]\text{W}(\text{H})\text{PMe}_3$ were contaminated with $[\text{HIPTN}_3\text{N}]\text{WPM}_3$ and BEt_3 . BEt_3 has a high boiling point (95 °C) and since $[\text{HIPTN}_3\text{N}]\text{W}(\text{H})\text{PMe}_3$ was also volatile BEt_3 could not be removed before $[\text{HIPTN}_3\text{N}]\text{W}(\text{H})\text{PMe}_3$ decomposed. Attempts to crystallize $[\text{HIPTN}_3\text{N}]\text{W}(\text{H})\text{PMe}_3$ from pentane only led to its decomposition and X-ray quality crystals could not be grown.

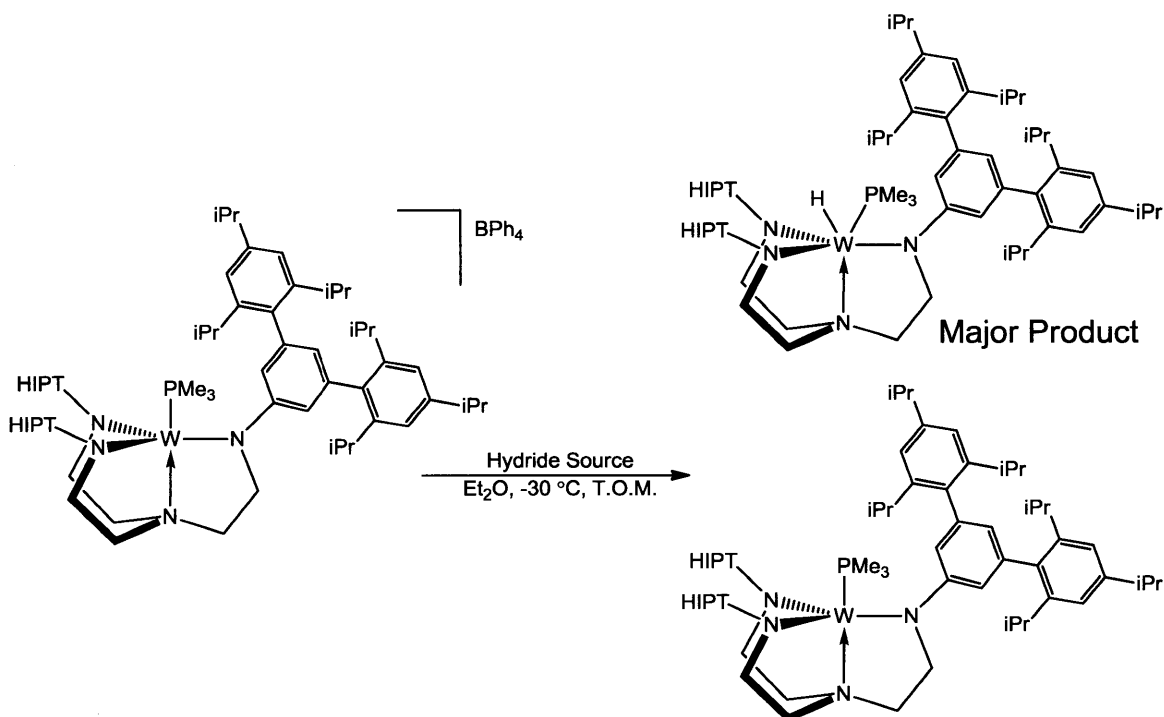


Figure 3.15: Synthesis of $[\text{HIPTN}_3\text{N}]\text{W}(\text{H})\text{PMe}_3$

In the mixture of $[\text{HIPTN}_3\text{N}]\text{W}(\text{H})\text{PMe}_3$ and $[\text{HIPTN}_3\text{N}]\text{WPMe}_3$ the resonance corresponding to the hydride of $[\text{HIPTN}_3\text{N}]\text{W}(\text{H})\text{PMe}_3$ was a doublet at δ 4.72 ppm (Figure 3.16) with a $J_{\text{PH}} = 119$ Hz. The hydride also exhibits a J_{WH} of 12.5 Hz. By comparison the $[\text{HIPTN}_3\text{N}]\text{WH}_3$ complex reported in the literature exhibits a J_{WH} of 24 Hz.²⁷ If LiDBEt₃ is employed, the resonance at δ 4.72 ppm disappears, but the rest of the spectrum remains the same. The resonance for $[\text{HIPTN}_3\text{N}]\text{W}(\text{H})\text{PMe}_3$ was further downfield than where it was observed for $[\text{HIPTN}_3\text{N}]\text{Mo}(\text{H})\text{PMe}_3$ (δ -1.10 ppm), but the J_{PH} values are similar. A ³¹P NMR spectrum shows a phosphorus resonance at δ -2.75 ppm which has a J_{WP} of 119 Hz. A proton coupled ³¹P NMR spectrum showed that the splitting of the $[\text{HIPTN}_3\text{N}]\text{W}(\text{H})\text{PMe}_3$

peak into a doublet in the ^1H NMR spectrum was from the phosphorus as a doublet appears at δ -2.75 ppm with a J_{PH} of 117 Hz.

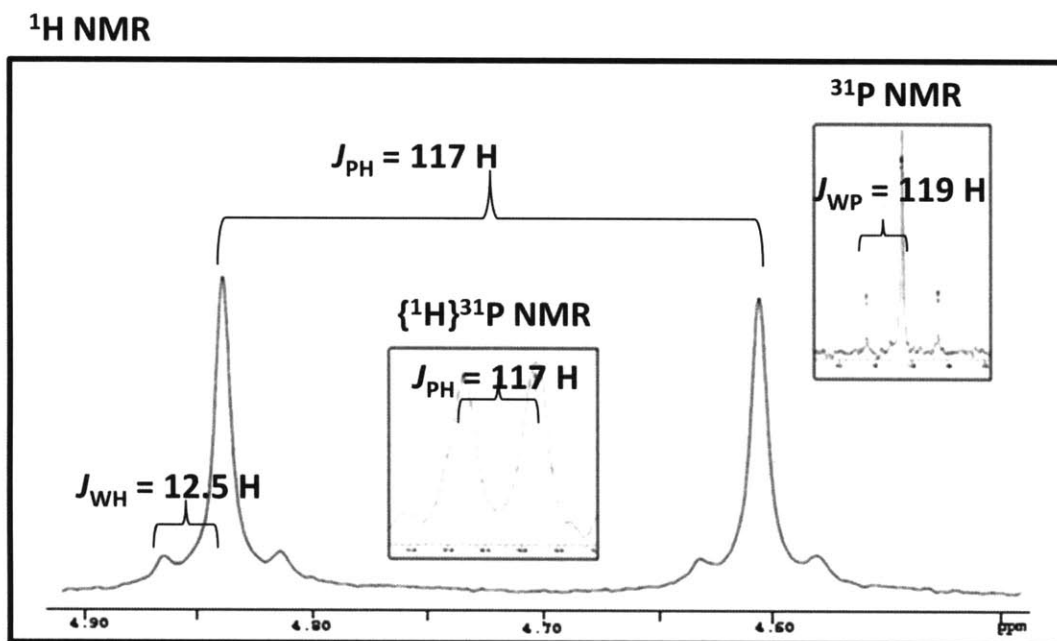


Figure 3.16: Selected Regions of ^1H and ^{31}P NMR Spectra for $[\text{HIPTN}_3\text{N}]\text{W}(\text{H})\text{PMe}_3$

Reactivity of Molybdenum and Tungsten Trimethylphosphine Complexes

After addition of $[\text{H}(\text{Et}_2\text{O})_2][\text{BAR}'_4]$ to $[\text{HIPTN}_3\text{N}]\text{MoPMe}_3$ a dramatic color change (red to green) was observed upon oxidation of $[\text{HIPTN}_3\text{N}]\text{MoPMe}_3$ (510 nm, with $\epsilon = 1657 \text{ M}^{-1}\text{cm}^{-1}$), to $[\text{HIPTN}_3\text{N}]\text{MoPMe}_3[\text{BAR}'_4]$ (630 nm, with $\epsilon = 865 \text{ M}^{-1}\text{cm}^{-1}$), and hydrogen gas was evolved (detected by GC). The ^1H and ^{19}F NMR spectra match with those of $[\text{HIPTN}_3\text{N}]\text{MoPMe}_3[\text{BAR}'_4]$ (Figure 3.17). The same reactivity was seen for $[\text{HIPTN}_3\text{N}]\text{WPMe}_3$. Similar reactivity was also observed by Peters with $\text{Si}(o\text{-C}_6\text{H}_4\text{PiPr}_2)_3\text{FeN}_2$. When an equivalent of $[\text{H}(\text{Et}_2\text{O})_2][\text{BAR}'_4]$ was added to $\text{Si}(o\text{-C}_6\text{H}_4\text{PiPr}_2)_3\text{FeN}_2$.

$C_6H_4PiPr_2)_3FeN_2$ 0.5 equivalents of H_2 were generated and $Si(o-C_6H_4PiPr_2)_3FeN_2[BAr'_4]$ resulted.²⁸

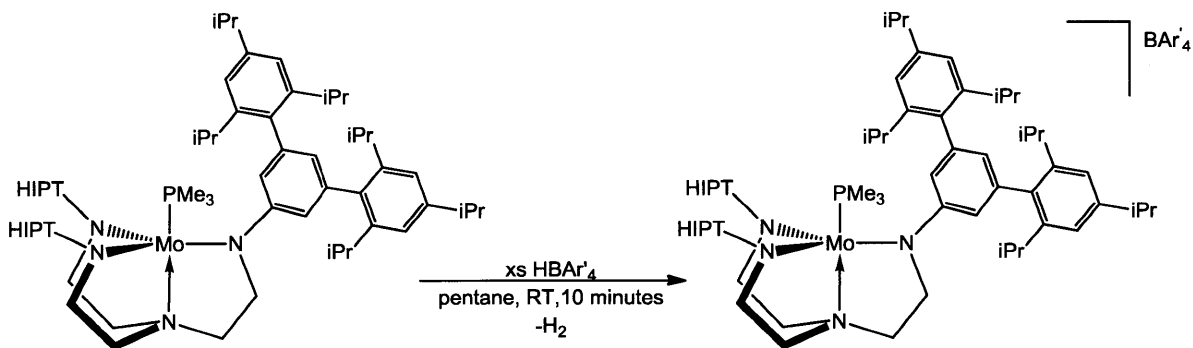


Figure 3.17: Oxidation of $[HIPTN_3N]MoPMe_3$ with $H(Et_2O)_2BAr'_4$

Suspecting that $[H(Et_2O)_2][BAr'_4]$ was too strong of an acid source for our purposes, other acid sources such as $[CollH][BAr'_4]$, $[N,N\text{-dimethylanilinium}][BAr'_4]$, $[Et_3NH][BAr'_4]$, and $[Et_3NH][OTf]$ were used. In each case only oxidation was observed.

When a stoichiometric amount of $B(C_6F_5)_3$ was employed $[HIPTN_3N]MoPMe_3[B(C_6F_5)_4]$ is formed according to 1H and ^{19}F NMR spectroscopy. The reaction was driven to completion using excess equivalents of $B(C_6F_5)_3$. Oxidation was not unexpected since $B(C_6F_5)_3$ can behave as an oxidant to give a radical anion.²⁹ The details of the oxidation of $[HIPTN_3N]MoPMe_3$ with $B(C_6F_5)_3$ are not well understood and were not clean. It should be noted that $B(C_6F_5)_3$ does not react with $[HIPTN_3N]MoN_2$, $[HIPTN_3N]MoN$ or $[HIPTN_3N]MoCl$. Similar results are obtained when $BF_3(Et_2O)$ was used. There was no reaction with BPh_3 , which is unsurprising due to its higher basicity compared to $BF_3(Et_2O)$ and $B(C_6F_5)_3$. Over the course of several days, a paramagnetic decomposition product became the predominant species in the 1H NMR spectrum. Addition of $MeOTf$ ($OTf =$

CF_3SO_3^-) and Me_3OPF_6 to $[\text{HIPTN}_3\text{N}]\text{MoPMe}_3$ both in stoichiometric proportions and in excess only led to decomposition.

$[\text{HIPTN}_3\text{N}]\text{MoNH}_3$ was oxidized by the same acid sources employed for oxidation of $[\text{HIPTN}_3\text{N}]\text{MoPMe}_3$ (Figure 3.17). One of the acid sources used was $[\text{CollH}][\text{BAR}'_4]$, which was commonly employed for catalytic reduction of dinitrogen to ammonia. Hydrogen formed during the catalytic reaction therefore could result through oxidation of $[\text{HIPTN}_3\text{N}]\text{MoNH}_3$ and other species to cationic species. Oxidation of both $[\text{HIPTN}_3\text{N}]\text{MoPMe}_3$ and $[\text{HIPTN}_3\text{N}]\text{MoNH}_3$ was slower (hours) when $[\text{CollH}][\text{BAR}'_4]$ was employed than when $[(\text{Et}_2\text{O})_2\text{H}][\text{BAR}'_4]$ was employed (minutes). The amount of hydrogen formed through oxidation of $[\text{HIPTN}_3\text{N}]\text{MoPMe}_3$ is likely to be negligible on the catalytic time scale.

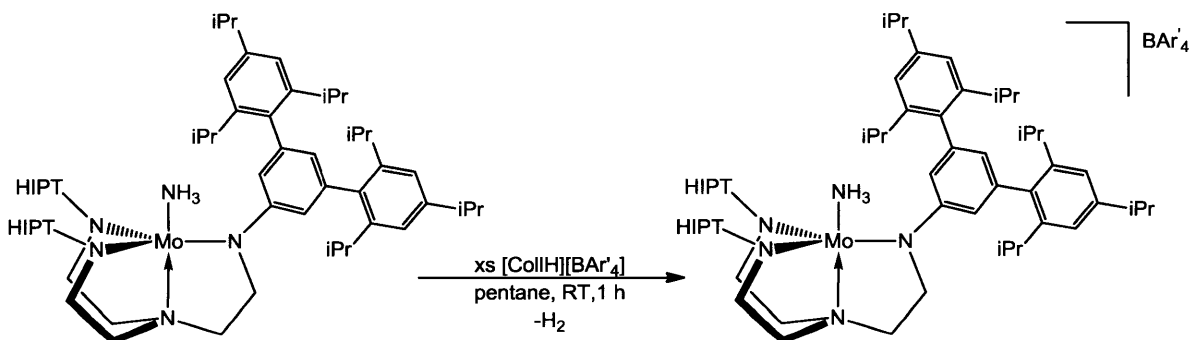


Figure 3.18: Oxidation of $[\text{HIPTN}_3\text{N}]\text{MoNH}_3$ with $[\text{H}(\text{Et}_2\text{O})_2][\text{BAR}'_4]$

Conclusions

$[\text{HIPTN}_3\text{N}]\text{MoPMe}_3$ was oxidized with strong acids. Since $[\text{HIPTN}_3\text{N}]\text{MoNH}_3$ was also oxidized by acids, during the oxidation of $[\text{HIPTN}_3\text{N}]\text{MoNH}_3$ some H₂ may be formed in this

manner during catalytic reduction of dinitrogen to ammonia. The instability of $[\text{HIPTN}_3\text{N}]\text{Mo}(\text{H})\text{PMe}_3$ was unfortunate. The rhenium phosphine hydrides were not reported as unstable under vacuum. Whether the instability of $[\text{HIPTN}_3\text{N}]\text{Mo}(\text{H})\text{PMe}_3$ is in any way relevant to the decomposition of $[\text{HIPTN}_3\text{N}]\text{MoH}_2$ described in Chapter 2 is unknown. Since $[\text{HIPTN}_3\text{N}]\text{Mo}(\text{H})\text{PMe}_3$ and $[\text{HIPTN}_3\text{N}]\text{MoH}_2$ are not stable, questions surrounding their reactivity and properties remain unanswered.

Experimental

General. Air and moisture sensitive compounds were manipulated utilizing standard Schlenk and dry-box techniques under a dinitrogen or argon atmosphere. All glassware was oven and/or flame dried prior to use. Pentane, diethyl ether, toluene, and benzene were purged with dinitrogen and passed through activated alumina columns. Benzene was additionally passed through a column containing copper catalyst. THF, heptane and tetramethylsilane were dried over Na/benzophenone, freeze-pump-thawed three times, and vacuum transferred. All dried and deoxygenated solvents were stored in a dinitrogen-filled glove box over molecular sieves or in Teflon[®] sealed glass solvent bombs. Molecular sieves (4 Å) and Celite were activated at 230 °C *in vacuo* over several days. BPh₃, B(C₆F₅)₃, AlEt₃, AlMe₃, PMe₃ (Strem), NaH, KH, NaBH₄, PPh₂Me, PMe₂Ph, LiHBET₃, NaHBET₃ (Aldrich), PH₃ (Electronic grade 99.9999% Aldrich) were used as received, unless indicated otherwise. KC₈, [HIPTN₃N]MoX,¹³ and [HIPTN₃N]WX¹² (X = H, Cl, N₂, NH₃) were prepared according to the published procedures or with slight modifications. All Mo and W complexes were stored under dinitrogen at -35 °C. ¹H, ¹³C, and ¹⁹F ³¹P NMR spectra were recorded on a Varian Mercury 300 and Varian Inova 500 spectrometers. ¹H and ¹³C NMR Spectra are referenced to the residual protons in solvent for ¹H or solvent in ¹³C s relative to tetramethylsilane (δ 0 ppm). ¹⁹F NMR spectra were referenced externally to fluorobenzene (δ -113.15 ppm upfield of CFC_l₃). ³¹P NMR spectra were referenced externally to H₃PO₄ (δ 0 ppm). Elemental analyses were performed by Midwest Microlabs, Indianapolis, Indiana, U.S.A.

Modified synthesis of [HIPTN₃N]MoPMe₃. In a 20 mL vial [HIPTN₃N]MoN₂ (320 mg, 0.19 mmol) was dissolved in 10 mL of pentane and an excess of PMe₃ (0.05 mL, 0.48 mmol) was added. The reaction mixture turned red after 30 minutes. The reaction was allowed to stir overnight, then the volatiles were removed *in vacuo* and the resultant red solid was crystallized from pentane, yield 171 mg (0.10 mmol, 52%). ¹H NMR (C₆D₆, 20 °C): δ 19.2 (br s, 9H, PMe₃), 15.8 (br s, 6H, NCH₂), 6.55 (s, 12H, 3,5,3'',5''-H), 2.43 (br septet, 6H, 4,4''-CHMe₂), 1.8 (br s, 36H, 2,6,2'',6''-CH(CH₃)₂), 0.94 (d, 36H, 4,4''-CH(CH₃)₂), 0.88 (br s, 15H, 2,6,2'',6''-CHMe₂ and 20-H), 0.55 (br s, 36H, 2,6,2'',6''-CH(CH₃)₂), -7.3 (br s, 6H, 4',6'-H), -25.9 (br s, 6H, NCH₂). Anal. Calcd. for C₁₁₇H₁₆₈MoN₄P: C, 79.91; H, 9.69; N, 5.46. Found: C, 79.50; H, 9.87; N, 5.06.

[HIPTN₃N]MoPMe[BAr'₄]. In a 20 mL vial [HIPTN₃N]MoCl (100 mg, 0.06 mmol) was added to NaBAr'₄ (52 mg, 0.06 mmol) in 10 mL of methylene chloride. An excess of 0.05 mL (0.48 mmol) of PMe₃ was added and the reaction mixture was stirred for 3 hours, turning green after a few minutes. The volatiles were then removed *in vacuo* and the solid was extracted with pentane and filtered through Celite. A green solid was then crystallized from the pentane solution, yield 106 mg (0.41 mmol, 70%). ¹H NMR (C₆D₆, 20 °C): δ 8.24 (br s, 8H, C₆H₃-3,5-(CF₃)₂), 7.58 (br s, 4H C₆H₃-3,5-(CF₃)₂), 7.11 (br s, 12H, 3,5,3'',5''-H), 2.0 (br m, 18H 2,2'',4'',4,6,6''-CHMe₂), 1.34 (br s, 36H, 4,4''-CH(CH₃)₂), 1.22 (br s, 72H, 2,6,2'',6''-CH(CH₃)₂), -10.3 (br s, 9H, PMe₃), -17 (br s, 6H, NCH₂), -96 (br s, NCH₂); ¹⁹F NMR (C₆D₆, 20 °C) δ -62.3 (s, C₆H₃-3,5-(CF₃)₂). Anal. Calcd. for C₁₄₉H₁₈₀ N₄BF₂₄MoP: C, 68.29; H, 6.92; N, 2.38. Found: C, 67.23; H, 6.93; N, 2.38.

[HIPTN₃N]MoPMe[BPh₄]. In a 20 mL vial [HIPTN₃N]MoCl (124 mg, 0.07 mmol) was added to NaBPh₄ (30 mg, 0.09 mmol) in 10 mL of methylene chloride. An excess of PMe₃ (0.05 mL 0.483 mmol) was added and the reaction mixture was stirred for 3 hours, turning green after a few minutes. The volatiles were then removed *in vacuo* and the solid was extracted with pentane and filtered through Celite. A green solid was then recrystallized from the pentane solution, yield 105 mg (0.05 mmol 70%). ¹H NMR (C₆D₆, 20 °C): δ 7.81 (br s, 20H, B(C₆H₅)₄), 7.11 (br s, 12H, 3,5,3'',5''-H), 3.1 (br m, 18H, 2,2'',4'',4,6,6''-CHMe₂), 1.35 (br s, 36H, 4,4''-CH(CH₃)₂), 1.2 (br s, 72H, 2,6,2'',6''-CH(CH₃)₂), -9.1 (br s, 9H PMe₃), -19 (br s, 6H NCH₂), -99 (br s, 6H, NCH₂). Anal. Found (Calcd.) for C₁₄₁H₁₈₈ N₄BMoP: C, 81.55; H, 9.25; N, 2.88. Found: C, 80.90; H, 9.12; N, 2.70.

[HIPTN₃N]Mo(H)PMe₃. In a 20 mL vial [HIPTN₃N]MoH (170 mg, 0.10 mmol) was dissolved in 5 mL of pentane. An excess of PMe₃ (0.48 mmol, 0.05 mL) was added and the solution immediately turned purple upon mixing. The reaction was allowed to stir for an additional 30 minutes, and the volatiles were removed *in vacuo*. The resultant solid was dissolved in pentane and filtered through Celite. Crystallization from pentane gave a purple solid, yield 135 mg (0.08 mmol, 76 %): ¹H NMR (C₆D₆, 20 °C): δ 7.17 (s, 12H, 3,5,3'',5'' Ar-H), 7.02 (d, *J*_{HH} = 1.2 Hz, 6H, 4',6'Ar-H), 6.69 (br t, 3H, 2' Ar-H), 3.67 (br t, 6H, NCH₂CH₂), 3.07 (sept, *J*_{HH} = 6.9 Hz, 12H, 2,6,2'',6'' -CHMe₂), 2.91 (sept, *J*_{HH} = 6.9 Hz, 6H, NCH₂CH₂), 2.28 (br t, 6H, NCH₂CH₂), 1.35 (d, *J*_{HH} = 6.9 Hz, 36H, 4,4''-CH(CH₃)₂), 1.22 (d, *J*_{HH} = 6.9 Hz, 36H, 2,6,2'',6''-CH(CH₃)₂), 1.14 (d, *J*_{HH} = 6.9 Hz, 36H, 2,6,2'',6''-CH(CH₃)₂), 1.01 (d, *J*_{PH} = 8.4 Hz, 9H, PMe₃), -1.19 (d, *J*_{PH} = 111 Hz, MoH). ³¹P NMR (C₆D₆, 20 °C) δ 15.5 (d, PMe₃)

[(HIPTN₃N)WPM₃][BPh₄]. In a 20 mL vial [HIPTN₃N]WCl (125 mg, 0.07 mmol) was added to 5 mL of CH₂Cl₂ and NaBPh₄ (33 mg, 0.10 mmol). After 20 minutes the solution turned pink. The volatiles were then removed *in vacuo* and the resultant solid was extracted with toluene then filtered through Celite. The volatiles removed *in vacuo* and the resultant solid rinsed with pentane to give a pink solid, yield 113 mg (0.05 mmol, 77 %): ¹H NMR (C₆D₆, 20 °C) δ 14.7 (s, 9H, PMe₃), 7.7 (br s, 12H, 3,5,3'',5''-H), 5.2 (br s, 3H, 2'-H), 3.7 (br septet, 6H, 4'',4-CHMe₂) 2.7 (br septet, 12H, 2,2'',6,6''-CHMe₂) 1.1 (br m, 108H, 2,2'',4,4'',6,6''-CH(CH₃)₂), -6.7 (br s, 6H, 4',6'H), -30 (br s, 6H, NCH₂), -68 (br s, 6H, NCH₂). Anal. Calcd. for C₁₄₁H₁₈₈N₄PBW: C, 78.23; H, 8.75; N, 2.59. Found: C, 77.87; H, 8.73; N, 2.66.

[HIPTN₃N]WPM₃. In a 20 mL vial [HIPTN₃N]WPM₃[BPh₄] (50 mg, 0.02 mmol) was dissolved in toluene and KC₈ (4 mg, 0.03 mmol) was added. The solution turned orange within 30 minutes but the reaction was allowed to stir overnight for 16 hours. The toluene solution was then filtered through Celite and the volatiles removed *in vacuo* to give an orange solid, yield 35 mg (0.02 mmol, 80%): ¹H NMR (C₆D₆, 20 °C) δ 19.0 (s, 9H PMe₃), 7.8 (br s, 12H, 3,5,3'',5''-H) 5.2 (br s, 3H, 2'-H), 3.2 (br m, 18H, 2,2'',4,4'',6,6''-CH(CH₃)₂) 2.7 (br s, 2,2'',4,4'',6,6''-CH(CH₃)₂), -2.6 (br s, 6H, NCH₂), -27.4 (br s, 6H, 4',6'H), -51 (br s, 6H, NCH₂). Anal. Calcd. for C₁₁₇H₁₆₈N₄PW; C, 75.90; H, 9.06; N, 3.14. Found: C, 76.15; H, 9.18; N, 3.04.

In situ preparation of [HIPTN₃N]W(H)PMe₃. In a 20 mL vial [HIPTN₃N]WPM₃[BPh₄] (30 mg, 0.02 mmol) was added to 10 mL of THF then cooled to -35° C. A solution of 1 M LiHBEt₃ was diluted 100:1 in THF and cooled. A 10 mM solution of LiHBEt₃ (1.5 mL,

0.02 mmol) in THF was added drop-wise with a syringe to a stirring solution of cold [HIPTN₃N]WPM_e[BPh₄] in THF. The solution slowly turned a dark red-purple color and the volatiles were gently removed. The resultant solid was then dissolved in C₆D₆ for NMR spectroscopy studies. ¹H NMR (C₆D₆, 20 °C): δ 7.83, (s, 12H, 3,5,3'',5'' Ar-H), 7.02 (d, *J*_{HH} = 1.2 Hz, 6H, 4',6'Ar-H), 6.69 (br t, 3H, 2' Ar-H), 4.74 (d, *J*_{PH} = 117 Hz, MoH). 3.67 (br t, 6H, NCH₂CH₂), 3.07 (sept, *J*_{HH} = 6.9 Hz, 12H, 2,6,2'',6'' -CHMe₂), 2.91 (sept, *J*_{HH} = 6.9 Hz, 6H, NCH₂), 2.28 (br t, 6H, NCH₂), 1.35 (d, *J*_{HH} = 6.9 Hz, 36H, 4,4''-CH(CH₃)₂), 1.22 (d, *J*_{HH} = 6.9 Hz, 36H, 2,6,2'',6''-CH(CH₃)₂), 1.14 (d, *J*_{HH} = 6.9 Hz, 36H, 2,6,2'',6''-CH(CH₃)₂), 1.01 (d, *J*_{PH} = 8.4 Hz, 9H, PMe₃), ³¹P NMR (C₆D₆, 20 °C) δ -2.75 (s, PMe₃). ³¹P{¹H} NMR (C₆D₆, 20 °C) δ -2.75 ppm (d, PMe₃).

References

1. (a) Hidai M.; Tominari K.; Uchida Y.; Misono A. *Chem. Commun.* **1969**, 814. (b) Hidai M.; Tominari K.; Uchida Y.; Misono A. *Chem. Commun.* **1969**, 1392. (c) Hidai, M.; Mizobe, Y. *Chem. Rev.* **1995**, *95*, 1115. (d) Hidai, M. *Coord. Chem. Rev.* **1999**, *185*, 99.
2. Chatt, J.; Dilworth, J. R.; Richards, R. L. *Chem. Rev.* **1978**, *78*, 589.
3. Richards, R. L. *Coord. Chem. Rev.* **1996**, *154*, 83.
4. Chatt, J.; Leigh, G. J. *Chem. Soc. Rev.* **1972**, *1*, 121.
5. Galindo, A.; Gutierrez, E.; Monge, A.; Paneque, M.; Pastor, A.; Perez, P. J.; Rogers, R. D.; Carmona E. *J. Chem. Soc., Dalton Trans.* **1995**, 3801.
6. Pickett, C. J.; Talarmin, J. *Nature* **1985**, *317*, 652.
7. Piro, N. A.; Cummins, C. C. *J. Am. Chem. Soc.* **2008**, *130*, 9524.
8. Spinney, H. A.; Piro, N. A.; Cummins, C. C. *J. Am. Chem. Soc.* **2009**, *131*, 16233.
9. Mösch-Zanetti N. C.; Schrock, R. R.; Davis W. M.; Wanninger K. Seidel S. W.; O'Donoghue, M. B. *J. Am. Chem. Soc.* **1997**, *119*, 11037.
10. Reid, S. M.; Neuner B.; Schrock, R. R.; Davis W. M. *Organometallics* **1998**, *17*, 4077.
11. Hetterscheid, D. G. H.; Hanna, B. S.; Schrock R. R. *Inorg. Chem.* **2009**, *48*, 8569.
12. Brookhart, M; Grant, B.; Volpe, A. F. Jr. *Organometallics* **1992**, *11*, 3920.
13. Yandulov, D. V.; Schrock, R.R., *Inorg. Chem.* **2005**, *44*, 1103.
14. Evans, D. F. J. *Chem. Soc.* **1959**, 2003.

-
15. Schrock, R. R.; Tonzetich, Z. J.; Lichtscheidl, A. G.; Müller, P.; Schattenmann, F. J. *Organometallics* **2008**, *27*, 3986.
 16. Brookhart, M.; Cox, K.; Cloke, F. G. N.; Green, J. C.; Green, M. L. H.; Hare, P. M.; Bashkin, J.; Derome, A. E.; Grebenik, P. D. *J. Chem. Soc., Dalton Trans.* **1985**, 423.
 17. Baya M.; Dub, P. A.; Houghton, J.; Daran, J. C.; Belkova, N. V.; Shubina, E. S.; Epstein, L. M.; Lledós, A.; Poil, R. *Inorg. Chem.* **2009**, *48*, 209.
 18. Yandulov, D. V.; Schrock, R. R. *Science* **2003**, *301*, 76.
 19. A search of the Cambridge Structural database gives 354 examples.
 20. Frenking, G.; Wichmann, K.; Frohlich, N.; Grobe, J.; Golla, W.; Le Van, V.; Krebs, B.; Lage, M. *Organometallics* **2002**, *21*, 2921.
 21. Vogel, U.; Scheer, M. Z. *Anorg. Allg. Chem.* **2001**, *627*, 1593.
 22. Huttner, G.; Schelle, S. *J. Cryst. Mol. Struct.* **1971**, *1*, 69.
 23. Huttner, G.; Schelle, S. *J. Organomet. Chem.* **1973**, *47*, 383.
 24. Fischer, O. E.; Louis, E.; Bathelt, W.; Müller, J. *Chem. Ber.* **1969**, *102*, 2547.
 25. Weare, W. W.; Schrock, R. R.; Hock, A. S.; Müller, P. *Inorg. Chem.* **2006**, *45*, 9185.
 26. Ritleng, V.; Yandulov, D. V.; Weare, W. W.; Schrock, R. R.; Hock, A. R.; Davis, W. M. *J. Am. Chem. Soc.* **2004**, *126*, 6150.
 27. Yandulov, D. V.; Schrock, R. R. *Can. J. Chem.* **2005**, *83*, 34.
 28. Lee, Y.; Mankad, N. P.; Peters, J. C. *J. Nat. Chem.* **2010**, *2*, 558.
 29. Kwaan, J. R.; Harlan, C. J.; Norton J. R. *Organometallics*, **2001**, *20*, 3818.

Chapter 4

Symmetric and C_s symmetric $[N_3N]$ Complexes

Chapter 4. Symmetric and C_s symmetric [N₃N] complexes**Introduction**

The syntheses of ligands based upon the [N₃N]Mo (N₃N = [(RNCH₂CH₂)N]³⁻) framework have been of interest in the Schrock group for many years.¹ Prior to the discovery of the reduction of dinitrogen to ammonia using [HIPTN₃N]Mo (HIPT = 2,4,6,2'',4'',6''-hexaisopropyl-1,1':3',1''-terphenyl), many steric and electronic variations of the N₃N ligand framework were synthesized.^{1,2,3} With the discovery that [HIPTN₃N]Mo complexes catalytically reduce dinitrogen to ammonia,⁴ variations of the terphenyl groups of the [N₃N] ligands were synthesized, including HTBT (HexaTertButylTerphenyl) and HMT (HexaMethylTerphenyl).⁵ Neither of these systems proved to catalytically reduce dinitrogen to ammonia. The only symmetric terphenyl ligand system, other than [HIPTN₃N], that was catalytically successful employed Tris(2'-bromo-2,4,6,2'',4'',6''-hexaisopropyl-1,1':3',1''-terphenyl)ethyl)amine (*p*BrHIPTN₃N), which yielded 7.1 equivalents of ammonia. *p*BrHIPTN₃N is electron withdrawing compared to HIPT and to synthesize an electron donating analogue for comparison was desired. An electron donating ligand should promote the exchange of NH₃ for N₂ and increase the turnover rate of the system. Therefore, *p*MeOHIPTN₃N (Tris(2'-methoxy-2,2'',4,4'',6,6''-hexaisopropyl-1,1':3',1''-terphenyl)ethyl)amine) was investigated.

Significant changes in the steric nature of the [HIPTN₃N] framework are detrimental to the catalytic activity of the system. Making small changes to the [HIPTN₃N] framework, numerous C_s symmetric ligand systems were synthesized. These C_s symmetric ligands consisted of two HIPT groups on two amines and a third aryl group was added to the third

amine, which could be varied.⁶ With one exception, [(TRIP)HIPT₂N₃N]Mo (TRIP = 1,3,5-triisopropylbenzene) none of these C_s symmetric systems was catalytic with respect to producing ammonia from dinitrogen.⁶ By retaining a substituted mono-aryl group on the third amine, the ligand is not as sterically demanding as [HIPTN₃N]. We wanted to continue to explore unsymmetric ligands with a terphenyl substituent that was sterically smaller than HIPT but not as small as those previously employed.

Results and Discussion

Synthesis of C_s Symmetric Ligands

The synthesis of C_s symmetric ligands requires forming a di-substituted TREN (TREN = N(CH₂CH₂NH₂)₃) ligand. Two equivalents of HIPTBr were coupled to TREN using a palladium cross-coupling reaction. The success of this reaction results from the significantly slower cross-coupling of the third aryl group compared to the first two couplings.⁵ H₄[HIPT₂N₃N] can be obtained in a 73% yield after silica gel column chromatography and crystallization. Published methods for isolation of H₄[HIPT₂N₃N] employ the pre-treatment of the silica gel with Et₃N, which allowed a 10:1 toluene:THF mixture to elute H₄[HIPT₂N₃N]. Ethyl acetate can be used to elute H₄[HIPT₂N₃N] once HIPTBr and H₃[HIPTN₃N] are removed. The resultant yellow solid, obtained upon removal of ethyl acetate *in vacuo*, was purified further by crystallization from acetone to yield a white solid in 73% yield. The use of THF to isolate H₄[HIPT₂N₃N], as published,⁶ leads to the contamination of H₄[HIPT₂N₃N] with BHT (butylated hydroxytoluene). BHT is commonly

used as a stabilizer for anhydrous THF and is difficult to remove from the product. The majority of the unrealized yield was recovered as $H_3[HIPT_3N_3N]$ or $HIPTBr$.

Addition of terphenyl bromide to the third amine was achieved by published methods.⁷ The desire was to increase the steric bulk of the C_s symmetric systems from the mono-aryl ligands originally used to a *meta*-terphenyl ligand such as 3,5-diphenylbromobenzene ($TerPhBr$). Other terphenyl groups were attempted to be incorporated into C_s symmetric ligands, (HMT, HTBT), however, the isolation of the molybdenum complexes with these ligands proved low yielding, (< 10%), and the complexes were not explored in depth.

$TerPhBr$ can be coupled with $H_4[HIPT_2N_3N]$ using a palladium cross-coupling reaction to give $H_3[(TerPh)HIPT_2N_3N]$ in 63% isolated yield (Figure 4.1).

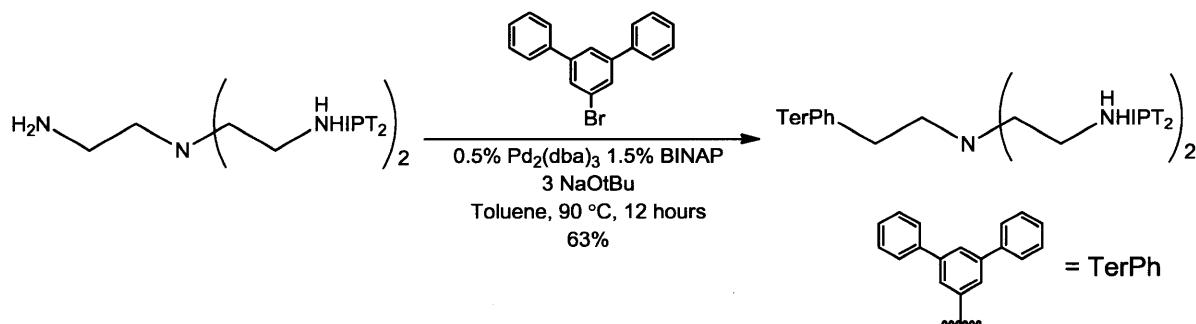


Figure 4.1: Synthesis of $H_3[(TerPh)HIPT_2N_3N]$

A silica gel column is required to separate the un-reacted $H_4[HIPT_2N_3N]$ and excess $TerPhBr$ from $H_3[(TerPh)HIPT_2N_3N]$. Un-reacted $H_4[HIPT_2N_3N]$ can be recovered by eluting the column with ethyl acetate. The 1H NMR spectrum of $H_3[(TerPh)HIPT_2N_3N]$ contains a broad resonance around δ 3.75 ppm corresponding to $CH_2CH_2NH(TerPh)$. A methine resonance appears at δ 3.13, and another methine resonance appears at 2.82 ppm

which overlaps with CH_2CH_2NH . The aryl resonances for the 2',6' protons of HIPT and TerPh are separated into two sets of inequivalent resonances at δ 6.44 and 6.48 ppm.

Synthesis of $[(\text{TerPh})\text{HIPT}_2\text{N}_3\text{N}]\text{MoCl}$ Complexes

Using $H_3[(\text{TerPh})\text{HIPT}_2\text{N}_3\text{N}]$, TREN based molybdenum complexes were synthesized. $[(\text{TerPh})\text{HIPT}_2\text{N}_3\text{N}]\text{MoCl}$ (Figure 4.2) is a common precursor to various catalytic intermediates, and can be stored for months at $-30\text{ }^\circ\text{C}$ under a dinitrogen atmosphere. To synthesize $[(\text{TerPh})\text{HIPT}_2\text{N}_3\text{N}]\text{MoCl}$, $H_3[(\text{TerPh})\text{HIPT}_2\text{N}_3\text{N}]$ was stirred with one equivalent of $\text{MoCl}_4(\text{THF})_2$ in THF (Figure 4.2). Ligand coordination to molybdenum was observed when $\text{MoCl}_4(\text{THF})_2$, which was insoluble in THF, was taken into solution. After $\text{MoCl}_4(\text{THF})_2$ coordinates to the $H_3[(\text{TerPh})\text{HIPT}_2\text{N}_3\text{N}]$, 3.1 equivalents of $\text{LiN}(\text{TMS})_2$ are added to deprotonate the ligand to form $[(\text{TerPh})\text{HIPT}_2\text{N}_3\text{N}]\text{MoCl}$ (Figure 4.2). Following crystallization from pentane or tetramethylsilane, $[(\text{TerPh})\text{HIPT}_2\text{N}_3\text{N}]\text{MoCl}$ is obtained as a red solid in 42% yield.

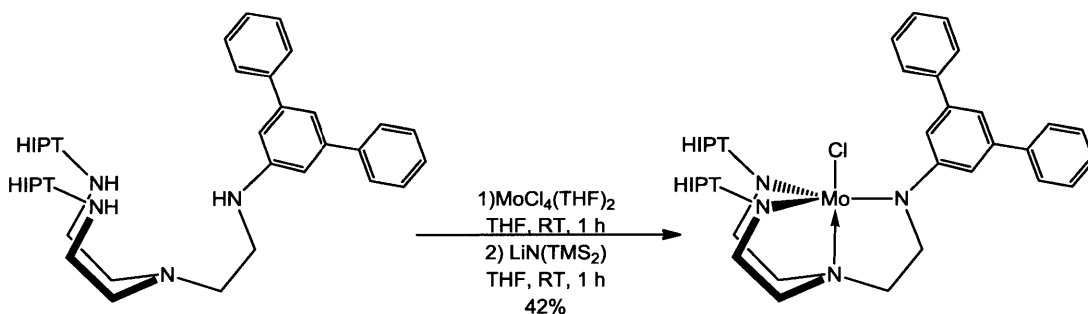


Figure 4.2: Synthesis of $[(\text{TerPh})\text{HIPT}_2\text{N}_3\text{N}]\text{MoCl}$.

$[(\text{TerPh})\text{HIPT}_2\text{N}_3\text{N}]\text{MoCl}$ is a paramagnetic high spin Mo(IV) complex. The broad resonances observed by ^1H NMR spectroscopy at δ -13, -19, and -24 ppm correspond to a set of $\text{N-CH}_2\text{CH}_2$ protons, and another set appears at δ -73 and -83 ppm. The two resonances at δ -19 and -24 ppm are broad and overlap significantly. The resonance at δ -13 ppm and the two overlapping resonances at δ -19 and -24 ppm taken together are in a 1:2 ratio, respectively, which is consistent with a C_s symmetric structure. The resonances at δ -73 and -83 ppm are also in a 1:2 ratio respectively because the resonance at -83 ppm does not split into two distinct resonances. The lack of diastereotopic splitting is not uncommon for resonances that are the furthest upfield in our C_s symmetric ligands.

$[\text{HIPT}_2(\text{TerPh})\text{N}_3\text{N}]\text{MoN}$ (Figure 4.3) was a convenient complex to use in the investigation of the catalytic cycle of the reduction of dinitrogen to ammonia, due to its superior stability compared to other intermediates. The d^0 Mo(VI), $[\text{HIPT}_2(\text{TerPh})\text{N}_3\text{N}]\text{MoN}$, can be synthesized and isolated cleanly on small scales by treating $[\text{HIPT}_2(\text{TerPh})\text{N}_3\text{N}]\text{MoCl}$ with TMSN_3 in toluene and heating the solution to $90\text{ }^\circ\text{C}$ for 16 hours. Crystallization from pentane or tetramethylsilane affords a yellow solid in 69% yield. Characteristic resonances for $[(\text{TerPh})\text{HIPT}_2\text{N}_3\text{N}]\text{MoN}$ were observed in the ^1H NMR spectrum.

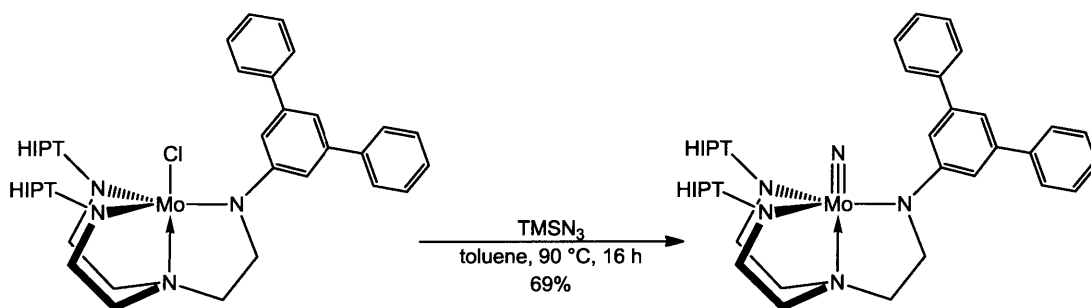
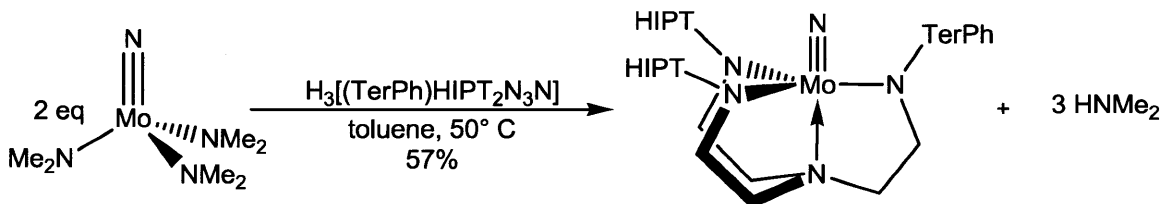


Figure 4.3: Synthesis of [(TerPh)HIPT₂N₃N]MoN

The synthetic route for the synthesis of $[N_3N]MoN$ directly from ligand described in Chapter 2, can also be used to synthesize $[HIPT_2(TerPh)N_3N]MoN$. Starting from $H_3[(TerPh)HIPT_2N_3N]$ the molybdenum nitride can be synthesized using $NMo(NMe_2)_3$. When two equivalents of $NMo(NMe_2)_3$ were combined with $H_3[HIPT_2(TerPh)N_3N]$ in a toluene or benzene solution and heated to 60 °C for 12 hours (Figure 4.4), $[(TerPh)HIPT_2N_3N]MoN$ was synthesized in 63% yield as a yellow solid. The isolated yield of $[(TerPh)HIPT_2N_3N]MoN$ from $NMo(NMe_2)_3$ and $H_3[(TerPh)HIPT_2N_3N]$ was lower than when employing $TMSN_3$ from $[HIPT_2(TerPh)N_3N]MoCl$, but the route employing $NMo(NMe_2)_3$ is more efficient with regard to ligand due to the low isolated yield for $[(TerPh)HIPT_2N_3N]MoCl$.

**Figure 4.4: Alternative Nitride Synthesis of [(TerPh)HIPT₂N₃N]MoN**

Molybdenum nitrides are the typical catalytic intermediate employed for catalytic reactions in our group. Upon performing two catalytic experiments as described by Yandulov⁴ with $[(TerPh)HIPT_2N_3N]MoN$ an average of 0.61 equivalents of ammonia was produced. One equivalent of ammonia is expected from the nitride so when less than one

equivalent of ammonia is generated by the complex, it was apparent that no ammonia was being synthesized from N_2 . The lack of catalytic activity for $[(\text{TerPh})\text{HIPT}_2\text{N}_3\text{N}]\text{MoN}$ was thought to be due to the less sterically demanding nature of TerPh compared to HIPT. The lack of steric protection allows for the decomposition of catalytic intermediates, before the system was able to reduce a measurable amount of atmospheric N_2 .

When $[(\text{TerPh})\text{HIPT}_2\text{N}_3\text{N}]\text{MoN}$ was treated with one equivalent of $[(\text{Et}_2\text{O})_2\text{H}][\text{BAR}'_4]$, ($[\text{BAR}'_4] = [\text{B}[3,5-(\text{CF}_3)_2\text{C}_6\text{H}_3]_4]^-$)⁸ in a $-30\text{ }^\circ\text{C}$ diethyl ether solution the solution turns deep red (Figure 4.5). A red solid is obtained by crystallization from pentane in 67% yield. A ^{19}F NMR spectrum of $\{[(\text{TerPh})\text{HIPT}_2\text{N}_3\text{N}]\text{MoNH}\}[\text{BAR}'_4]$ shows a single resonance at $\delta -62$ ppm consistent with the presence of a coordinating $[\text{BAR}'_4]^-$. A resonance in the ^1H NMR spectrum that integrates to one proton appears at $\delta 6.5$ ppm which corresponds to the NH proton, which is consistent with other compounds of this type.^{6,9} The methine resonances are also shifted from $\delta 2.85$ and 2.00 ppm to 2.86 and 2.70 ppm as observed by ^1H NMR spectroscopy.

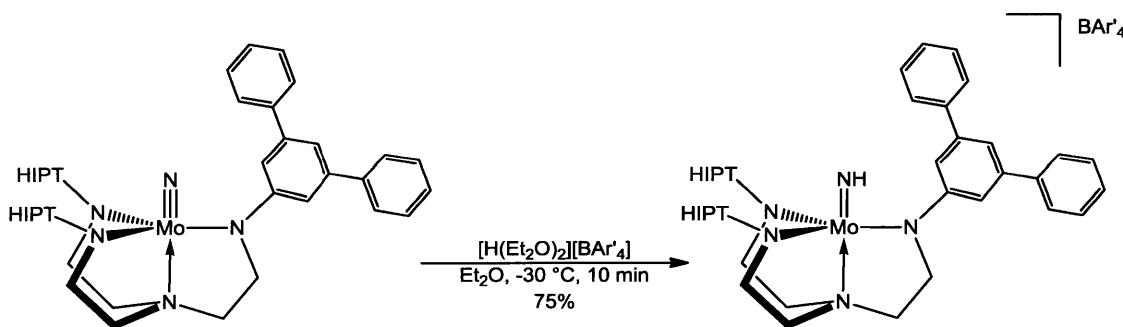


Figure 4.5: Synthesis of $[(\text{TerPh})\text{HIPT}_2\text{N}_3\text{N}]\text{MoNH}[\text{BAR}'_4]$

$\{[(\text{TerPh})\text{HIPT}_2\text{N}_3\text{N}]\text{MoNH}_3\}[\text{BAR}'_4]$ can be synthesized from $[(\text{TerPh})\text{HIPT}_2\text{N}_3\text{N}]\text{MoCl}$ using NaBAR'_4 and ammonia gas (Figure 4.6). The ammonia gas is dried over sodium before

being introduced to a CH_2Cl_2 solution of $[(TerPh)HIPT_2N_3N]MoCl$ and $NaBAR'_4$. After the reaction is allowed to proceed for two hours, the volatiles are removed *in vacuo* and $[(TerPh)HIPT_2N_3N]MoNH_3[BAR'_4]$ is crystallized from pentane as a red solid in 74% yield. A ^{19}F NMR spectrum contains a resonance for $[BAR'_4]^-$ at δ -62 ppm. Characteristic resonances for the backbone protons are observed at δ -22 ppm and -107 ppm.

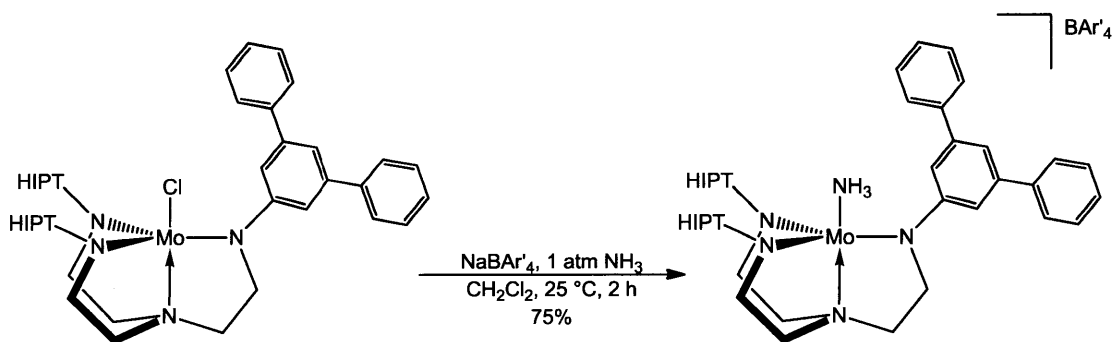


Figure 4.6: Synthesis of $[(TerPh)HIPT_2N_3N]MoNH_3[BAR'_4]$

Introduction of N_2 to the $[(TerPh)HIPT_2N_3N]Mo$ complex was achieved by reducing $[(TerPh)HIPT_2N_3N]MoCl$ under an N_2 atmosphere. Molybdenum chlorides can be reduced by a variety of reducing agents to give anionic N_2 complexes. Since the N_β carries a formal negative charge the metal center remains unchanged with respect to its oxidation state (Mo(IV)). The Mo(IV) center becomes low spin and the resulting complexes are diamagnetic. The metal center can then be reduced to Mo(III) by the use of an oxidizing agent which oxidizes the N_2 anion and creates a neutral Mo(III)(N_2) complex.

When a 0.5% Na/Hg amalgam was added to $[(TerPh)HIPT_2N_3N]MoCl$ in THF, a green solution resulted within minutes, and was allowed to react for an additional hour yielding $[(TerPh)HIPT_2N_3N]MoN_2Na(THF)_x$ (Figure 4.7). Upon removing THF *in vacuo* the

product turned purple. The purple solid was crystallized from pentane and was isolated in 65% yield. When THF was added to the purple solid, the color returned to green. The color change from green to purple and back suggests that THF coordination was responsible for the green color.

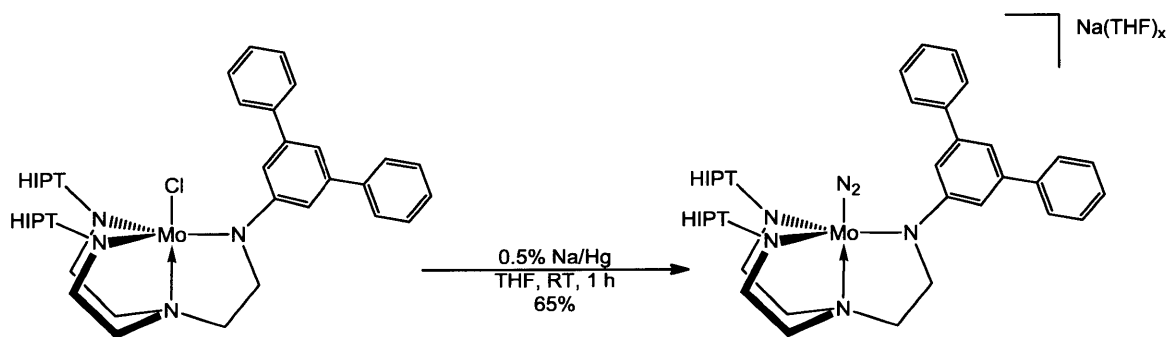


Figure 4.7: Synthesis of $[(\text{TerPh})\text{HIPT}_2\text{N}_3\text{N}]\text{MoN}_2\text{Na}(\text{THF})_x$

Since $[(\text{TerPh})\text{HIPT}_2\text{N}_3\text{N}]\text{MoN}_2\text{Na}(\text{THF})_x$ is low spin Mo(IV), it is diamagnetic as observed by ^1H NMR spectroscopy. The ^1H NMR spectrum is consistent with other C_s complexes showing the backbone protons in a 2:1 ratio. THF resonances were also observed by ^1H NMR spectroscopy and the integration of the THF resonances versus an internal standard were not consistent from one spectrum to another. This suggests that THF coordinates to sodium and is partial labile. The quantity of THF coordinated to Na in a sample of $[(\text{TerPh})\text{HIPT}_2\text{N}_3\text{N}]\text{MoN}_2\text{Na}(\text{THF})_x$ depended upon the isolation technique. IR spectroscopy reveals that the diazenido anion has a ν_{NN} at 1790 cm^{-1} and $\nu^{15\text{N}15\text{N}}$ is observed at 1730 cm^{-1} , consistent with other diazenido sodium salts synthesized in our lab.^{6,9}

Reduction of $[(\text{TerPh})\text{HIPT}_2\text{N}_3\text{N}]\text{MoCl}$ with 0.5% Na/Hg resulted in a sample of $[(\text{TerPh})\text{HIPT}_2\text{N}_3\text{N}]\text{MoN}_2\text{Na}(\text{THF})_x$ in which the stoichiometry, in terms of THF was variable. A cleaner synthetic route to $[(\text{TerPh})\text{HIPT}_2\text{N}_3\text{N}]\text{MoN}_2\text{X}$ employed KC_8 . Although

KC_8 is a powerful reductant, a two electron reduction is not observed for $[N_3N]Mo$ complexes. Therefore, an excess of KC_8 can be used to ensure complete conversion of $[N_3N]MoCl$ to $[N_3N]MoN_2K$. When $[(TerPh)HIPT_2N_3N]MoCl$ was treated with excess (2-3 equivalents) of KC_8 in THF the solution changes from red to purple within minutes (Figure 4.8). Volatiles were then removed *in vacuo* and the resulting solid was extracted with pentane and the solution filtered through Celite. Upon crystallization from pentane, a purple solid, $[(TerPh)HIPT_2N_3N]MoN_2K$, was obtained in 61% yield. Due to asymmetry observed by 1H NMR spectroscopy and the lack of a coordinating solvent, it was believed that the potassium coordinates to an aryl ring of the ligand. A ν_{NN} of 1802 cm^{-1} was observed by IR spectroscopy for $[(TerPh)HIPT_2N_3N]MoN_2K$ compared to ν_{NN} at 1798 cm^{-1} observed for $[HIPTN_3N]MoN_2K$.

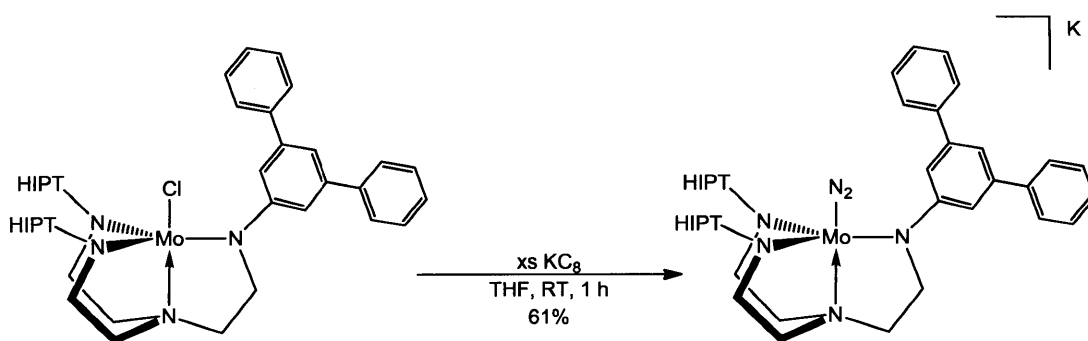


Figure 4.8: Synthesis of $[(TerPh)HIPT_2N_3N]MoN_2K$

$[(TerPh)HIPT_2N_3N]MoN_2$ is an essential catalytic intermediate if ammonia is to be generated from dinitrogen. The previously employed method of oxidizing the diazenido anion was to treat a solution of $[N_3N]MoN_2X$ with $ZnCl_2$ /dioxane. When $ZnCl_2$ /dioxane is reacted with $[N_3N]MoN_2X$, it was shown to produce a small amount of $[N_3N]MoCl$;

therefore, we now employ $Zn(OAc)_2$, a milder oxidant. While $ZnCl_2$ /dioxane oxidized $[(TerPh)HIPT_2N_3N]MoN_2X$ to $[(TerPh)HIPT_2N_3N]MoN_2$ in several minutes, $Zn(OAc)_2$ requires twelve hours, (overnight). Oxidation of $[(TerPh)HIPT_2N_3N]MoN_2X$ with $Zn(OAc)_2$ yields a green solid, which can be isolated in 67% yield after crystallization from tetramethylsilane (Figure 4.9). $[(TerPh)HIPT_2N_3N]MoN_2$ was determined to be a paramagnetic Mo(III) complex as observed by 1H NMR spectroscopy.

$[(TerPh)HIPT_2N_3N]MoN_2$ contains three characteristic resonances downfield of the aryl resonances in the 1H NMR spectrum at δ 19.7, 18.7, and 16.3 ppm. Three resonances are also observed upfield at δ -27.2, -31.1, -32.9 ppm. There are again three resonances in a 1:1:1 ratio due to the diastereotopic nature of the $HIPT-NCH_2CH_2N$ backbone methylene protons. Another resonance also appears at δ -6.5 ppm in the 1H NMR spectrum, which corresponds to the 2',6' aryl protons (*ortho* protons on terphenyl substituents with respect to the amide). The IR spectrum of $[(TerPh)HIPT_2N_3N]MoN_2$ contains a ν_{NN} at 1984 cm^{-1} and the ^{15}N labeled complex has a $\nu^{15N^{15}N}$ at 1918 cm^{-1} .

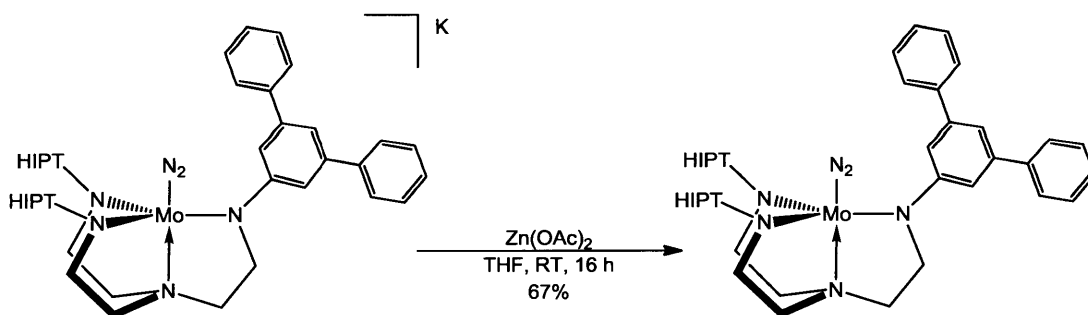


Figure 4.9: Synthesis of $[(TerPh)HIPT_2N_3N]MoN_2$

The diazenido complex, $[N_3N]MoN_2H$ is an interesting and difficult to isolate proposed intermediate in the catalytic cycle of the reduction of dinitrogen to ammonia. Diazenido

complexes for the C_s symmetric ligand systems investigated by Weare were decomposed to the dinitrogen complexes;⁶ $[\text{HIPT}_3\text{N}_3\text{N}]\text{MoN}_2\text{H}$ investigated by Yandulov decomposes to the hydride.⁹ For other C_s symmetric ligands Mo(IV) diazenido complexes were also observed to decompose to Mo(III) dinitrogen complexes.⁶

Few other structurally characterized examples of $[\text{M}]\text{N}_2\text{H}$ (M = transition metal) complexes exist in the literature.^{9,10} $[(\text{TerPh})\text{HIPT}_2\text{N}_3\text{N}]\text{MoN}_2\text{X}$ (X = Na, Mg, K) is a potential precursor to $[(\text{TerPh})\text{HIPT}_2\text{N}_3\text{N}]\text{MoN}_2\text{H}$. Unfortunately the C_s symmetric $[\text{N}_3\text{N}]\text{MoN}_2\text{H}$ complexes were not as stable as $[\text{HIPTN}_3\text{N}]\text{MoN}_2\text{H}$, and performing studies on them proved difficult.^{6,9} One interesting aspect of the diazenido species is its varied stability depending on the steric environment of the supporting ligand. For $[\text{HIPTN}_3\text{N}]\text{MoN}_2\text{H}$, the species decomposes to $[\text{HIPTN}_3\text{N}]\text{MoH}$ at 60 °C.⁹ In the case of the C_s symmetric supporting ligand systems $[\text{N}_3\text{N}]\text{MoN}_2\text{H}$ decomposed to $[\text{N}_3\text{N}]\text{MoN}_2$.⁶

$[(\text{TerPh})\text{HIPT}_2\text{N}_3\text{N}]\text{MoN}_2\text{H}$, like other C_s symmetric diazenido complexes, also rearranges to the dinitrogen complex, $[(\text{TerPh})\text{HIPT}_2\text{N}_3\text{N}]\text{MoN}_2$. Previous C_s symmetric complexes contained only a single aryl substituent on one of the amines.⁶ In the case of $[(\text{TerPh})\text{HIPT}_2\text{N}_3\text{N}]\text{MoN}_2\text{H}$ a terphenyl added more steric bulk, but did not prevent decomposition.

$[(\text{TerPh})\text{HIPT}_2\text{N}_3\text{N}]\text{MoN}_2\text{H}$ can be generated *in situ* easily from $[(\text{TerPh})\text{HIPT}_2\text{N}_3\text{N}]\text{MoN}_2\text{X}$ using acids such as $[\text{H}(\text{Et}_2\text{O})_2][\text{BAR}'_4]$, $[\text{Et}_3\text{NH}][\text{OTf}]$, or $[\text{CollH}][\text{BAR}'_4]$ (Figure 4.10). As with the other diazenido complexes, $[(\text{TerPh})\text{HIPT}_2\text{N}_3\text{N}]\text{MoN}_2\text{H}$ has a characteristic resonance in the ^1H NMR spectrum appearing at δ 8.58 ppm corresponding to the N_β bound hydrogen.

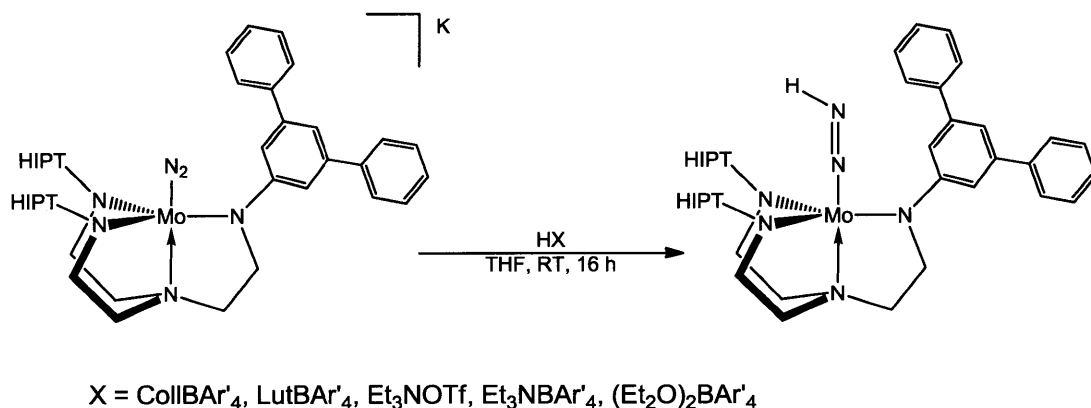


Figure 4.10: [(TerPh)HIPT₂N₃N]MoN₂H

When one equivalent of [H(Et₂O)₂][BAR'₄] was added to [(TerPh)HIPT₂N₃N]MoN₂K the major product was [(TerPh)HIPT₂N₃N]MoN₂H₂[BAR'₄]. Due to the formation of [(TerPh)HIPT₂N₃N]MoN₂H₂[BAR'₄] weaker acids were typically chosen. [Et₃NH][OTf], or [CollH][BAR'₄] can both be employed to synthesize [(TerPh)HIPT₂N₃N]MoN₂H. A significant portion of [(TerPh)HIPT₂N₃N]MoN₂ was also generated, regardless of the acid source. Since the goal was to isolate [(TerPh)HIPT₂N₃N]MoN₂H quickly and cleanly, [Et₃NH][OTf] was chosen because Et₃N is much easier to remove than collidine. There is a trend for the decomposition of [(TerPh)HIPT₂N₃N]MoN₂H based on the strength of the base used and Et₃N is among the strongest counter bases, so the rate at which it promotes the decomposition of [(TerPh)HIPT₂N₃N]MoN₂H is quicker than others.⁶

When [(TerPh)HIPT₂N₃N]MoN₂K was treated with 0.9 equivalents of [Et₃NH][OTf] in diethyl ether, and rapidly isolated within a few hours, it still contains [(TerPh)HIPT₂N₃N]MoN₂. The amount of [(TerPh)HIPT₂N₃N]MoN₂ increases during isolation, resulting in a 1:1 N₂ complex to NNH complex ratio on any given attempt. There were no longer any observed ¹⁹F NMR spectroscopy resonances and no observed Et₃N by ¹H

NMR spectroscopy, so it was proposed that only $[(\text{TerPh})\text{HIPT}_2\text{N}_3\text{N}]\text{MoN}_2$ and $[(\text{TerPh})\text{HIPT}_2\text{N}_3\text{N}]\text{MoN}_2\text{H}$ were present. Each time $[(\text{TerPh})\text{HIPT}_2\text{N}_3\text{N}]\text{MoN}_2\text{H}$ was isolated, a significant portion of $[(\text{TerPh})\text{HIPT}_2\text{N}_3\text{N}]\text{MoN}_2$ co-crystallized. A similar problem was encountered for $[\text{HIPTN}_3\text{N}]\text{MoN}_2\text{H}$, where there was some contamination of the sample with $[\text{HIPT}_3\text{N}_3\text{N}]\text{MoH}$. Due to the much slower rate of rearrangement of $[\text{HIPTN}_3\text{N}]\text{MoN}_2\text{H}$ the product contains far more $[\text{HIPTN}_3\text{N}]\text{MoN}_2\text{H}$ than $[\text{HIPTN}_3\text{N}]\text{MoH}$.

While rearrangement studies have been performed with $[(\text{TerPh})\text{HIPT}_2\text{N}_3\text{N}]\text{MoN}_2\text{H}$ generated *in situ*, none were performed on the isolated mixture of $[(\text{TerPh})\text{HIPT}_2\text{N}_3\text{N}]\text{MoN}_2$ and $[(\text{TerPh})\text{HIPT}_2\text{N}_3\text{N}]\text{MoN}_2\text{H}$. The *in situ* decomposition of $[(\text{TerPh})\text{HIPT}_2\text{N}_3\text{N}]\text{MoN}_2\text{H}$ was calculated to have a half life of 15 hours. We have found a similar half life for $[(3,5\text{-bisCF}_3)\text{HIPT}_2\text{N}_3\text{N}]\text{MoN}_2\text{H}$ (bis- CF_3 = 3,5-bis(trifluoromethyl)benzene) when $[\text{CollH}]\text{BAR}'_4$ was used (17 hours).⁶ When an acid with Et_3N as the conjugate base was used, the half life of $[(\text{bis-}\text{CF}_3)\text{HIPTN}_3\text{N}]\text{MoN}_2\text{H}$ was not measured because the complex was almost completely decomposed by the time a ^1H NMR spectrum could be taken. The increased steric encumbrance of the TerPh ligand along with the change in electronic effect has slowed the decomposition of $[(\text{TerPh})\text{HIPT}_2\text{N}_3\text{N}]\text{MoN}_2\text{H}$ compared to $[(\text{bis-}\text{CF}_3)\text{HIPTN}_3\text{N}]\text{MoN}_2\text{H}$.

It was difficult to know accurately how much $[(\text{TerPh})\text{HIPT}_2\text{N}_3\text{N}]\text{MoN}_2\text{H}$ is present in the sample because $[(\text{TerPh})\text{HIPT}_2\text{N}_3\text{N}]\text{MoN}_2$ is paramagnetic. Accurate integration of a single proton attached to a quadrupolar nitrogen nucleus is difficult, and the necessity of running these reactions *in situ* adds a component of uncertainty necessary to remove.

When $[\text{Et}_3\text{NH}][\text{BAR}'_4]$ or $[\text{Et}_3\text{NH}][\text{OTf}]$ was employed for the generation of $[(\text{TerPh})\text{HIPT}_2\text{N}_3\text{N}]\text{MoN}_2\text{H}$ from $[(\text{TerPh})\text{HIPT}_2\text{N}_3\text{N}]\text{MoN}_2\text{K}$ and solvent and Et_3N are removed *in vacuo*, a 1:1 mixture of $[(\text{TerPh})\text{HIPT}_2\text{N}_3\text{N}]\text{MoN}_2$ to $[(\text{TerPh})\text{HIPT}_2\text{N}_3\text{N}]\text{MoN}_2\text{H}$

was found upon crystallization of crude residue from tetramethylsilane. Other acids with different conjugate bases (Lut, Coll) were used and similar results were found. For these higher boiling conjugate bases (Lut, Coll), it was difficult to remove them efficiently without decomposing $[(\text{TerPh})\text{HIPT}_2\text{N}_3\text{N}]\text{MoN}_2\text{H}$. A major impediment to isolation of $[(\text{TerPh})\text{HIPT}_2\text{N}_3\text{N}]\text{MoN}_2\text{H}$ is the several hours required for $[(\text{TerPh})\text{HIPT}_2\text{N}_3\text{N}]\text{MoN}_2\text{H}$ to crystallize from a tetramethylsilane solution, thus leading to further decomposition to $[(\text{TerPh})\text{HIPT}_2\text{N}_3\text{N}]\text{MoN}_2$.

A different approach was tried by synthesizing $[(\text{TerPh})\text{HIPT}_2\text{N}_3\text{N}]\text{MoN}_2\text{H}_2[\text{BAr}'_4]$ using two equivalents of $[\text{HEt}_2\text{O}][\text{BAr}'_4]$ starting with $[(\text{TerPh})\text{HIPT}_2\text{N}_3\text{N}]\text{MoN}_2\text{K}$. $[(\text{TerPh})\text{HIPT}_2\text{N}_3\text{N}]\text{MoN}_2\text{H}_2[\text{BAr}'_4]$ can be synthesized in a 90% yield after crystallization from tetramethylsilane. $[(\text{TerPh})\text{HIPT}_2\text{N}_3\text{N}]\text{MoN}_2\text{H}_2[\text{BAr}'_4]$ can then be deprotonated to $[(\text{TerPh})\text{HIPT}_2\text{N}_3\text{N}]\text{MoN}_2\text{H}$ with Et_3N and $[\text{Et}_3\text{NH}][\text{BAr}'_4]$ was filtered. Unfortunately, crystallization of $[(\text{TerPh})\text{HIPT}_2\text{N}_3\text{N}]\text{MoN}_2\text{H}$ synthesized through this route, still led to the decomposition of $[(\text{TerPh})\text{HIPT}_2\text{N}_3\text{N}]\text{MoN}_2\text{H}$ to $[(\text{TerPh})\text{HIPT}_2\text{N}_3\text{N}]\text{MoN}_2$. *In situ* reactions run by this method and monitored by ^1H NMR spectroscopy show the half life of $[(\text{TerPh})\text{HIPT}_2\text{N}_3\text{N}]\text{MoN}_2\text{H}$ to be 17 hours. Studies with the 1:1 mixture of $[(\text{TerPh})\text{HIPT}_2\text{N}_3\text{N}]\text{MoN}_2:[(\text{TerPh})\text{HIPT}_2\text{N}_3\text{N}]\text{MoN}_2\text{H}$ were not performed due to the difficulty associated with integration of ^1H NMR spectrum taken where a paramagnetic species was present.

Due in part to the difficulty of isolating C_s symmetric $[\text{N}_3\text{N}]$ ligands for mechanistic investigation, and their lack of catalytic activity, symmetric $[\text{N}_3\text{N}]$ variations were sought.

Symmetric $[N_3N]$ Variations

Since the C_s symmetric ligand systems do not lead to an increase in catalytic turnover of dinitrogen to ammonia, attention was turned towards developing a symmetric ligand. The electron withdrawing [*p*BrHIPTN₃N] ligand had been synthesized and it was shown that the N_2 for ammonia exchange was slowed.⁵ In hopes of increasing the rate of N_2 for ammonia exchange to improve catalytic activity of the $[N_3N]$ system, an electron donating terphenyl ligand was developed.

Introducing an oxygen atom to the *para* position of the HIPT ligand relative to the amine, and using it as a nucleophile to add a methyl group, was explored after Power's reported 2,2'',4,4'',6,6''-hexaisopropyl-[1,1':3',1''-terphenyl]-2'-ol, (2,6-(TRIP)₂phenol, HIPTOH) (Figure 4.11).¹¹ It was proposed that the phenol could be deprotonated with a variety of bases.^{12,13} The nucleophilic oxygen would then be reacted with an electrophilic methyl group¹⁴ to synthesize 2,2'',4,4'',6,6'''-hexaisopropyl-2'-methoxy-1,1':3',1''-terphenyl, (2,6-(TRIP)₂anisole).

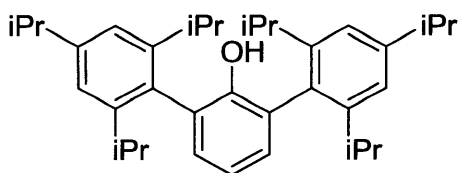


Figure 4.11: (2,6-(TRIP)₂phenol); HIPTOH.

It was believed that the methoxy group would electronically promote bromination of the *para* position, as observed for 2'-methoxy-1,1':3',1''-terphenyl. Bromination of 2,6-(TRIP)₂anisole, unlike 2'-methoxy-1,1':3',1''-terphenyl, only proceeded to ~33% by a variety

of methods. Since 2,6-(TRIP)₂anisole was not brominated efficiently, 2,6-(TRIP)₂phenol was brominated first.^{15,16}

2,6-(TRIP)₂phenol was synthesized by published methods¹¹ with slight modifications similar to those utilized in lab for the synthesis of HIPTBr.⁹ A 92% conversion of 2,6-(TRIP)₂phenol to 3,5-(TRIP)₂-4-phenolbromide was realized by addition of one equivalent of Br₂ to an acetic acid slurry of 2,6-(TRIP)₂phenol.^{13,17} The ratio of brominated phenol to unbrominated phenol was determined by integration of the ¹H NMR spectrum using the ratio of phenol peaks at δ 4.58 ppm for 3,5-(TRIP)₂-4-phenolbromide and 4.54 ppm for 2,6-(TRIP)₂phenol. When 1.5 equivalents of bromine were used, the reaction went to completion with no 2,6-(TRIP)₂phenol observable by ¹H NMR spectroscopy.

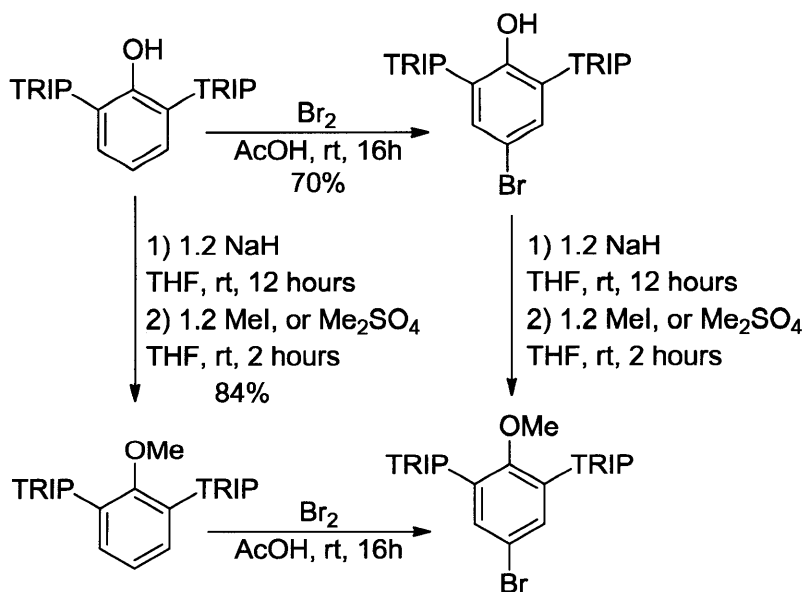


Figure 4.12: Synthetic Routes to 3,5-(TRIP)₂-4-anisolebromide.

Methylation of 3,5-(TRIP)₂-4-phenolbromide to 3,5-(TRIP)₂-4-anisolebromide was achieved by treating 3,5-(TRIP)₂-4-phenolbromide with 1.2 equivalents of NaH in THF

(Figure 4.12). This was followed by addition of either iodomethane or dimethylsulfate (Figure 4.12). The reaction proceeded for one hour until a sodium salt began to precipitate, and was allowed to proceed for an additional hour.

Synthesis of $H_3[pMeOHIPTN_3N]$

When a palladium cross-coupling reaction was performed in toluene employing 1.5% $Pd_2(dba)_3$ catalyst loading and BINAP,¹⁸ a 57% isolated yield of $H_3[pMeOHIPTN_3N]$ was obtained (Figure 4.13). Lower catalyst loadings gave lower yields, and higher catalyst loadings did not increase yields.

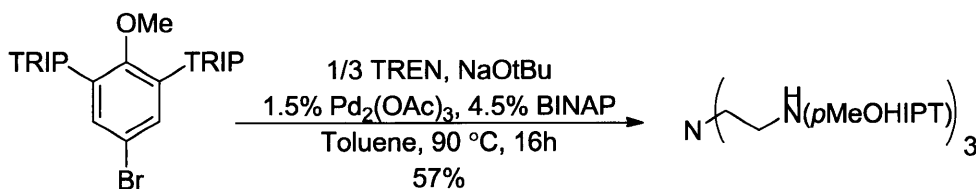


Figure 4.13: Synthesis of $H_3[pMeOHIPTN_3N]$

The isolation techniques for $H_3[pMeOHIPTN_3N]$ were similar to that used for $H_3[HIPTN_3N]$. A 1:1 mixture of toluene/hexanes was used to elute tri-substituted $H_3[pMeOHIPTN_3N]$. Additional bi-substituted $H_4[pMeOHIPT_2N_3N]$ was obtained by eluting the column with ethyl acetate. The bi and tri-substituted products are further purified by crystallization from acetone; $H_3[pMeOHIPTN_3N]$ was isolated in 57% yield.

Synthesis of [*p*MeOH IPTN₃N] Molybdenum Complexes

Conditions for the synthesis of HIPT based triamidoamine molybdenum complexes were first described by Yandulov.^{1,9} These same conditions have proven effective in the syntheses of numerous other variations of the [HIPTN₃N] framework, and H₃[*p*MeOH IPTN₃N].

[*p*MeOH IPTN₃N]MoCl was the main precursor employed to access various catalytic intermediates. It was synthesized in the method described for [HIPTN₃N]MoCl. H₃[*p*MeOH IPTN₃N] was reacted with MoCl₄(THF)₂, followed by the addition of three equivalents of LiN(TMS)₂ (Figure 4.14).

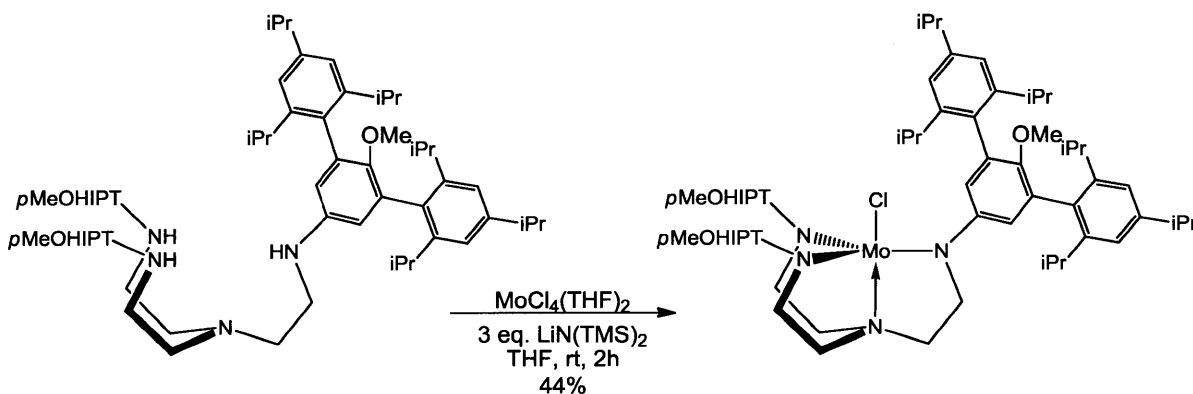


Figure 4.14: Synthesis of [*p*MeOH IPTN₃N]MoCl

While [HIPTN₃N]MoCl can be isolated from pentane, [*p*MeOH IPTN₃N]MoCl does not crystallize from pentane. When a saturated pentane solution of [*p*MeOH IPTN₃N]MoCl is cooled to -30 °C, it solidifies into a gel. Crystallization of [*p*MeOH IPTN₃N]MoCl from SiMe₄ at room temperature proved effective and the product was isolated in 44% yield, as a red solid.

A ¹H NMR spectrum of [*p*MeOH IPTN₃N]MoCl, which is a paramagnetic high spin Mo(IV) complex, reveals characteristic resonances at δ 13.5 ppm, for the six (2',6') protons

on the internal aryl ring of p MeOHIPT, and δ -19.9 ppm and δ -82.1 ppm for the backbone protons. These backbone resonances for $[p\text{MeOHIPTN}_3\text{N}]\text{MoCl}$ are comparable to the backbone proton resonances for $[\text{HIPTN}_3\text{N}]\text{MoCl}$ at δ -21.4 and -76.3 ppm.

$[p\text{MeOHIPTN}_3\text{N}]\text{MoN}_2\text{Na}$ complexes were synthesized by reduction of $[p\text{MeOHIPTN}_3\text{N}]\text{MoCl}$. The published synthesis of $[\text{HIPTN}_3\text{N}]\text{MoN}_2\text{X}$ used magnesium as the reductant, but sodium was used for these syntheses. Ten equivalents of sodium sand were added to a red solution of $[p\text{MeOHIPTN}_3\text{N}]\text{MoCl}$ in THF and the solution quickly became dark green (Figure 4.15). When THF was removed, the $[p\text{MeOHIPTN}_3\text{N}]\text{MoN}_2\text{Na}(\text{THF})_x$ turned purple, and the IR spectrum contains a ν_{NN} at 1856 cm^{-1} , similar to that observed for $[\text{HIPTN}_3\text{N}]\text{MoN}_2\text{Na}(\text{THF})_x$.

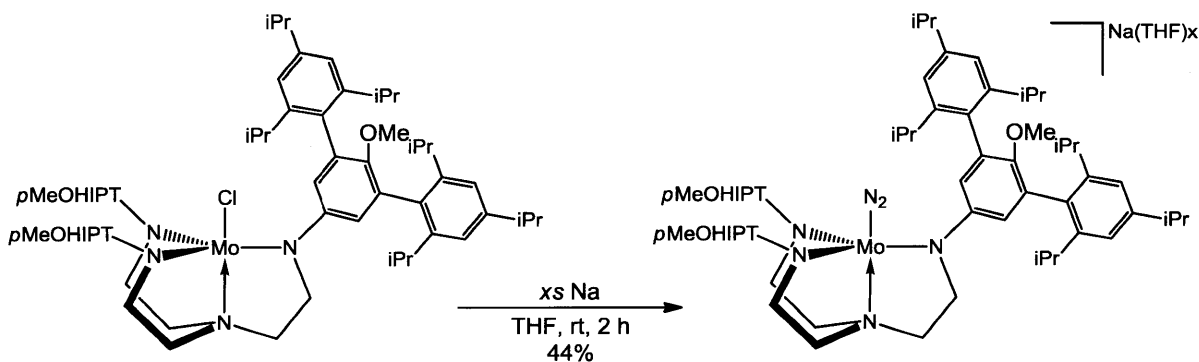


Figure 4.15: Synthesis of $[p\text{MeOHIPTN}_3\text{N}]\text{MoN}_2\text{Na}(\text{THF})_x$

To synthesize $[p\text{MeOHIPTN}_3\text{N}]\text{MoN}_2$ a THF solution containing $[p\text{MeOHIPTN}_3\text{N}]\text{MoN}_2\text{Na}(\text{THF})_x$ was filtered through Celite into a solution containing two equivalents of $\text{ZnCl}_2/\text{dioxane}$. The solution turns brown upon mixing, and after crystallization from heptane, $[p\text{MeOHIPTN}_3\text{N}]\text{MoN}_2$ is isolated in 34% yield. A ^1H NMR spectrum contains three resonances corresponding to paramagnetic Mo(III)

$[p\text{MeOHIPTN}_3\text{N}]\text{MoN}_2$. The resonance for the 2',6' HIPT protons was observed at δ 21.2 ppm, and the backbone resonances are observed at δ -7.6 and -21.2 ppm. These resonances for $[p\text{MeOHIPTN}_3\text{N}]\text{MoN}_2$ were compared to δ 23.3, -4.8, and -33.5 ppm for $[\text{HIPTN}_3\text{N}]\text{MoN}_2$. Upon closer inspection of the ^1H NMR spectrum of $[p\text{MeOHIPTN}_3\text{N}]\text{MoN}_2$, by enlarging the vertical scale, it was noticed that the resonances of $[p\text{MeOHIPTN}_3\text{N}]\text{MoCl}$ are observable in the isolated product (Figure 4.16). When a 20 equivalents excess of $\text{ZnCl}_2/\text{dioxane}$ was used, the majority of the isolated product was $[p\text{MeOHIPTN}_3\text{N}]\text{MoCl}$ after a twelve hour reaction time.

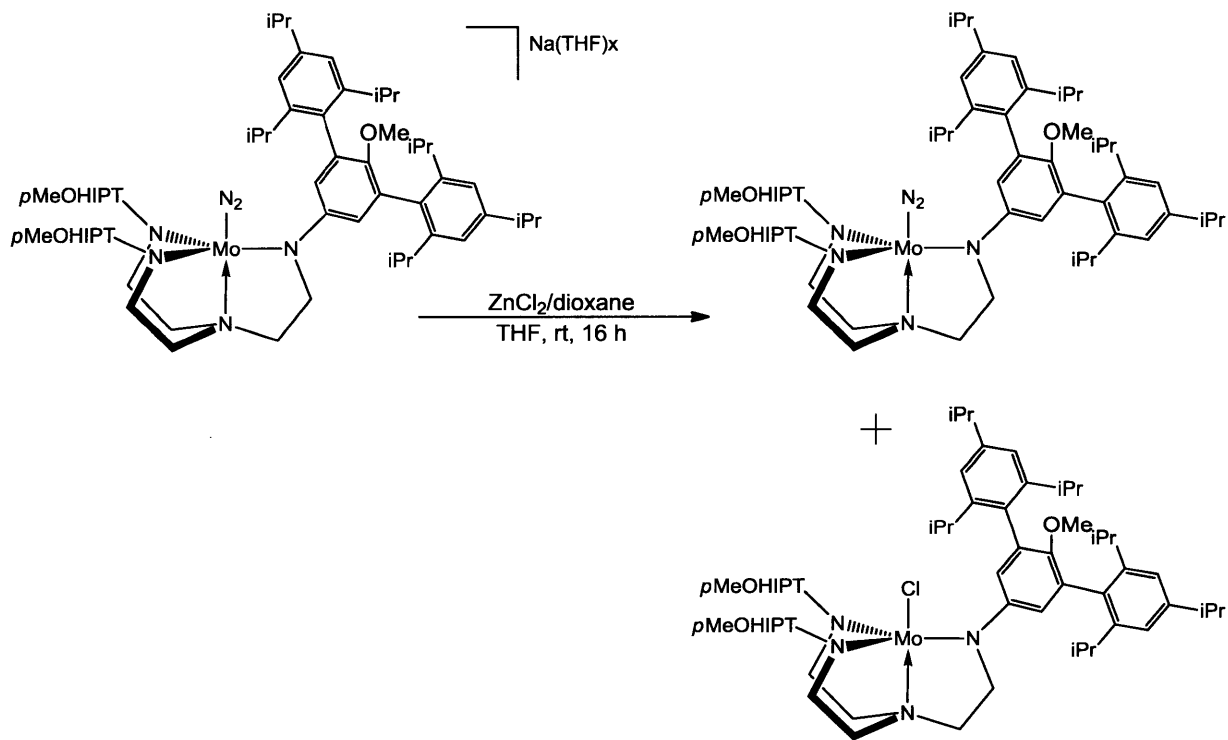


Figure 4.16: Synthesis of $[p\text{MeOHIPTN}_3\text{N}]\text{MoN}_2$

The reduction product of $[p\text{MeOH IPTN}_3\text{N}]\text{MoCl}$, with ten equivalents of sodium in diethyl ether, $[p\text{MeOH IPTN}_3\text{N}]\text{MoN}_2\text{Na}(\text{Et}_2\text{O})_x$, contained no resonances corresponding to a paramagnetic species as observed by ^1H NMR spectroscopy. The ^1H NMR spectrum for the oxidation product of $[p\text{MeOH IPTN}_3\text{N}]\text{MoN}_2\text{Na}(\text{Et}_2\text{O})_x$ with $\text{ZnCl}_2/\text{dioxane}$ does contain three resonances δ 13.5, -19.6, and -80.6 ppm which correspond to $[p\text{MeOH IPTN}_3\text{N}]\text{MoCl}$.

The ν_{NN} of $[p\text{MeOH IPTN}_3\text{N}]\text{MoN}_2$ observed at 1984 cm^{-1} by IR spectroscopy in C_6D_6 is similar to the ν_{NN} of $[\text{HIPTN}_3\text{N}]\text{MoN}_2$ at 1990 cm^{-1} . The methoxy groups appear to have only a small electronic effect on the molybdenum center, at least according to ν_{NN} .

$[p\text{MeOH IPTN}_3\text{N}]\text{MoN}_2$ was synthesized cleanly by adding $\text{Zn}(\text{OAc})_2$ to a THF solution of $[p\text{MeOH IPTN}_3\text{N}]\text{MoN}_2\text{Na}(\text{THF})_x$ and allowing the reaction to proceed for 16 hours (Figure 4.17). The spectral data are as discussed for the oxidation of $[p\text{MeOH IPTN}_3\text{N}]\text{MoN}_2\text{Na}(\text{THF})_x$, but without contamination of $[p\text{MeOH IPTN}_3\text{N}]\text{MoCl}$.

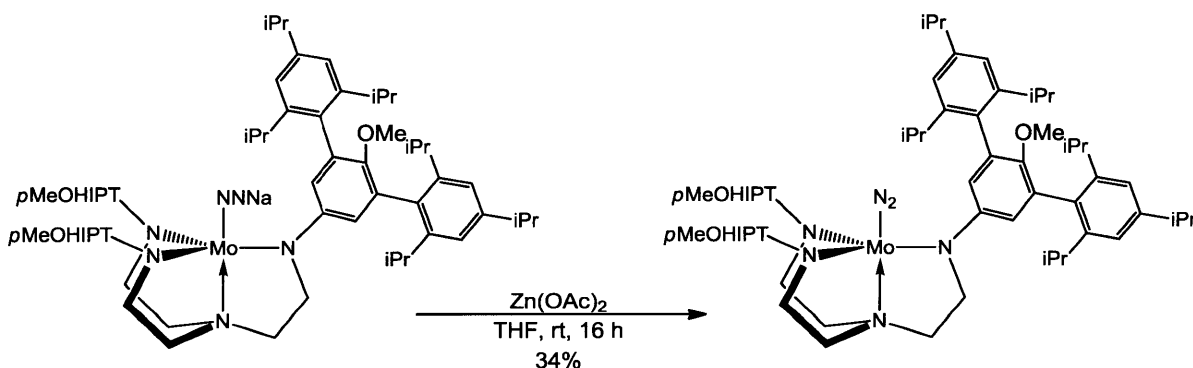


Figure 4.17: Clean Synthesis of $[p\text{MeOH IPTN}_3\text{N}]\text{MoN}_2$

One equivalent of $[\text{CollH}][\text{BAR}'_4]$ can be added to a C_6D_6 solution (31 mM) of $[p\text{MeOH IPTN}_3\text{N}]\text{MoN}_2\text{Na}(\text{THF})_x$ to synthesize $[p\text{MeOH IPTN}_3\text{N}]\text{MoN}_2\text{H}$ *in situ*. $[p\text{MeOH IPTN}_3\text{N}]\text{MoN}_2\text{H}$ rearranges to $[p\text{MeOH IPTN}_3\text{N}]\text{MoH}$ at $60\text{ }^\circ\text{C}$, which is the same

as was observed for $[HIPTN_3N]MoH$. A rigorous kinetic study was not performed on this molecule, however, the rearrangement was shown to decompose to half of its original concentration in approximately one week, as observed by 1H NMR.

$[pMeOHIPTN_3N]MoN$ was synthesized by two methods. From $[pMeOHIPTN_3N]MoCl$, $[pMeOHIPTN_3N]MoN$ was synthesized by adding $TMSN_3$ to a solution of $[pMeOHIPTN_3N]MoCl$ in toluene and heating the solution to $90\text{ }^\circ C$ overnight (Figure 4.18).

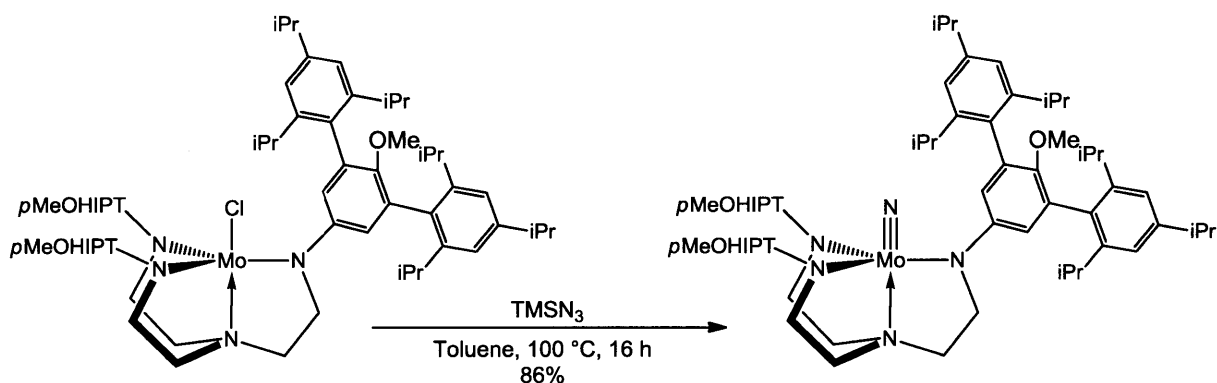


Figure 4.18: Synthesis of $[pMeOHIPTN_3N]MoN$

The second method was employed by reacting $H_3[pMeOHIPTN_3N]$ with two equivalents of $NMo(NMe_2)_3$ in toluene and heating the solution to $60\text{ }^\circ C$ overnight. $[pMeOHIPTN_3N]MoN$ was isolated by filtration through Celite followed by the removal of volatiles *in vacuo*. Crystallization of $[pMeOHIPTN_3N]MoN$ from $SiMe_4$ at room temperature yielded $[pMeOHIPTN_3N]MoN$ in 86% yield. The 1H NMR spectrum resonances of the backbone protons of $H_3[pMeOHIPTN_3N]$ are at δ 2.82, and 2.28 ppm; these protons shift to δ 3.44, and 1.90 ppm for $[pMeOHIPTN_3N]MoN$.

Crystallization of $[p\text{MeOHIP}T\text{N}_3\text{N}]\text{MoN}$ from tetramethylsilane yielded X-ray quality crystals in the $C2/c$ space group. Tetramethylsilane is not an optimal solvent for solving X-ray crystal structures because of the tendency for the methyl groups to be disordered, however it was the only solvent employed which resulted in X-ray quality crystals. The volatility of tetramethylsilane (bp, 26 °C) also led to some cracking of the crystals prior to their mounting on the X-ray diffractometer; however an acceptable solution was found with an $R1$ equal to 0.0758 (Figure 4.19). Crystallographic data tables are shown in appendix C.

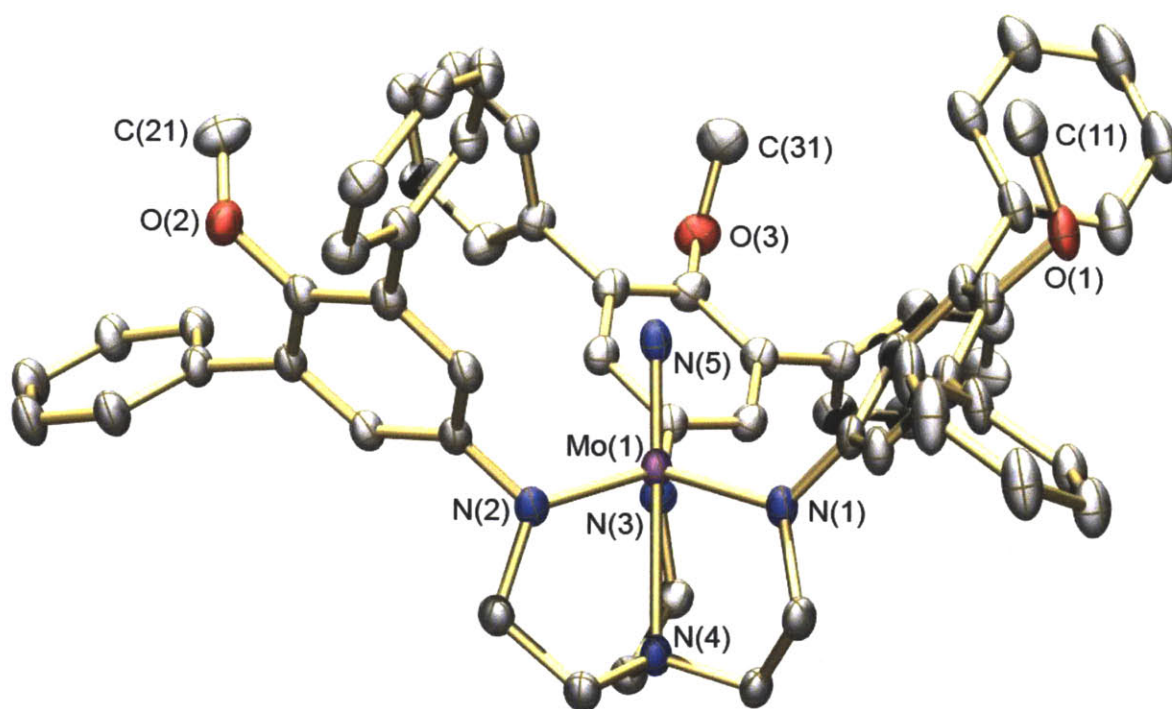


Figure 4.19: X-ray Crystal Structure of $[p\text{OMeHIPTN}_3\text{N}]\text{MoN}$ Thermal ellipsoid representation $[p\text{MeOHIP}T\text{N}_3\text{N}]\text{MoN}$. Isopropyl groups and hydrogen atoms omitted for clarity. Selected bond distances (Å) and angles (°): $\text{Mo}(1)\text{-N}(5) = 1.650(4)$, $\text{Mo}(1)\text{-N}(4) = 2.433(4)$. $\text{Mo}(1)\text{-N}(1)\text{-C}_{\text{ipso}} = 126.17$, $\text{N}_{\text{amide}}\text{-Mo}(1)\text{-N}(4) = 77.00$

The parameters for $[p\text{MeOHIP}T\text{N}_3\text{N}]\text{MoN}$ are comparable to $[\text{HIPTN}_3\text{N}]\text{MoN}$ (Table 4.1) the structure of which was previously reported.⁹ The electron donating nature of the

ligand is evident in that the Mo-N_{amine} distance is longer by nearly 0.04 Å. This elongation of the Mo-N_{amine} bond is comparable to that observed for the difference between {[HIPTN₃N]MoPMe₃}[BAR'₄] and {[HIPTN₃N]MoNH₃}[BAR'₄] (0.05 Å) discussed in Chapter 3.

Table 4.1: Selected Bond Lengths (Å) and Angles (°) for [pMeOHIPTN₃N]MoN compared to [HIPTN₃N]MoN

Selected Bonds (Å) and Angles (°)	[pMeOHIPTN ₃ N]MoN	[HIPTN ₃ N]MoN
Mo-N _{amide} (av)	1.988	2.003
Mo-N _{amine}	2.433(4)	2.395(5)
Mo-N(5) _{Nitride}	1.650(4)	1.652(5)
N _{amine} -Mo-N _{amide} (av)	77.00	78.02
Mo-N _{amide} -C _{ipso} (av)	126.17	128.64

Catalytic reactions employing [pMeOHIPTN₃N]MoN, were performed under standard conditions⁴ for which an average of 6.5 equivalents of ammonia was generated. Since the steric constraints of the [pMeOHIPTN₃N] ligand are similar to the [HIPTN₃N] ligand, the system does catalytically reduce dinitrogen to ammonia. The 6.5 equivalents of ammonia generated from [pMeOHIPTN₃N]MoN was less than obtained from [pBrHIPTN₃N]MoN, however, this is presumably from the differences in the catalytic reactions inherent to the quality of reagents.

{[pMeOHIPTN₃N]MoNH₃}[BAR'₄] is synthesized in the same manner as reported for {[HIPTN₃N]MoNH₃}[BAR'₄]. [pMeOHIPTN₃N]MoCl was added to methylene chloride then reacted with NaBAR'₄ under an NH₃ atmosphere at room temperature for two hours (Figure 4.20). After removal of volatiles *in vacuo*, the solid was dissolved in toluene and the solution

was filtered through Celite. The toluene was removed from the filtrate *in vacuo* and the solid was triturated in pentane and a ruby red solid is isolated in 90% yield.

The 1H NMR backbone resonances for $[pMeOHIPTN_3N]MoNH_3[Bar'_4]$ are observed at, δ -16 and, -105 ppm compared to the reported values of δ -21, and -103 ppm for $[HIPTN_3N]MoNH_3[Bar'_4]$. The 2,4-aryl proton resonances for $[Bar'_4]^-$ are observed at δ 8.28 and 7.62 ppm, with a single ^{19}F NMR resonance for the $-CF_3$ groups observed at δ -62.2 ppm.

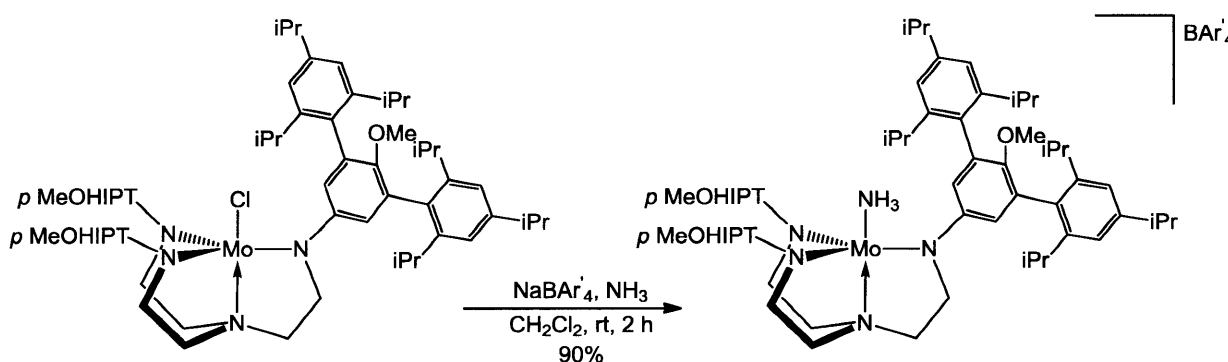


Figure 4.20: Synthesis of $[pMeOHIPTN_3N]MoNH_3[Bar'_4]$

The N_2 for ammonia exchange is an important part of the catalytic cycle. As shown in Chapter 2, the exchange of dinitrogen for ammonia must be competitive with the exchange of hydrogen for ammonia or the complex will not be a catalyst. Exchange of dinitrogen for ammonia in $[HIPTN_3N]MoNH_3$ requires 110 minutes to proceed to ~50%, and $[pBrHIPTN_3N]MoNH_3$ required 120 minutes (Table 4.2). A primary reason for synthesizing $[pMeOHIPTN_3N]Mo$ was to promote faster exchange of NH_3 for N_2 , due to the increased electronic donating nature of the $pMeOHIPT$ ligand.

To determine the half-life of the N_2 for ammonia exchange the procedures utilized for other $[N_3N]$ ligands were employed.^{5,6,9} $\{[pMeOHIPTN_3N]MoNH_3\}[Bar'_4]$ in toluene

reduced with Cp_2^*Cr and the solution was stirred at a controlled rate. Aliquots of the reaction solution were taken, and the formation of $[pMeOH IPTN_3N]MoN_2$ was observed by the presence of the ν_{NN} resonance at 1986 cm^{-1} by IR spectroscopy (Figure 4.21). The area of the N_2 resonance as observed by IR spectroscopy was integrated, and calculations were done using first order kinetics.

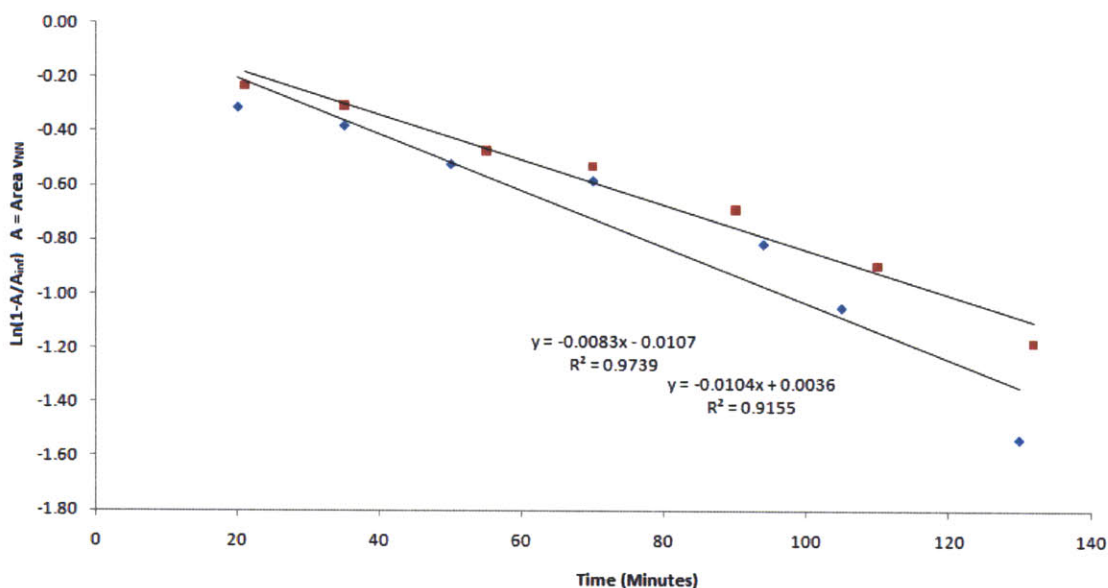


Figure 4.21: Area of N_2 peak observed by IR Spectroscopy; $\ln(1 - (Area/Area_{inf})/$ vs. time

The kinetics of the N_2 for ammonia exchange were extremely sensitive to the stir rate of the solution and amount of time it took to make aliquots for IR spectroscopy, due to the limited solubility of N_2 in toluene. Employing first order kinetics, $t_{1/2} = (\ln(2)/k)$, was calculated to be 75 minutes. As shown in Table 4.2, the $t_{1/2}$ of the N_2 for ammonia exchange was shown to be affected by the electronic donating nature of $[pMeOH IPTN_3N]Mo$, when compared with various $[N_3N]$ ligands.

Table 4.2: Half Life of Ammonia for Dinitrogen Exchange

[Ligand]MoNH ₃	T _{1/2} of N ₂ for NH ₃ exchange (min)
[<i>p</i> BrHIPTN ₃ N] ⁵	120
[HIPTN ₃ N] ⁹	110
[<i>p</i> MeOHIPTN ₃ N]	75
[3,5-dimethoxyHIPT ₂ N ₃ N]	< 45
[HTBTN ₃ N] ⁵	> 6000

The HIPTN₃N framework allowed for the catalytic reduction of dinitrogen to ammonia. The electron donating nature of the ligand appears to have an effect on the N₂ for ammonia exchange, though not as pronounced as we had hoped for, and was observed for C_s symmetric ligands previously developed. Crystallinity of the [N₃N] complexes continued to be an issue for the exploration of [N₃N] chemistry, so new t-butyl containing ligands were explored.

Synthesis of DTBA and DTBAT Ligands

There have been problems isolating HIPT-containing [N₃N] complexes due to their high solubility and the difficulty crystallizing them. This led to the development of aryl and terphenyl ligands containing 3,5-ditert-butyl groups, and investigation of symmetric [N₃N]Mo complexes. 3,5-ditertbutyl aryl groups were shown to promote crystallinity¹⁹ and it was believed that enhanced crystallinity could be used to further examine difficult to isolate intermediates. 5-bromo-1,3-di-tert-butyl-2-methoxybenzene (DTBA = DiTertButylAnisole

= 1,3-di-tert-butyl-2-methoxybenzene) and 1-bromo-3,5-di-tert-butylbenzene are both commercially available. However, the former is significantly cheaper and can be synthesized easily from inexpensive starting materials in high yields and on a large scale.²⁰

Using three equivalents of DTBABr per equivalent of TREN employing a palladium cross-coupling reaction using $Pd_2(dba)_3$ and BINAP, $H_3[DTBAN_3N]$ can be isolated in 20% yield (Figure 4.22). Despite using the three equivalents of DTBABr per TREN, over-arylation of the secondary amines to tertiary amines, was a significant problem. Reaction conditions may be modified to give a higher yield of the desired product, however, this has been a problem seen in the past with small aryl groups.³ Fortunately the over-arylated products were easily separable by silica gel column chromatography using a 1:1 toluene:hexanes mixture, and the desired ligand, $H_3[DTBAN_3N]$, was further purified by crystallization from hot acetone yielding a white solid in 20% yield $H_3[DTBAN_3N]$.

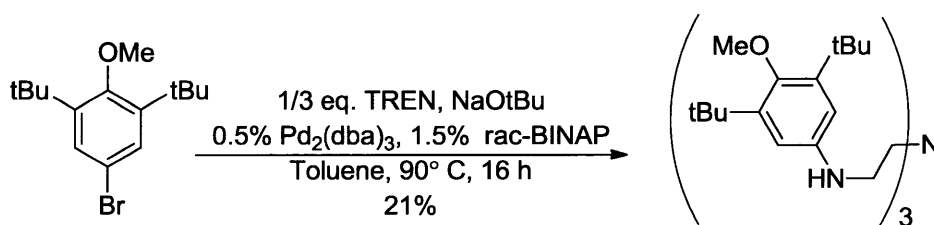


Figure 4.22: Synthesis of $H_3[DTBAN_3N]$

Isolated $H_3[DTBAN_3N]$ can then be reacted with $NMo(NMe_2)_3$ to yield $[DTBAN_3N]MoN$. When $H_3[HIPTN_3N]$ was reacted with $NMo(NMe_2)_3$, heating was required to promote the protonolysis reaction and two equivalents of $NMo(NMe_2)_3$ were required due to thermal decomposition of $NMo(NMe_2)_3$ at 60 °C.

For $[\text{DTBAN}_3\text{N}]\text{MoN}$ only one equivalent of $\text{NMo}(\text{NMe}_2)_3$ was needed because the reaction proceeded quickly at room temperature in contrast to the $[\text{HIPTN}_3\text{N}]$ ligand discussed in Chapter 2. When one equivalent of $\text{NMo}(\text{NMe}_2)_3$ was added to a toluene solution of $\text{H}_3[\text{DTBAN}_3\text{N}]$ and stirred, the solution immediately turns orange (Figure 4.23). After ten minutes the mixture becomes gel-like and stirring is stopped

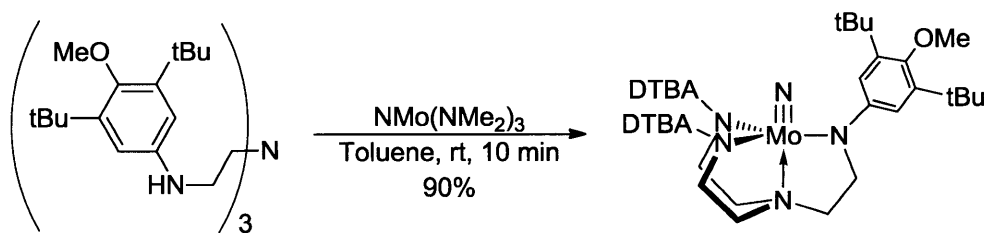


Figure 4.23: Synthesis of $[\text{DTBAN}_3\text{N}]\text{MoN}$

$[\text{DTABN}_3\text{N}]\text{MoN}$ is soluble in toluene but the ligand structure appears to enforce a crystallinity that is similar in consistency to cotton candy and the product crystallizes out of solution. The initial concentration was too high (25 mM) to keep the product in solution, and the necessary amount of toluene required to take all product into solution was impractical. Upon removal of volatiles *in vacuo* a yellow-orange solid can be isolated and $[\text{DTBAN}_3\text{N}]\text{MoN}$ can be further purified by trituration with cold pentane resulting in a 90% yield. $[\text{DTABN}_3\text{N}]\text{MoN}$ was soluble in diethyl ether, so using a pentane layered diethyl ether solution provided crystallization.

Attempts to synthesize $[\text{DTABN}_3\text{N}]\text{MoNH}[\text{BAR}'_4]$ from $[\text{DTABN}_3\text{N}]\text{MoN}$ using $[\text{H}(\text{Et}_2\text{O})_2][\text{BAR}'_4]$ have proven ineffective. When a cold diethyl ether solution of $[\text{DTABN}_3\text{N}]\text{MoN}$ was added to a cold $[\text{H}(\text{Et}_2\text{O})_2][\text{BAR}'_4]$ diethyl ether solution, the mixture turns immediately orange-red after ten minutes. The solution of $[\text{DTBAN}_3\text{N}]\text{MoN}$ and

[H(Et₂O)₂][BAR'₄] then begins to turn dark purple and an intractable black precipitate forms. Attempts to determine the results of the reaction by ¹H NMR spectroscopy were not successful, because the product is paramagnetic and no characteristic resonances were observed. The protonation reaction was also unsuccessful when stopped within a minute of mixing, as the solution appears to decompose upon removal of volatiles *in vacuo*. Another method of adding [H(Et₂O)₂][BAR'₄] drop-wise over five minutes to a -30 °C [DTABN₃N]MoN diethyl ether solution, or reverse addition has also not been successful. [H(Et₂O)₂][BAR'₄] may be too strong of an acid, causing decomposition of the complex by protonating the ligand arms and causing the ligand to detach from the metal. Another possibility that should be considered, was that [DTABN₃N]MoNH[BAR'₄] may be initially formed, but the steric nature of the complex does not promote the stability of the complex under these conditions. Another acid source, [CollH][BAR'₄] was also employed. The use of one equivalent of [CollH][BAR'₄] left un-reacted [DTABN₃N]MoN, as observed by ¹H NMR spectroscopy and no [*p*MeOHIPN₃N]MoNH[BAR'₄] was observed after seven days at 80 °C.

Synthesis of DTABT and [DTABTN₃N]Mo

The method used to synthesize DBTATBr was the same as the method employed to synthesize HIPTBr. Three equivalents of DTBABr were reacted with Mg in refluxing THF to form the Grignard, after which 2,4,6-tribromoiodobenzene was then added (Figure 4.24).

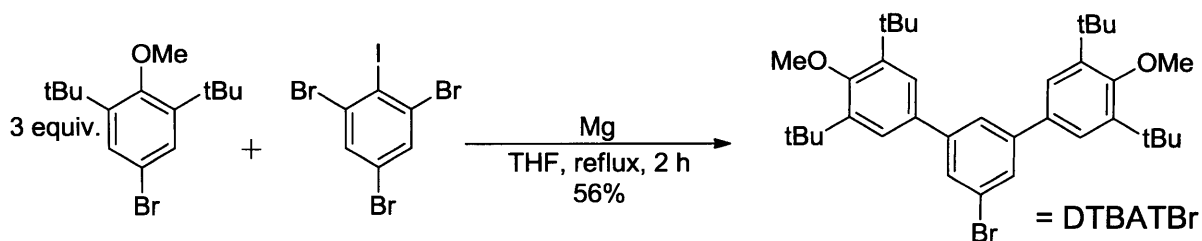


Figure 4.24: Synthesis of DTBATBr

One equivalent of DTBABr was consumed for the trans-metalation of 2,4,6-tribromoiodobenzene. After isolation of the resultant solid from this reaction the material contained both DTBAT and DTBA. Crystallization from hot hexanes led to the isolation of the desired terphenyl, DTBAT, as a white solid in 56% yield.

Using DTBATBr, $H_3[DTBATN_3N]$ can be synthesized employing the same palladium cross-coupling technique used for DTBABr, and many other aryl bromides (Figure 4.25).¹⁸ After purification by silica gel chromatography as described for previous terphenyls,⁹ a white solid was obtained in a 72% yield. There does not appear to be an issue with over-arylation, as observed by TLC and 1H NMR spectroscopy.

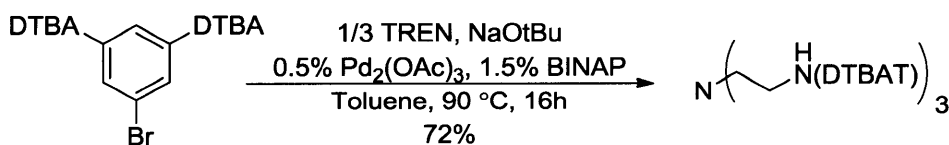


Figure 4.25: Synthesis of $H_3[DTBATN_3N]$

$H_3[DTBATN_3N]$ was then reacted with a single equivalent of $NMo(NMe_2)_3$ at room temperature in C_6D_6 . The reaction does not proceed to completion as observed by 1H NMR spectroscopy. When the reaction conditions are changed to those used to synthesize

[HIPN₃N]MoN (60 °C for two hours with two equivalents of NMo(NMe₂)₃), a yellow solid was obtained in 80% yield (Figure 4.26). As observed by ¹H NMR spectroscopy [DTBATN₃N]MoN is shown to contain similar backbone resonances, as other characterized [N₃N] nitrides. The backbone resonances for [DTBATN₃N]MoN appear at δ 3.59 and 2.11 ppm compared to δ 3.55 and 1.79 ppm for [HIPTN₃N]MoN.⁴



Figure 4.26: Synthesis of [DTBATN₃N]MoN

The hope was that the DTBAT may be sterically protecting enough to allow for the catalytic reduction of dinitrogen to ammonia. Catalytic reactions performed using [DTBATN₃N]MoN under standard conditions were not successful, resulting in the formation of 0.82 equivalents of ammonia per molybdenum center.

[DTBATN₃N]MoCl was synthesized in the same fashion as other [N₃N]MoCl complexes. MoCl₄(THF)₂ was added to a THF solution of H₃[DTBATN₃N] and stirred for one hour followed by addition of LiN(TMS)₂ (Figure 4.27). Upon isolation and crystallization from tetramethylsilane, a red solid was obtained in 40% yield. Since [DTBATN₃N]MoCl is paramagnetic the characteristic ¹H NMR resonances corresponding to the backbone protons were observed at δ -27.6, and -68.0 ppm, compared to δ -21.4 and -76.3

ppm for $[\text{HIPTN}_3\text{N}]\text{MoCl}$.⁹ The yield for this reaction was fairly low considering the reasoning for synthesizing these compounds was their increased crystallinity compared to $[\text{HIPTN}_3\text{N}]$, but the reaction was run on a relatively small scale (200 mg).

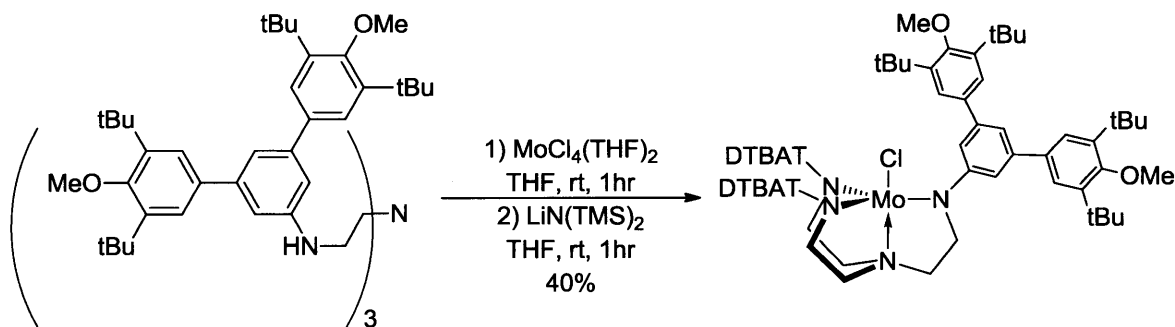


Figure 4.27: Synthesis of $[\text{DTBATN}_3\text{N}]\text{MoCl}$

$[\text{DTBATN}_3\text{N}]\text{MoN}_2\text{K}$ was synthesized *in situ* through the addition of KC_8 to a sample of $[\text{DTBATN}_3\text{N}]\text{MoCl}$ (Figure 4.28). A ν_{NN} of 1807 cm^{-1} was observed for $[\text{DTBATN}_3\text{N}]\text{MoCl}$ in C_6D_6 by IR spectroscopy, a ν_{NN} of 1798 cm^{-1} was observed for $[\text{DTBATN}_3\text{N}]\text{MoN}_2\text{K}$ in C_6D_6 by IR spectroscopy, a ν_{NN} of 1990 cm^{-1} was observed for $[\text{HIPTN}_3\text{N}]\text{MoN}_2\text{K}$.¹⁹ $[\text{DTBATN}_3\text{N}]\text{MoN}_2\text{K}$ was then oxidized to $[\text{DTBATN}_3\text{N}]\text{MoN}_2$ with $\text{Zn}(\text{OAc})_2$ and a ν_{NN} of 1984 cm^{-1} was observed by IR spectroscopy compared to $[\text{HIPTN}_3\text{N}]\text{MoN}_2$ which has a ν_{NN} of 1990 cm^{-1} .

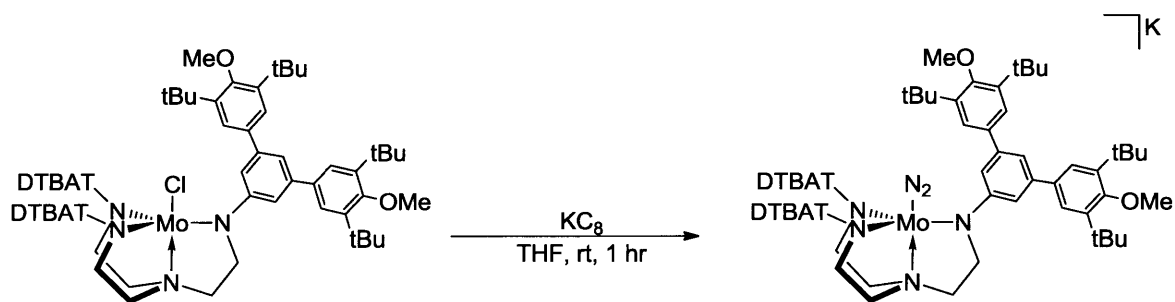


Figure 4.28: Synthesis of $[\text{DTBATN}_3\text{N}]\text{MoN}_2\text{K}$

Conclusions**Table 4.3: Summary of Catalytic Reactions**

Complex	Avg. Eq. of NH ₃
[HIPTN ₃ N]MoN	7.3
[<i>p</i> MeOHIPTN ₃ N]	6.5
[DTBATN ₃ N]	0.8

As with multiple previous attempts, improving the catalytic activity of the [N₃N] system appears to depend on the steric nature of the ligand system. The ligand system, [*p*MeOHIPTN₃N], which has the same steric constraints as [HIPTN₃N], proved catalytically active in the reduction of dinitrogen to ammonia (Table 4.3). This is the same result seen for [*p*BrHIPTN₃N], and in neither case, was the catalytic activity of the system improved. Since neither electronic change of the ligand appears to alter the catalytic activity of the system, it can be proposed that the steric constraints of the ligand, which protect key catalytic intermediates, were the most important aspect of the ligand system. The electron donating nature of the methoxy group does increase the rate of exchange of N₂ for ammonia. This increase does not translate into an increase in the yield of ammonia from the catalytic reaction of [*p*MeOHIPTN₃N]MoN. Since the yield of ammonia does not increase, it is likely that different intermediates or substrates (H₂, Chapter 2)²¹ are responsible for the failure of the [HIPTN₃N] systems, rather than a turnover rate problem.

In the case of the C_s symmetric ligand systems, it appears that reducing the steric bulk of just one amine arm has a drastic impact on the catalytic ability of the system (Table 4.3). Increasing the third amine arm from a mono-aryl to a terphenyl ligand, (TerPh) did not

provide enough steric encumbrance to sufficiently protect key intermediates, specifically $[(\text{TerPh})\text{HIPTN}_3\text{N}]\text{MoN}_2\text{H}$ which decomposes to $[(\text{TerPh})\text{HIPTN}_3\text{N}]\text{MoN}_2$ as was seen for previous C_s symmetric ligands.⁶ The nature and reactivity of $[(\text{TerPh})\text{HIPTN}_3\text{N}]\text{Mo}$ complexes parallel those observed for C_s symmetric ligands previously developed.⁶ Attempts to utilize larger terphenyl groups for the synthesis of C_s symmetric ligands proved difficult as the increasing solubility of these larger terphenyls made isolation of products low yielding (< 10%).

In an effort to synthesize a more crystalline catalyst compared to $[\text{HIPTN}_3\text{N}]\text{Mo}$, DTBA, and DTBAT were explored. DTBA was not greatly sterically encumbering, and though $[\text{DTBAN}_3\text{N}]\text{MoN}$ could be synthesized and was highly crystalline, no reactivity beyond this species was realized. The terphenyl, DTBAT, based on DTBA was also synthesized. The $[\text{DTBATN}_3\text{N}]$ system was more crystalline than $[\text{HIPTN}_3\text{N}]$ and the molybdenum complexes were easier to isolate. Unfortunately it appears that the positioning of the tert-butyl groups in the 3- and 5- positions does not provide sufficient steric protection for the reduction of dinitrogen to ammonia (Table 4.3). While using DTBAT with C_s symmetric ligands might provide a system that could prove catalytic, these systems were not explored as it was unlikely that the catalytic activity of these complexes would exceed $[\text{HIPTN}_3\text{N}]\text{Mo}$.

Experimental

General. Air and moisture sensitive compounds were manipulated utilizing standard Schlenk and dry-box techniques under a dinitrogen or argon atmosphere. All glassware was oven and/or flame dried prior to use. Pentane, diethyl ether, toluene, and benzene were purged with dinitrogen and passed through activated alumina columns. Benzene was additionally passed through a column containing copper catalyst. THF, heptane and tetramethylsilane were dried over Na/benzophenone, freeze-pump-thawed three times, and vacuum transferred. Nitrobenzene and fluorobenzene were dried over CaH_2 and distilled. All dried and deoxygenated solvents were stored in a dinitrogen-filled glove box over molecular sieves or in Teflon[®] sealed glass solvent bombs. Molecular sieves (4 Å) and Celite were activated at 230 °C *in vacuo* over several days. Br_2 , $Pd_2(dba)_3$, BINAP, TREN, *n*-BuLi, *t*-BuLi TMSN₃, and $MoCl_5$ were purchased from (Strem) and used as received. Cp_2^*Cr , $LiN(TMS)_2$, and $Zn(OAc)_2$ were purchased from Strem and purified by sublimation. 4-bromo-2,6-di-*tert*-butylphenol, (Aldrich) TRIPBr, PhBr, and NBS (Alfa Aesar), 2,6-dichloroaniline, (Matrix Scientific). KI, $MgSO_4$, and $NaSO_3$ (Mallinckrodt Baker Chemicals) were used as received. 2,6-TRIP₂(Phenol),¹¹ $MoCl_4(THF)_2$,²² KC_8 , $NMo(NMe_2)_3$,²³ $[H(Et_2O)_2][BAR'_4]$,⁸ $[CollH][BAR'_4]$, and $[LutH][BAR'_4]$ ⁹ were synthesized by published methods. All Mo and W complexes were stored under dinitrogen at -35 °C. ¹H, ¹³C, ¹⁹F and, ³¹P NMR spectra were recorded on a Varian Mercury 300 and Varian Inova 500 spectrometers. ¹H and ¹³C NMR Spectra are referenced to the residual protons in solvent for ¹H or solvent in ¹³C s relative to tetramethylsilane (δ 0 ppm). ¹⁹F NMR spectra were referenced externally to fluorobenzene (δ -113.15 ppm upfield of $CFCl_3$). ³¹P NMR spectra

were referenced externally to H₃PO₄ (δ 0 ppm). IR spectroscopy was performed on a FTIR spectrometer from and analyzed using IR spectroscopy software. UV-Vis spectroscopy was performed on an agilent 8315, and analyzed using Chem Station. Elemental analyses were performed by Midwest Microlabs, Indianapolis, Indiana, U.S.A. and H. Kolbe Mikroanalytisches Laboratorium, Mülheim an der Ruhr, Germany

H₃[(TerPh)HIPT₂N₃N]. To a 50 mL Schlenk bomb with a Teflon[®] stopper containing 50 mL of toluene, H₄[HIPT₂N₃N] (5.5 g, 4.96 mmol), TerPhBr (1.62 g, 5.24 mmol), and NaOtBu (1 g, 10.41 mmol) a Pd catalyst was added. The Pd catalyst was pre-formed by combining Pd₂(dba)₃ (0.024g, 26.21 μ mol) and BINAP (0.0483g, 77.6 μ mol) in 5 mL of toluene. The catalyst was allowed to stir overnight to yield an orange solution. The catalyst solution was then filtered through Celite into the reaction mixture and heated to between 85-90 °C for 24 hours. The reaction mixture was then filtered through Celite and the toluene was removed *in vacuo*. The crude solid was re-dissolved in hexanes. The hexanes solution was then filtered through a 300 mL frit loaded with silica gel to remove HIPTBr. Once the hexanes filtrate contained no HIPTBr as monitored by TLC, toluene was used to obtain H₃[(TerPh)HIPT₂N₃N], 4.18 g (3.13 mmol, 63 % yield). ¹H NMR: (C₆D₆, 20 °C) δ 7.53 (m, 2H, TerPh-3',3''H), 7.51 (m, 2H, TerPh-5',5''H), 7.24-7.08 (aryl region m, 15H, contains TerPh-2',2''-6'6''H, TerPh-4H, TerPh-4',4''H, HIPT-3',3''-5',5''-H) 6.75 (d, 2H, HIPT-4-H) 6.48 (br t, 2H, TerPh-2,6-H), 6.44 (m, 4H, HIPT-2,6-H), 3.7 (br s 3H, NH) 3.11 (septet, 8H, HIPT-2',6'-2'',6''-CH(CH₃)₂), 2.82 (septet, 4H, HIPT-4',4''-CH(CH₃)₂), 2.81 (m, 6 H, NCH₂CH₂ under methine) and 2.19 (br m, 6H, NCH₂CH₂), 1.4-1 (methyl region, 72 H, HIPT-CH(CH₃)₂). MS (ESI m/z) calcd. for C₉₆H₁₂₆N₄Na⁺: 1358.9914, found 1358.9914.

[(TerPh)HIPT₂N₃N]MoCl. In a 50 mL round bottom flask, H₃[(TerPh)HIPT₂N₃N] (2.63 g, 1.97 mmol), and MoCl₄(THF)₂ (0.82 g, 2.15 mmol) were added to 20 mL of THF. After allowing the reaction to proceed for an hour LiN(TMS)₂ (1.04 g, 6.2 mmol) was added slowly to avoid an exotherm, and the reaction was allowed to stir for an additional hour. The volatiles were then removed *in vacuo* and the resultant black solid was dissolved in pentane and the mixture was filtered through Celite. The solid product was then crystallized from pentane in two crops to afford a red solid, 1.20 g (0.83 mmol, 42% yield): ¹H NMR (C₆D₆, 20 °C) δ 11.7 (br s, ArH), 7.7-6.7 (br m, ArH's), 3.3-2.7 (br m, CHMe₂), 1.8-0.7 (br s, CH(CH₃)₂), -13 (br s, TerPhNCH₂CH₂) -19 (br s, HIPTNCH₂CH₂), -24 (br s, HIPTNCH₂CH₂), -73 (br s, TerPhNCH₂CH₂), -83 (br s, HIPTNCH₂CH₂). Anal. Calcd. for : C, 78.95; H, 8.63; N, 3.83; Cl, 2.62. Found: C, 78.73; H, 8.47; N, 3.83; Cl 2.42.

[(TerPh)HIPT₂N₃N]MoN. In a 50 mL Schlenk bomb, [HIPT₂(TerPh)N₃N]MoCl (400 mg, 0.273 mmol), was added to 25 mL of toluene and TMSN₃ (31 mg, 0.27 mmol). The reaction mixture was then heated to 90 °C overnight and results in a dark yellow solution. Toluene was then removed *in vacuo* and crude product was dissolved in pentane and filtered through Celite. Recrystallization from pentane in two crops gave a yellow solid, 270 mg (0.19 mmol, 69 % yield): ¹H NMR (C₆D₆, 20 °C) δ 7.84 (d, 2H, TerPh-2,6-*H*), 7.81 (d, 4H, HIPT-2,6-*H*), 7.52 (m 2H TerPh-3',3''-*H*), 7.50 (m 2H TerPh-5',5''-*H*), 7.34 (t 1H TerPh-4*H*), 7.26-7.1 (14H aryl region contain HIPT-3',5'-3'',5''-4 *H* and TerPh-3',5'-3''5''*H*) 6.67 (br t 2H TerPh-4',4'') 3.55 (br t, 4H, HIPT-NCH₂CH₂), 3.39 (br, t, 2H, TerPh-NCH₂CH₂), 3.1 (septet, 8H, HIPT-3',5'-3'',5''CH(CH₃)₂), 2.85 (septet, 4H, HIPT-4'-4'', CH(CH₃)₂) 2.00 (br m 6H includes HIPT-NCH₂CH₂ and TerPh-NCH₂CH₂), 1.28 (dd, 6H, HIPT-2',2''-CH(CH₃)₂), 1.80

(dd, 6H,HIPT-4',4''-CH(CH₃)₂), 1.07 (d, 6H,HIPT-6',6''-CH(CH₃)₂). Anal. Calcd. for C₉₆H₁₂₃MoN₅: C, 79.91; H, 8.59; N, 4.85. Found: C, 79.72; H, 8.65; N, 4.73.

Alternative Synthesis of [HIPT₂(TerPh)₃N₃N]MoN. In a 50 mL Schlenk bomb, NMo(NMe₂)₃ (34 mg, 0.10 mmol) was added to H₃[TerPhHIPT₂N₃N] (100 mg, 0.06 mmol) in 10 mL of toluene. The reaction was stirred at 60 °C, and turned dark yellow within 5 minutes. After 12 hours the reaction was cooled and toluene was removed under high vacuum. The remaining solid was extracted with pentane and the mixture was filtered through Celite to yield a bright yellow filtrate. The filtrate volume was reduced under vacuum until a yellow solid began to precipitate. The solution was then cooled to -35 °C for 12 hours and the product was collected on a glass frit, yield 61 mg (0.04 mmol, 57%). Characterization as reported previously.

[HIPT₂(3,5-diphenyl)₃N₃N]MoNN[Na(THF)_x]. In a 20 mL vial 500 mg of [(TerPh)HIPT₂N₃N]MoCl was added to a THF solution with 4.69 g of 0.5% Na/Hg amalgam. The reaction mixture was stirred for 2 hours and turned a dark purple. The reaction was then dried and filtered through Celite. Crystallization from pentane gave a purple solid, 360 mg (0.22 mmol, 65%).(THF coordination was assumed to be 2 equivalents per molybdenum center) ¹H NMR: (C₆D₆, 20 °C) δ 7.69-7.67 (m 6H, 2,6-HIPT 2,6-TerPh), 7.45 (m, 4H, 3',3''-5',5''-TerPh), 7.20-7.12 (Aryl region 14H, 3',3'', 5',5''-HIPT, 2',2'', 4',4'', 6',6''-TerPh), 6.46 (t, 2H 4-HIPT, 1H 4-TerPh) , 3.80 (m, 6H ,ArNCH₂CH₂), 3.33, 3.07 (septet, 8H, HIPT-3',5'-3'',5''CH(CH₃)₂), 2.86 (septet, 4H, HIPT-4'-4'', CH(CH₃)₂), 2.07 (br, t, 2H, TerPh-NCH₂CH₂), 1.99 (br t, 4H, HIPT-NCH₂CH₂) , 1.4-1.0 (HIPT-2',2'', 4',4'', 6',6''-CH(CH₃)₂, coordinated THF. IR: ν_{NN} at 1790 cm⁻¹.

[HIPT₂(3,5-diphenylphenyl)N₃N]MoN₂K. In a 20 mL vial, 200 mg of [HIPT₂(3,5-diphenylphenyl)N₃N]MoCl was stirred in 10 mL of THF and 50 mg of KC₈ is added. The reaction mixture was stirred for 3 hours producing a deep purple solution within 10 minutes. The volatiles were then removed *in vacuo* and the purple solid is dissolved into pentane and dried three times. The resultant purple solid was crystallized from pentane and isolated as a purple solid, 120 mg (0.08 mmol, 61%). ¹H NMR (C₆D₆, 20 °C) δ 7.64 (s, Ar), 7.46, (d, Ar), 7.39 (s, Ar), 7.21 (s, Ar), 7.13 (s, Ar), 7.11 (s, Ar), 7.07 (t, Ar) 7.04 (t, Ar), 7.03 (br s, Ar), 7.01 (t, Ar), 6.49 (s, Ar), 6.46 (s, Ar), 3.84 (m, backbone CH₂), 3.41 (sept, methine CH(CH₃)₂), 3.32-3.22 (m, overlapping methines CH(CH₃)₂), 2.80 (sept, methine CH(CH₃)₂), 2.19 (t, backbone CH₂), 2.08 (m, overlapping backbone CH₂), 2.00 (m, overlapping backbone CH₂), 1.25 (two d, two overlapping CH₃s) 1.22 (d, CH₃) 1.16-1.10, (m, multiple CH₃) 0.99 (d, CH₃). IR: ν_{NN} 1802 cm⁻¹. Anal. Calcd., for C₉₆H₁₂₃MoN₆K: C, 77.07; H, 8.29; N, 5.62. Found: C, 77.06; H, 8.30; N, 5.65.

[(TerPh)HIPT₂N₃N]MoN₂. In a 20 mL vial, 20 mg of Zn(OAc)₂ is added to a 5 mL THF solution containing 500 mg of [HIPT₂(3,5-diphenylphenyl)N₃N]MoN₂K. The solution begins to turn brownish-green within an hour, and the reaction is allowed to proceed for 16 hours. Volatiles are then removed *in vacuo*, and the solid extracted with pentane and filtered through Celite. A yellowish green solid was crystallized from pentane, 325 mg (0.23 mmol, 67 %) ¹H NMR (C₆D₆, 20°C): 19.7, (br s, 2H, NCH₂CH₂N) 18.7, (br s, 2H, NCH₂CH₂N) 16.3, (br s, 2H, NCH₂CH₂N) 7.4-6.4 (Aryl protons) 2.8 (m, 12H, 2,4,6,2'',4'',6''-CH(CH₃)₂), 1.8-0.4 (br m, Methyl protons), -6.5 (2,6-HIPT 2,6-TerPh), -27.2, (br s, 2H, NCH₂CH₂N), -31.1, (br s, 2H, NCH₂CH₂N), -32.9, (br s, 2H, NCH₂CH₂N); IR: ν_{NN} 1984 cm⁻¹.

Partial Synthesis of [(TerPh)HIPT₂N₃N]MoN₂H. In a 20 mL vial 100 mg of [(TerPh)HIPT₂N₃N]MoN₂K was dissolved in 2 mL of -35 °C Et₂O. To the Et₂O solution 15 mg of [Et₃NH][OTf] was added and stirred for 2 minutes. The solution was then rapidly dried *in vacuo* and the yellow-green solid dissolved in 2 mL of 5:1 pentane:toluene and filtered through Celite. The filtrate was again dried rapidly *in vacuo* and placed under vacuum on a Schlenk line to remove the last traces of toluene. The resultant dark yellow-green solid was then triturated with 0.5 mL of tetramethylsilane and placed in the freezer at -35 °C for 15 minutes until the solution becomes cold. The tetramethylsilane was then carefully removed using a micro syringe and the remaining solid triturated once more with 0.1 mL of cold tetramethylsilane which is removed again with a micro syringe. The resultant solid is then dried *in vacuo* to give a yellow-green solid in 53% yield which still contains some [(TerPh)HIPT₂N₃N]MoN₂. ¹H NMR (C₆D₆): δ 8.58 (br s, 1H, NNH), 7.65-6.44 (m, 27H, Aryl Region), 3.62, 3.51 (br t, 6H, Ar-NCH₂CH₂), 3.13 (br m, 8H, HIPT-2',6'-2'',6''CH(CH₃)₂), 2.84 (br m HIPT-4',4''-CH(CH₃)₂), 2.36 (q, N(CH₂CH₃)₃) 2.23, 2.08, (br t, 6H, Ar-NCH₂CH₂), 1.35-1.05 (m, 72H, Methyl Region).

General Method for Kinetic studies of [(TerPh)HIPT₂N₃N]MoN₂H decomposition. A solution of approximately of MoN₂K (30 mg, 0.02 mmol) in C₆D₆ (0.7 mL, 0.3 mM) was added to a 20 mL vial. An acid source, 0.9 equivalents, ([Et₃NH][OTf], [CollH][BAR'₄], [LutH][BAR'₄]) was then added and the solution was quickly filtered into a J-Young tube which was sealed removed from the nitrogen glove box and frozen in liquid nitrogen. The NMR tube was warmed prior to insertion into the NMR instruments. A file was set up to continuously record a ¹H NMR spectrum every 30 minutes, or a ¹H NMR spectrum was

taken every half hour with identical parameters. The area of the MoNNH peak was integrated versus time to calculate the half-life of MoNNH.

[[TerPh]HIPT₂N₃N]MoNH][BAr'₄]. In a 20 mL vial [(TerPh)HIPT₂(3,5-diphenyl)N₃N]MoN (200 mg, 0.14 mmol) was dissolved in diethyl ether and the solution was cooled to -30 °C. Another vial was charged with [H(Et₂O)₂][BAr'₄] (171 mg, 0.15 mmol) in 2 mL of diethyl ether and cooled to -30 °C. The nitride solution was stirred vigorously and the [H(Et₂O)₂][BAr'₄] solution was added drop-wise over 2 minutes. The solution turned deep red upon mixing, and the reaction was allowed to proceed until the solution has come to room temperature. Volatiles were then removed *in vacuo* and the resultant solid was then dissolved in pentane and filtered through Celite. The filtrate was dried *in vacuo* to yield a red solid, 239 mg. (0.10 mmol, 75%) ¹H NMR (C₆D₆, 20 °C): δ 8.39 (br s, 8H, C₆H₃-3,5-CF₃), 7.66 (br s, 4H, C₆H₃-3,5-CF₃), 7.44 (s, 1H, 4-TerPh), 7.25-7.11 (m, 18H, Aryl Region), 6.88 (s, 4H, 2,6-HIPT), 6.70 (s, 2H, 2,6-TerPh) 6.50 (br s, 1H, Mo-NH⁺), 3.65 (m, 4H, HIPT-NCH₂CH₂) 3.41 (t, 2H, TerPh-NCH₂CH₂), 2.86 (septet, 4H, 4'4''-HIPT, CH(CH₃)₂) 2.70 (septet, 8H, 3',5'- 3'',5''-HIPT, CH(CH₃)₂) 2.23 (m, 6H, HIPT-NCH₂CH₂), 1.39-0.96 (72H Methyl Protons); ¹⁹F NMR δ (C₆D₆, 20°C): -62.2 (s, CF₃).

2,4,6,2'',4'',6''-hexaisopropyl-[1,1':3',1''-terphenyl]-2'-ol Variation of 2,6-(TRIP)₂phenol synthesis. In a 1 L Schlenk flask, (50 g, 82.14 mmol) of 2,6-(TRIP)₂-iodobenzene was dissolved in 150 mL of anhydrous diethyl ether, and 350 mL of anhydrous pentane. The reaction mixture was cooled to -78 °C in a CO₂/acetone bath and 1.6 M n-BuLi (55 mL, 88 mmol) was injected slowly. The reaction mixture was allowed to slowly warm to room temperature, then re-cooled to -78 °C in a CO₂/acetone bath. Nitrobenzene (40 mL, 390 mmol) was added drop-wise to the cold solution. The solution turns dark red, and after 5

minutes of stirring and 400 mL of methanol were added slowly so the solution turns dark amber. Once the solution has warmed to room temperature the solution was extracted with 3 x 300 mL of ether and the combined organic fractions are dried over MgSO₄ treated with Na₂SO₃ (8 g 63.5 mmol) and the solids are filtered through Celite. The solvent was removed *in vacuo* and excess nitrobenzene was removed by vacuum distillation. The resultant solid was triturated with methanol to yield an off white solid. The off white solid was then purified by silica gel column chromatography to remove un-reacted 2,6-(TRIP)₂-iodobenzene which elutes in hexanes. 2,6-(TRIP)₂phenol was then flushed through the column by using ethyl acetate as the elutant. A white solid was then isolated by removal of volatiles *in vacuo*. Characterization data as reported.¹¹

5'-bromo-2,4,6,2'',4'',6''-hexaisopropyl-[1,1':3',1''-terphenyl]-2'-ol (3,5-(TRIP)₂-4-phenolbromide). In a 500 mL flask, of 2,6-(TRIP)₂phenol (15 g, 30 mmol) was slurried in 200 mL of glacial acetic acid. To the reaction mixture Br₂ (5 g, 31.3 mmol) was added, and the reaction was allowed to stir for 12 hours. Upon completion, a solution of 200 mL of water and Na₂SO₃ (5.9 g, 46.8 mmol) was added. The product was then collected on a frit and rinsed with a 10:1 methanol/acetone solution to yield an off white solid, 14 g, (20.8 mmol, 70 %): ¹H NMR (CDCl₃, 20° C): 7.24 (s, 2H, (TRIP)₂(HO)C₆H₂Br), 7.10 (s, 4H, iPr₃C₆H₂), 4.57 (s, 1H, OH), 2.95 (sept, *J*_{HH} = 6.9 Hz, 2H, 4',4''-CH(CH₃)₂) 2.71 (sept, *J*_{HH} = 6.7 Hz, 4H, 2',6',2'',6''-CH(CH₃)₂) 1.31 (d, *J*_{HH} = 7.0 Hz, 12H, Ar-CH₃) 1.17 (d, *J*_{HH} = 6.8 Hz, 12H, Ar-CH₃) 1.09 (d, *J*_{HH} = 6.8 Hz, 12H, Ar-CH₃). ¹³C NMR (CDCl₃, 20° C): 150.46, 149.43, 147.72, 132.54, 129.65, 128.83, 121.42, 112.23, 34.51, 30.92, 24.47 24.21. HRMS (ESI m/z): Calcd for C₃₆H₅₀BrO⁺: 577.3045, found 577.3040.

5'-Bromo-2,4,6,2'',4'',6''-hexaisopropyl-2'-methoxy-1,1':3',1''-terphenyl

2,6-(TRIP)₂anisolebromide. In a 1 L Schlenk flask 300 mL of THF was added to a NaH mineral oil dispersion (3.4 g, 142 mmol) and purged with nitrogen for 10 minutes. Under steady nitrogen flow, 2,6-(TRIP)₂phenolbromide (35 g, 60.6 mmol) was added slowly and the mixture was stirred for 12 hours. Excess NaH was removed by filtering the reaction mixture through a swivel frit into a 1 L 3-neck round bottom flask. The round bottom flask was kept under nitrogen flow and 12 g (84.5 mmol, 5.25 mL) of CH₃I is injected. The solution was then stirred for three hours. After an hour, NaI begins to precipitate out of solution and the reaction was allowed to stir for an additional 2 hours. The reaction mixture was then treated with 300 mL of distilled water. The resultant solution was extracted with 3 x 200 mL of diethyl ether and 100 mL of concentrated aqueous NaCl solution. The combined organic layers were dried with MgSO₄ and filtered through Celite. The volatiles were removed *in vacuo* and the resultant brown powder was triturated with methanol and recrystallized from hot chloroform to yield 30g. (50.7 mmol, 84%) ¹H NMR (CDCl₃, 20° C): δ 7.23 (s, 2H, (TRIP)₂CH₃OC₆H₂Br), 7.05 (s, 4H, iPr₃C₆H₂), 3.05 (s, 3H, CH₃OHIPT), 2.93 (sept, *J*_{HH} = 6.9 Hz, 2H, 4',4''-CH(CH₃)₂), 2.70 (sept, *J*_{HH} = 7.0 Hz, 4H, 2',6',2'',6''-CH(CH₃)₂), 1.30 (d, 12H, Ar-CH₃) 1.16 (d, 12H, Ar-CH₃) 1.13 (d, 12H, Ar-CH₃). ¹³C NMR (CDCl₃, 20° C): δ 155.14, 148.53, 146.65, 135.29, 133.50, 132.38, 120.96, 115.03, 34.44, 31.02, 25.37, 24.28, 23.61. HRMS (ESI *m/z*): Calcd. for C₃₇H₅₁BrONa⁺ 613.3021, found 613.2997.

Tris(2-(2,4,6,2'',4'',6''-hexaisopropyl-1,1':33',1''-terphenyl-2'-methoxy-5'-

amino)ethyl)amine H₃[*p*MeOHIPTN₃N]. In a 0-8, 150 mL Schlenk bomb, 50 mL of toluene was slurried with 2,6-(TRIP)₂anisole bromide (7.86 g, 13.3 mmol), TREN (590 mg,

4.03 mmol), and NaOtBu (1.74 g, 18.1 mmol) and Pd catalyst. The Pd catalyst was preformed by stirring Pd₂(dba)₃ (165 mg, 0.18 mmol) and BINAP (338 mg, 0.54 mmol) for three hours and was filtered through a sintered glass frit containing Celite into the Schlenk bomb. The reaction mixture was heated to 85 °C which dissolves the solids into the toluene solution, and stirred for 16 hours. After cooling, the solution was filtered through Celite and rinsed with 300 mL of toluene. The volatiles were removed *in vacuo* and the solid was dissolved in 1:1 toluene/hexanes. Product was isolated by column chromatography with 1:1 toluene/hexanes as the elutant followed by crystallization from acetone 3.82 g. Additional bi-substituted product was obtained by eluting the silica gel column with ethyl acetate. (2.28 mmol, 57%): ¹H NMR (C₆D₆, 20° C): δ 7.26 (s, 12H, iPr₃C₆H₂), 6.43 (s, 6H, (TRIP)₂CH₃OC₆H₂), 3.47 (br t, 3H, (CH₂)₂NH-Ar), 3.19 (sept, J_{HH} = 6.8 Hz, 6H, 4',4''-CH(CH₃)₂), 3.04 (s, 9H, OCH₃), 2.90 (sept, J_{HH} = 7.0 Hz, 12H, 2',6',2'',6''-CH(CH₃)₂), 2.82 (q, 6H, CH₂CH₂NH) 2.28 (t, J_{HH} = 6.2 Hz, 6H, CH₂CH₂NH) 1.40 (d, J_{HH} = 7.0 Hz, 36H, Ar-CH₃) 1.29 (d, J_{HH} = 6.9 Hz, 36H, Ar-CH₃) 1.24 (d, J_{HH} = 6.9 Hz, 36H, Ar-CH₃); ¹³C NMR: δ 148.27, 147.72, 146.68, 142.79, 134.15, 133.92, 120.73, 115.43, 59.70, 53.32, 42.05, 34.37, 30.84, 25.69, 24.32 23.68. MS ESI Calcd. for C₁₁₇H₁₆₉N₄O₃⁺: 1679.3228, found 1679.3209.

[pMeOHIPN₃N]MoCl. In a 50 mL Schlenk bomb H₃[pMeOHIPN₃N] (2.5 g, 1.49 mmol) was added to 10 mL of THF and MoCl₄(THF)₂ (566 mg, 1.49 mmol) and stirred at room temperature. After several minutes, MoCl₄(THF)₂ was no longer visible, and the solution turns dark red. After an hour of stirring, LiN(TMS)₂ (750 mg, 4.48 mmol) was added to the solution and stirred for another hour. The volatiles were then removed *in vacuo* at 60° C, and the remaining solid dissolved in pentane was filtered through Celite. The pentane was removed *in vacuo* and product was crystallized from tetramethylsilane at room

temperature, to yield 1.18 g of an orange solid. (0.65 mmol, 44%): ¹H NMR (C₆D₆, 20° C): δ 13.5, (br s, 6H, (TRIP)₂CH₃OC₆H₂) 7.45-7.06 (br, m, 12H, aryl region), 3.4-2.73, (br, m, 39H, 2,4,6,2'',4'',6''-CH(CH₃)₂, Ar-OCH₃) 2.2-0.75 (br m, 128H, Ar-CH(CH₃)₂), -19.9 (NCH₂CH₂N), -82.1 ((NCH₂CH₂N). Anal. Calcd. for C₁₁₇H₁₆₅ClMoN₄O₃: C, 77.77; H, 9.20; N, 3.10; Cl, 1.96. Found: C, 77.49; H, 9.15; N, 3.02; Cl 2.09.

[pMeOHIPTN₃N]MoN. In a 50 mL Schlenk Bomb, 10 mL of toluene was added to H₃[pMeOHIPTN₃N] (100 mg, 0.059 mmol) and NMo(NMe₂)₃ (30 mg 0.124 mmol). The reaction is then heated to 60° C for 4 hours and cooled. After filtering the solution through Celite and the volatiles were removed, and the resultant solid was then crystallized from tetramethylsilane to yield a yellow solid, 92 mg. (0.052 mmol, 86%) ¹H NMR (C₆D₆, 20° C): δ 7.35 (s, 6H, (TRIP)₂CH₃OC₆H₂), 7.28 (s, 12H, iPr₃C₆H₂), 3.44 (t, 6H, NCH₂CH₂N), 3.18 (sept, *J*_{HH} = 6.8 Hz, 12H, 2,6,2'',6''-CH(CH₃)₂), 3.04 (s, 9H, OCH₃), 2.92 (sept, *J*_{HH} = 7.0 Hz, 6H, 4',4''-CH(CH₃)₂), 1.90 (t, 6H, NCH₂CH₂N), 1.46 (d, *J*_{HH} = 7.0 Hz, 36H, Ar-CH₃), 1.32 (d, *J*_{HH} 7.0 Hz, 36H, Ar-CH₃), 1.15 (d, *J*_{HH} = 7.0 Hz, 36H, Ar-CH₃): Anal. Calcd. for C₁₁₇H₁₆₅MoN₅O₃: C, 78.70; H, 9.31; N, 4.14. Found: C, 78.36; H, 8.83; N, 4.14.

***In situ* [pMeOHIPTN₃N]MoN₂Na(THF)_x.** In a 20 mL scintillation vial, [pMeOHIPTN₃N]MoCl (118 mg, 0.065 mmol) was added to 10 mL of THF. To this solution Na sand (25 mg, 1.09 mmol) was added and the reaction was allowed to stir. After an hour the solution turns green. When THF was removed *in vacuo*, from an aliquot of the solution, the solid becomes dark purple. IR (THF): 1856 cm⁻¹ (ν(N-N(THF)_x)).

[pMeOHIPTN₃N]MoN₂. The remaining solution of [pMeOHIPTN₃N]MoN₂Na(THF)_x in THF was filtered through Celite into a stirring solution ZnCl₂/dioxane (30 mg, 0.134 mmol) in 5 mL of THF. The solution turned brown upon mixing and was allowed to stir for

an additional 10 minutes. The THF was then removed *in vacuo*, and the solids redissolved in pentane which was filtered through Celite. An un-optimized crystallization from heptane yielded a brown solid, 40 mg. (0.02 mmol, 34%): ¹H NMR (C₆D₆, 20° C): δ 21.2 (s, 6H, (TRIP)₂CH₃OC₆H₂), -7.6 (s, 6H, NCH₂CH₂N), -32.74 (s, 6H, NCH₂CH₂N); IR (C₆D₆): = 1986 cm⁻¹(ν(N-N)); 1920 cm⁻¹ (ν(N¹⁵-N¹⁵))

[pMeOHIPN₃N]MoNH₃[BAr'₄]. In a 50 mL Schlenk bomb, 10 mL of methylene chloride was added to [pMeOHIPN₃N]MoCl, (200 mg, 0.11 mmol) and NaBAr'₄ (113 mg, 0.128 mmol). In a separate 50 mL Schlenk Bomb, a mirror of Na metal was made and the flask was filled with an atmosphere of NH₃. The flask was then immersed in liquid N₂ and re-warmed three times to dry the ammonia. The two 50 mL Schlenk flasks were then connected by a vacuum-transfer bridge and the flask containing methylene chloride was degassed. Both flasks were opened and the NH₃ was condensed into the methylene chloride solution. After warming to room temperature and stirring for two hours, the solution turns deep red. The volatiles were removed *in vacuo* and the solid was dissolved in toluene and filtered through Celite. The toluene was removed *in vacuo*, and the solid triturated with pentane twice and tetramethylsilane once to remove a green solution yielding a ruby red solid, 263 mg. (0.10 mmol 90%): ¹H NMR (C₆D₆, 20° C) δ 8.28 (br s, 8H, BAr'₄), 7.62, (br s, 4H, BAr'₄), 7.32 (br s, 12H, Aryl) 3.4-2.7 (br, m, 39H, 2,4,6,2'',4'',6''-CH(CH₃)₂, Ar-OCH₃), 1.5-1.0 (Ar-CH₃), -16.2 (br s, 6H, NCH₂CH₂N) -105.3 (NCH₂CH₂N); ¹⁹F NMR (C₆D₆, 20° C): δ -62.2 (BAr'₄); Anal. Found Calcd., for C₁₄₉H₁₈₀BF₂₄MoN₅O₃: C, 67.49; H, 6.84; N, 2.64. Found: C,67.12; H, 6.47; N, 2.75.

Kinetic Studies of N₂ for ammonia exchange. In a 20 mL scintillation vial [pMeOHIPN₃N]MoNH₃[BAr'₄] (50 mg, 0.02 mmol) was added to 2 mL of heptane. With

stirring at medium speed (marked line on stirplate) of Cp_2^*Cr (7 mg, 0.02 mmol) was added. Aliquots of 0.5 mL were taken approximately every 20 minutes and observed by IR spectroscopy. Using the IR software integrations were taken of the resonance $\nu_{NN} = 1986\text{ cm}^{-1}$ and treated by first order kinetics and analyzed using Microsoft Excel.

Tris(2-((3,5-di-tert-butyl-4-methoxyphenyl)amino)ethyl)amine $H_3(DTBAN_3N)$. In a 100 mL Schlenk bomb, DTBABr (5 g, 16.7 mmol) was dissolved in 25 mL of Toluene. To the solution, TREN (0.81 g, 5.5 mmol), NaOtBu (2.01 g, 21.7 mmol) $Pd_2(dba)_3$ (76 mg, 0.084 mmol), and BINAP (148 mg, 0.16 mmol) were added and the flask was sealed and heated to 90°C for 16 hours. The reaction was then allowed to cool, filtered through Celite, and volatiles removed *in vacuo*. Product was isolated by a silica gel column using hexanes followed by toluene. The toluene fraction was taken and dried *in vacuo* resulting in a mixture of both product and an over-arylated product. The 72% over-arylated product was removed by crystallization from acetone. A white product was obtained in 21% yield (890 mg, 1.1 mmol). 1H NMR (C_6D_6 , 20°C): δ 6.66 (s, 6H, 2,6-ArH), 3.91 (br s, 3H, DTBA-NH), 3.48 (s, 9H, OCH_3), 3.01 (t, $J_{HH} = 6.0\text{ Hz}$, 6H, $NHCH_2CH_2N$) 2.44 (t, $J_{HH} = 5.9\text{ Hz}$, 6H, $NHCH_2CH_2N$) 1.51 (s, 54H, $ArCCH_3$); ^{13}C NMR ($CDCl_3$, 20°C): δ 151.88, 144.43, 143.48, 111.61, 64.47, 54.09, 42.76, 36.06, 32.44; HRMS (ESI m/z) Calcd. for $C_{51}H_{85}N_4O_3^+$: 801.6616, found 801.6603.

$[DTBAN_3N]MoN$. In a 20 mL scintillation vial with a small stirbar, $H_3(DTBAN_3N)$ (100 mg, 0.13 mmol) was dissolved in 10 mL of toluene. $NMo(NMe_2)_3$ (68 mg, 0.13 mmol) was added at room temperature and the solution was allowed to stir as the color changed from yellow to orange within a minute. After 10 minutes the solution became a gel-like and the vial was shaken to allow stirring to continue. After an additional 10 minutes the gel was

again shaken to promote stirring. After 10 additional minutes the volatiles were carefully removed as stirring was negligible. The solid was then triturated with 5 mL of pentane and isolated on a frit, as a yellow solid in 90% yield (92 mg, 0.10 mmol). ¹H NMR (C₆D₆, 20° C): δ 7.73 (s, 6H, ArH), 3.63 (br t, 6H, NCH₂CH₂N), 3.47 (s, 9H, Ar-OCH₃), 2.21 (br t, 6H, NCH₂CH₂N), 1.53 (s, 54H, ArCCH₃). Anal. Calcd. for C₅₁H₈₁MoN₅O₃: C, 67.45; H, 8.99; N, 7.71. Found: C, 67.23; H, 9.01; N, 7.42.

5'-Bromo-3,3'',5,5''-tetra-tert-butyl-4,4''-dimethoxy-1,1':3',1''-terphenyl

(DTBATBr). 100 mL of a THF solution containing of, 5-bromo-1,3-di-tert-butyl-2-methoxybenzene (DTBABr) (5g, 16.7 mmol) was added drop-wise to a 500 mL 3-necked round bottom flask containing of magnesium (800 mg, 32.9 mmol) in 100 mL of refluxing THF. The solution was refluxed for 2 hours, then a 50 mL solution of 2,4,6-tribromiodobenzene (2.5 g, 5.6 mmol) in THF was added drop-wise under reflux. The solution was allowed to reflux for an additional 2 hours, upon which time the solution was cooled and poured into 1L of ice-water. The mixture was separated with 3 x 100 mL portions of diethyl ether. The organic fractions were combined, and washed twice with water and once with a conc. aqueous NaCl solution. The organic fraction was then dried over MgSO₄, and the volatiles removed *in vacuo*. The resultant solid was triturated with methanol and isolated as a white powder. The white powder was crystallized from hot hexanes to yield a white solid, 3.1g (5.2 mmol, 56%): ¹H NMR (CDCl₃, 20° C): δ 7.66 (s, 1H, 2'-H) 7.65 (s, 2H, 4',6'-H), 7.51 (s, 4H, 2,6,2'',6''-H) 3.80 (s, 6H, 4,4''-OCH₃) 1.54 (s, 32H, 3,5,3'',5''-C(CH₃)₃); ¹³C NMR (CDCl₃, 20° C): δ 159.87, 144.48, 144.42, 134.50, 128.62, 125.83, 125.08, 123.11, 64.55, 36.156, 32.32; HRMS (ESI m/z) Calcd. for CHNOBr⁺: 593.2989, found 593.2976.

Tris(2-((3,5,3'',5''-di-tert-butyl-4,4''-methoxyphenyl)-1,1':3',1''-terphenyl-5'-amino)ethyl)amine H₃(DTBATN₃N). In a 100 mL Schlenk bomb, DTBATBr (3 g, 5.05 mmol), TREN (246 mg, 1.7 mmol), NaOtBu (630 mg, 6.6 mmol), Pd₂(dba)₃ (25 mg, 0.03 mmol), BINAP (50 mg, 0.1 mmol) were added to 50 mL of toluene. The flask was then sealed and heated to 90° C for 16 hours. The reaction was allowed to cool, filtered through Celite and the volatiles removed *in vacuo*. Product was isolated employing a silica gel column using hexanes as an elutant followed by toluene as an elutant. The toluene fractions was combined and dried over MgSO₄. Volatiles were removed *in vacuo* leading to an off white powder, 2.1 g (1.2 mmol, 72%). ¹H NMR (C₆D₆, 20° C): δ 7.78 (s, 12H, 2,6,2'',6''-H), 7.72(br s, 6H,) 7.53 (s, 3H, 2'-H), 6.99 (s, 6H, 4',6'-H) 3.75 (br s, 3H, DTBA-NHCH₂-), 3.39 (s, 18H, 4,4''- OCH₃) 3.08 (br t, 6H, NHCH₂CH₂N) 2.47 (t, 6H, NHCH₂CH₂N) 1.46 (s, 108H, 3,5,3'',5''-C(CH₃)₃); ¹³C NMR (CDCl₃, 20° C): δ 159.43, 148.91, 144.03, 143.96, 136.50, 126.03, 116.88, 110.88, 64.58, 53.82, 42.24, 36.21, 32.49. HRMS (ESI m/z) Calcd. for C₁₁₄H₁₆₃N₄O₆⁺: 1684.2567, found 1685.2662.

[DTBATN₃N]MoN. In a 50 mL Schlenk flask with a small stirbar, H₃[DTBATN₃N] (200 mg, 0.12 mmol) was dissolved in 10 mL of toluene. NMo(NMe₂)₃ (58 mg, 0.25 mmol) was added and the reaction was heated to 60 °C for 2 hours. The volatiles were removed *in vacuo* and the resultant solid was extracted with pentane and filtered through Celite. The resultant yellow solution was dried *in vacuo* and the resultant yellow solid was crystallized from tetramethylsilane to yield a yellow solid 170 mg (0.09 mmol, 80%). ¹H NMR (C₆D₆, 20° C): δ 7.96 (s, 6H, 4',6'-H), 7.91 (s, 3H, 2'-H), 7.89 (s, 12H, 2,6,2'',6''-H) 3.59 (t, J_{HH} = 4.77Hz, 6H, -NCH₂CH₂N), 3.39 (s,18H, 4,4''-OCH₃), 2.11 (t, J_{HH} = 5.48 Hz, 6H, -NCH₂CH₂N), 1.44

(s, 108H, 3,5,3'',5''-C(CH₃)₃); Anal. Found (Calcd., %) for C₁₁₄H₁₅₉MoN₅O₆: C, 75.43; H, 8.45; N, 3.91. Found: C, 75.96; H, 8.65; N, 3.72.

[DTBATN₃N]MoCl. In a 100 mL round-bottom flask, H₃[DTBATN₃N] (200 mg, 0.12 mmol) and MoCl₄(THF) (45 mg, 0.12 mmol) were added to 30 mL of THF and stirred for 1 hour at room temperature. LiN(TMS)₂ (65 mg 0.40 mmol) was added and the mixture was allowed to stir for an additional hour. The volatiles were removed *in vacuo* and the solid was dissolved in pentane and filtered through Celite. Product was isolated by crystallization from pentane, 87 mg (0.05 mmol, 40%). ¹H NMR (C₆D₆, 20° C): δ 7.78 (s, 12H, 2,6,2'',6''-H), 7.72 (br s, 6H, 4',6'-H), 6.99–3.41 (s, 18H, 4,4''-OCH₃), 1.43 (s, 108H, 3,5,3'',5''-C(CH₃)₃), -27 (br s, 6H, NCH₂CH₂N), -67 (br s, 6H, NCH₂CH₂N).

***In situ* synthesis of [DTBATN₃N]MoN₂K.** In a 20 mL scintillation vial [DTBATN₃N]MoCl (50 mg, .03 mmol) was added to 5 mL of THF. To this solution, excess KC₈ (11 mg, 0.09 mmol) was added and stirred for 1 hour. The THF solution was filtered through Celite and the volatiles were removed *in vacuo* resulting in a crude purple product. IR (C₆D₆): = 1807 cm⁻¹ (ν(N-N⁻)); ¹H NMR (C₆D₆, 20° C): δ 7.86 (s, 12H, 2,6,2'',6''-H), 7.77 (br s, 6H, 4',6'-H), 6.99 (s, 3H, , 2'-H), 3.93, (br t, 6H, NCH₂CH₂N), 3.38 (s, 18H, 4,4''-OCH₃), 2.16 (br t, 6H, NCH₂CH₂N), 1.46 (s, 108H, 3,5,3'',5''-C(CH₃)₃),

***In situ* synthesis of [DTBATN₃N]MoN₂.** To the crude purple of [DTBATN₃N]MoN₂K product an excess of Zn(OAc)₂ (10 mg, 0.01 mmol) was added resulting in a crude brown product. 1984 cm⁻¹ (ν(N-N)).

References

1. Schrock, R. R. *Acc. Chem. Res.* **1997**, *30*, 9.
2. a) Siedel, S. W.; Schrock, R. R. *Organometallics* **1998**, *17*, 1058. b) Greco, G. E.; O'Donoghue, M. B.; Seidel, S. W.; Davis, W. M.; Schrock, R. R. *Organometallics* **2000**, *19*, 1132.
3. a) Greco, G. E.; Schrock, R. R. *Inorg. Chem.* **2001**, *40*, 3850. b) Greco, G. E.; Schrock, R. R. *Inorg. Chem.* **2001**, *40*, 3861. c) Greco, G. E.; Popa, A. I.; Schrock, R. R.; *Organometallics* **1998**, *17*, 5591.
4. Yandulov, D. V.; Schrock, R. R. *Science* **2003**, *301*, 76.
5. Ritleng, V.; Yandulov, D. V.; Weare, W. W.; Schrock, R. R.; Hock, A. S.; Davis, W. M. *J. Am. Chem. Soc.* **2004**, *126*, 6150.
6. Weare, W. W.; Schrock, R. R.; Hock, A. S.; Müller P. *Inorg. Chem.* **2006**, *45*, 9185.
7. a) Du, C. J. F.; Hart, H.; Ng, K. K. D. *J. Org. Chem.* **1986**, *51*, 3162. b) Kehlbeck, J. D.; Dimise, E. J.; Sparks, S. M.; Ferrara, S.; Tanski, J. M.; Anderson, C. M. *Synthesis* **2007**, *13*, 1979.
8. Brookhart, M.; Grant, B.; Volpe, A. F. Jr. *Organometallics* **1992**, *11*, 3920.
9. Yandulov, D. V.; Schrock, R. R.; *Inorg. Chem.* **2005**, *44*, 1103.
10. a) Reithofer, M. R.; Schrock, R. R.; Muller, P. *J. Am. Chem. Soc.* **2010**, *132*, 8349. b) Yandulov, D. V.; Schrock, R. R. *Can. J. Chem.* **2005**, *83*, 34.
11. Stanciu, C.; Olmstead, M. M.; Phillips, A. D.; Stender, M.; Power, P. P. *Eur. J. Inorg. Chem.* **2003**, *18* 3495.
12. a) Vougioukalakis, G. C.; Chronakis, N.; Orfanopoulos, M. *Org. Lett.* **2003**, *5*, 4603.

-
13. Brown, M. L.; Eidam, H. A.; Paige, M.; Jones, P. J. Patel, M. K. *Bioorg. Med. Chem.* **2009**, *17*, 7056.
 14. Bates, R. B.; Siahaan, T. J.; Suvannachut, K.; Vasey, S. K.; Yager, K. M. *J. Org. Chem.* **1987**, *52*, 4605.
 15. Rajagopal, R.; Jarikote, D. V.; Lahoti, R. J.; Daniel, T.; Srinivasan, K. V. *Tetrahedron* **2003**, *44*, 1815.
 16. Gutsche, D. C.; Pagoria, P. F. *J. Org. Chem.* **1985**, *50*, 5795.
 17. a) Irlapari, N. R.; Baldwin, J. E.; Adlington, R. M.; Pritchard, G. J.; Cowley, A.R. *Tetrahedron* **2006**, *62*, 4603. b)
 18. a) Hartwig, J. F. *Nature* **2008**, *455*, 314. b) Surry, D. S.; Buchwald, S. L. *Angew. Chem., Int. Ed.* **2008**, *47*, 6338. Cacchi, S.; Fabrizi, G.; Goggiamani, A.; Licandro E. *Org. Let.* **2005**, *7*, 1497.
 19. Chin, J. *Syntheses and Studies of Molybdenum and Tungsten Complexes For Dinitrogen Reduction*. Ph.D. Thesis, Massachusetts Institute of Technology, Cambridge, MA, 2010.
 20. Atsuko, O.; Ito, H.; Sawamura, M. *J. Am. Chem. Soc.* **2006**, *128*, 16486.
 21. Hetterscheid, D. G. H.; Hanna, B. S.; Schrock, R. R. *Inorg. Chem.* **2009**, *48*, 8569.
 22. Stoffelbach, F.; Saurenz, D.; Poli, R. *Eur. J. Inorg. Chem.* **2001**, *10*, 2699.
 23. Johnson, M. J. A.; Lee, M. P.; Odom, A. L.; Davis, W. M.; Cummins, C. C. *Angew. Chem., Intl. Ed.* **1997**, *36*, 87.

Appendix A

Investigation of Triamidophosphine Ligands

Appendix A. Investigation of Triamidophosphine Ligands

Introduction

Some aryl substituted triamidoamine ligands, were synthesized by George Greco employing a DCC (dicyclohexylcarbodiimide) coupling.¹ DCC couplings are commonly used to couple primary amines with carboxylic acids to synthesize amino acids.² DCC couplings with TREN (TREN = (*N*¹,*N*¹-bis(2-aminoethyl)ethane-1,2-diamine), (H₂NCH₂CH₂)₃N) were typically low yielding and required multiple steps. When palladium cross-coupling between aryl bromides and amines were published the DCC synthetic route was no longer used.^{1,3} With our increased interest in synthesizing functionalized triamidophosphine (TRAP, 2,2',2''-phosphinetriyltriethanamine, [N₃P]) ligands (Figure A.1), we began to further investigate amide coupling reactions.

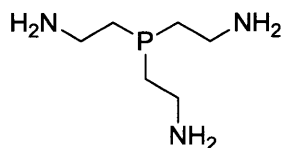


Figure A.1: TRAP or [N₃P] Ligand

Results and Discussion

A ligand with the steric bulk of HIPT (HexaIsoPropylTerphenyl, 2,4,6-2'',4'',6''-hexaisopropyl-1',3'-terphenyl)⁴ had not been reported with DCC coupling. Since the [N₃P] ligands are difficult to synthesize, HIPTNH₂ was reacted with 2,2',2''-nitrilotriacetic acid (Figure A.2) as a test reaction.

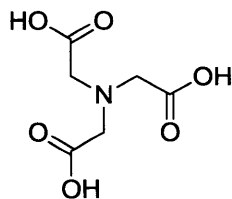


Figure A.2: 2,2',2''-nitrilotriacetic acid

HIPTNH₂ can be synthesized by a variety of routes. A synthesis performed by Nathan Smythe has been shown to be efficient but cost prohibitive as benzophenoneimine is expensive (Figure A.3).⁵

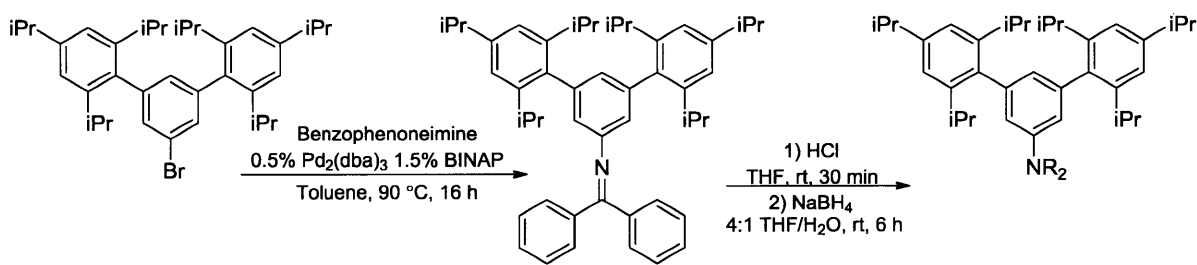


Figure A.3: Synthesis of HIPTNH₂ done by Nathan Smythe.

Other published routes, call for the palladium cross-couplings of HIPTBr with lithium hexamethyldisilazide⁶ or ammonia⁷ (Figure A.4).

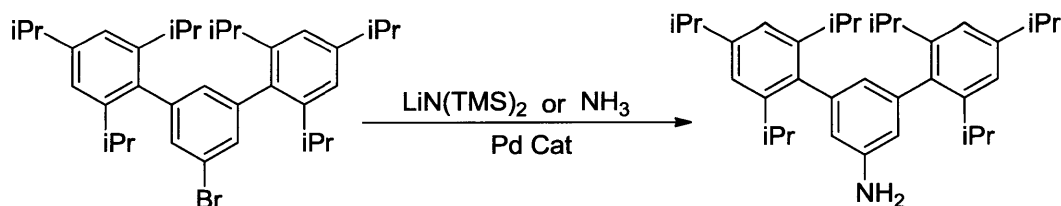


Figure A.4: General Palladium Cross-coupling Reactions for Synthesis of HIPTNH₂

DCC-couplings were performed by published methods.¹ The reaction employed THF and water in roughly a 1:1 ratio with one equivalent of 2,2',2''-nitrilotriacetic acid, three

equivalents of HIPTNH₂ and 1.1 equivalents of DCC. As the reaction proceeds by the mechanism shown in (Figure A.5) the intermediate *o*-acylisourea must undergo nucleophilic attack of the now activated carbonyl before an unproductive rearrangement occurs to form *N*-acylisourea. Reaction yields tend to be low because in the case of 2,2',2''-nitrilotriacetic acid the reaction must go through the correct pathway three times without a single rearrangement.

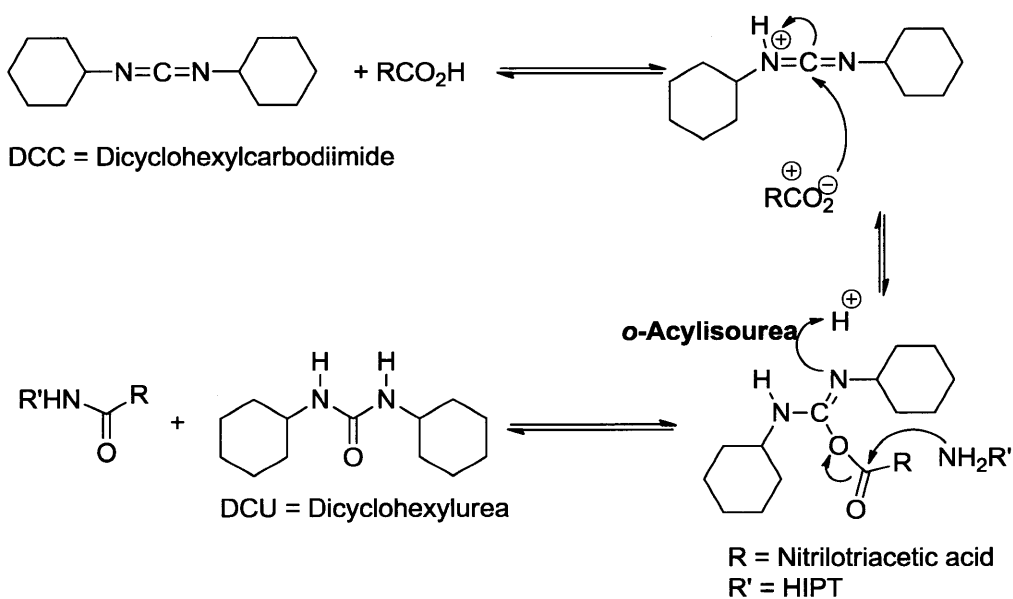


Figure A.5: DCC Coupling Mechanism

The reaction has a large concentration dependence because there is competition between product formation and intermolecular decomposition of *o*-acylisourea. The requirement for three successful nucleophilic substitutions per molecule of 2,2',2''-nitrilotriacetic acid, along with the steric influences of HIPT favors the decomposition pathway at published concentrations (1M). The major product, confirmed by ¹H NMR spectroscopy and MALDI-TOF (Matrix Assisted LASER Desorption Ionization Time of Flight), was an undesired decomposition product.

When the DCC coupling of 2,2',2''-nitrilotriacetic acid with HIPTNH₂ was run at high concentrations with excess HIPTNH₂, H₃[HIPT(N₃N)_{amide}] ([N₃N]_{amide} = Tris(2-(2,4,6,2'',4'',6''-hexaisopropyl-1,1':3',1'',3'''-terphenyl 5'-amide)ethyl)amine) was obtained. Separation of HIPTNH₂ and H₃[HIPT(N₃N)_{amide}] was achieved using a 4:1 hexanes/ethyl acetate elutant. While HIPTNH₂ and H₃[HIPT(N₃N)_{amide}] were separable by TLC, half of the fractions contained both compounds due to streaking on the column. A 12% isolated yield of H₃[HIPT(N₃N)_{amide}] was realized after one column, and the total isolated yield was increased to 54% by running additional columns.

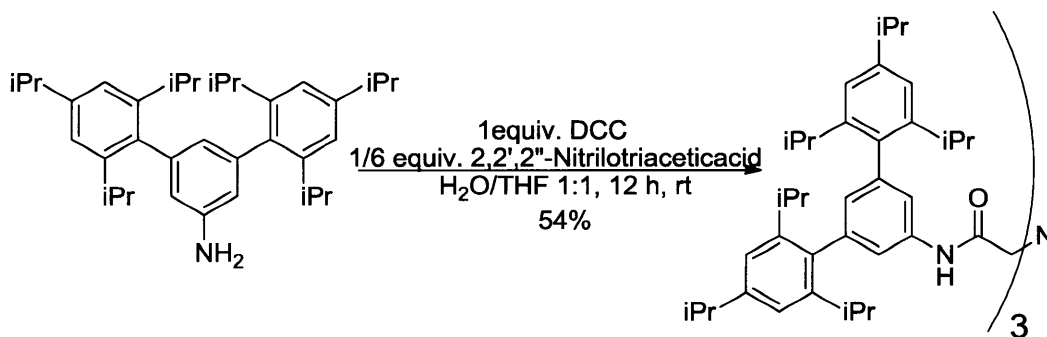


Figure A.6: Synthesis of H₃[HIPT((N₃N)_{amide})]

H₃[HIPT((N₃N)_{amide})] was utilized in an attempt to synthesize molybdenum complexes with a carbonyl in the ligand backbone. The nitride synthesis using NMo(NMe₂)₃, described in Chapter 2, yielded a paramagnetic complex as observed by ¹H NMR spectroscopy. Attempts to crystallize product only yielded crystallization of free ligand. The published method for metallation of ligand employing MoCl₄(THF)₂ was also attempted.⁴ To deprotonate the ligand LiN(TMS)₂ was tried first, but a milder base, Et₃N was also tried to avoid enol formation. After several minutes MoCl₄(THF)₂, which is typically insoluble in THF, appeared to be dissolved into the solution. The THF solution becomes brown-yellow,

suggesting a pre-complex was formed similar to those observed for [HIPTN₃N] complexes. Upon addition of LiN(TMS)₂ or Et₃N the color changed from yellow to orange. A ¹H NMR spectrum of the crude reaction mixture showed a paramagnetic substance was present in solution. Attempts to remove THF and crystallize product from pentane yielded only free ligand. One of the explanations for these problems may be the numerous tautomers available to amides (Figure A.7) that are not available for [N₃N] ligands. With the addition of a strong base the complex may have formed enols or iminols, which prevented the metal center from binding to the ligand. The carbonyl group may also coordinate to the metal center allowing the molybdenum precursor to be dissolved into solution, but rendering the complex unstable towards isolation.

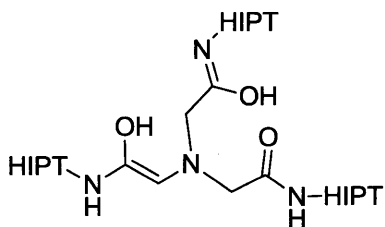


Figure A.7: Possible Tautomers of H₃[HIPT(N₃N)_{amide}]

TRAP

The functionalized TRAP (2,2',2''-phosphinetriyltriethanamine, (RNCH₂CH₂P)₃³⁻, N₃P) ligand analogous to TREN has been explored in our group.^{5,8} Nathan Smythe and Steven Kolchinski developed phosphorus ligands with various levels of functionalization, though triaryl-substituted TRAP remained elusive.^{5,8}

TRAP·3HCl (Figure A.8) was first synthesized by Steven Kolchinski,⁸ and slight modifications to the synthesis were made by Nathan Smythe.⁵ Prior to functionalization

TRAP·3HCl must be deprotonated, but low yields (~20%) have resulted. TRAP is a difficult ligand to synthesize on a large scale due to the use of PH_3 and tBuLi . Losing a significant amount of yield in the second step has made investigation of functionalized TRAP ligands difficult.^{5,8}

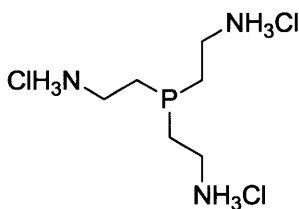


Figure A.8:TRAP·3HCl

TRAP·3HCl synthesized by Nathan Smythe showed one major resonance by ^{31}P NMR spectroscopy, at δ -46.5 ppm (reported) and two minor resonances at -35.80, -39.05 ppm (~ 5 %). The ^1H -NMR spectrum also showed some unidentified impurities. Elemental analysis of chlorine percentages of the compound suggests a combination of the *bis*- or *tris*- HCl salts. The TRAP·3HCl synthesized by Nathan Smythe was used for a handful of reactions in anticipation that the compound, which was water soluble, would become soluble in organic solvents upon deprotonation. Fresh TRAP·3HCl was also synthesized by published methods for further exploration.^{5,8}

Deprotonation of TRAP·3HCl by the reported procedures gives a 22% yield.^{5,8} In hopes of improving on the yield of TRAP various methods were attempted. Using THF, methanol, or diethyl ether with excess Et_3N , and heating to 80 °C did not produce higher yields. When TRAP·3HCl was dissolved in degassed water and excess NaOH was added, an oil (TRAP) was obtained in 60% yield (Figure A.9).

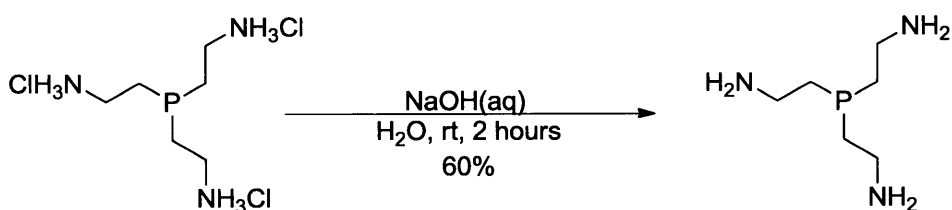


Figure A.9: Deprotonation of TRAP·3HCl

TRAP Chalcogenides

Nathan synthesized TRAP-oxide in an attempt to avoid phosphine coordination to palladium during the palladium cross-coupling reaction of TRAP with aryl bromide.⁵ TRAP-oxide was not soluble in either THF or toluene, which are common solvents employed for palladium cross-coupling reactions.^{3,5} To improve upon the solubility of protected TRAP ligands synthesizing TRAP-sulfide⁹ was investigated, and the sulfide would be removed after the amine was functionalized.¹⁰

Eight equivalents of sulfur were dissolved in benzene then added drop-wise to another benzene solution of TRAP. After fifteen minutes, the solution turned orange and an hour later a dark orange-red solid began to precipitate out of solution. A ³¹P NMR spectrum of the crude orange C₆D₆ solution obtained after the mixing of sulfur and TRAP contained two major resonances, δ 46.01, (60%) 46.74 (35%) ppm and another minor resonance 46.74 ppm (5%). After allowing the reaction to proceed for sixteen hours (Figure A.10), the ³¹P NMR spectrum remains unchanged, suggesting the reaction was complete in fifteen minutes. When the orange reaction mixture was filtered through Celite, a colorless solution was obtained. The orange-red solid removed with Celite was insoluble in common organic solvents kept in the dry-box, as well as water and methanol employed outside of the dry-box. As the volatiles were removed from the colorless filtrate *in vacuo*, another orange-red solid is

formed. The orange-red solid that resulted contained some soluble compound, which was extracted with methylene chloride. An off-white solid was obtained in 20% yield after filtration and removal of methylene chloride *in vacuo*. The off-white solid was not highly soluble in CH_2Cl_2 , THF, or toluene. A ^{31}P NMR spectrum taken in CD_2Cl_2 contains a phosphorus resonance at δ 46.01 ppm shifted downfield of starting material (TRAP -46.5 ppm (CD_2Cl_2)). Attempts to use the small amount of material (50 mg) obtained for a palladium cross-coupling reaction produced no recoverable ligand.

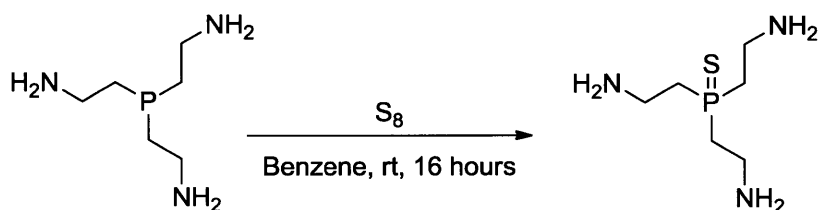


Figure A.10: Synthesis of TRAP-sulfide.

Silylated TRAP

With the difficulty in arylation of TRAP, the easier to install SiMe_3 group was tried. $\text{H}_3[(\text{TMS})_3\text{N}_3\text{P}]$ (Figure A.11) was first synthesized by Kolchinski, however no metal complexes were obtained with this ligand.⁸ Attempts to use $\text{MoCl}_3(\text{THF})_3$ or $(\text{MoCl}_4(\text{THF})_2)$ were unsuccessful in reactions with $[(\text{TMS})_3\text{N}_3\text{P}][\text{Li}_3]$. No Mo(VI) starting materials were employed by Kolchinski.⁸

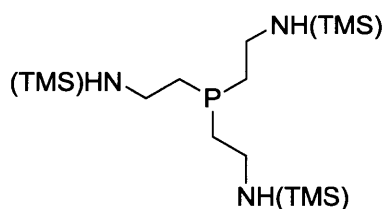


Figure A.11: $\text{H}_3[(\text{TMS})_3\text{N}_3\text{P}]$

$\text{NMo}(\text{NMe}_2)_3$ has been used to successfully metallate a variety of $[\text{N}_3\text{N}]$ ligands (Chapter 2). Using a Mo(VI) starting material limits possible red-ox chemistry, and the protonolysis reaction of $\text{NMo}(\text{NMe}_2)_3$ with $[\text{N}_3\text{N}]$ ligands was a clean way to form $[\text{N}_3\text{N}]\text{MoN}$ complexes.

$\text{H}_3[\text{TMS}_3\text{N}_3\text{P}]$ was synthesized by published methods⁸ and reacted with one equivalent of $\text{NMo}(\text{NMe}_2)_3$. A downfield shift of the phosphine resonance from $\delta -47.14$ ppm for $\text{H}_3[(\text{TMS})_3\text{N}_3\text{P}]$ to $\delta 35.29$ ppm was observed in the ^{31}P NMR spectrum. Two minor peaks were also observed at $\delta 42.38$ and 37.90 ppm in the ^{31}P NMR spectrum. No remaining resonances corresponding to starting material are observed by ^1H NMR spectroscopy. The ^1H NMR spectrum is diamagnetic; however, assignment of resonances was not possible due to the multiple products which were present. No single product was isolable from this reaction mixture. When two equivalents of $\text{NMo}(\text{NMe}_2)_3$ were reacted with $\text{H}_3[(\text{TMS})_3\text{N}_3\text{P}]$, 80% of the excess $\text{NMo}(\text{NMe}_2)_3$ was recovered by crystallization. No ^{31}P NMR resonance was observed in the ^{31}P NMR spectrum of the material.

A proposed method to avoid a palladium cross-coupling was to first add the aryl group to 2-chloroethylamine. Unsuccessful attempts were also made to use an *N*-functionalized 2-chloroethylamine, which could be reacted with a phosphorus source to form a functionalized $[\text{N}_3\text{P}]$ ligand. More than one substitution was not achieved by this method and only LPH_2 (L = *N*-phenylethylamine, *N*-Boc-*N*-HIPTethylamine; Boc = tertbutoxycarbonyl) was recovered.^{5,8} With the Boc protected amine additional reactions of LPH_2 with tBuLi produced no results. Since Boc contains a carbonyl which is unfavorable when using tBuLi ,³ attempts to use a more tolerant protecting group such as TBS (TBS = tert-butyldimethylsilane) or TMS were tried. Silyl protected *N*-aryl-2-chloroethylamine closely resemble the STABASE

(1,2-*Bis*(chlorodimethylsilyl)ethane) protected amine that was used successfully for the synthesis of TRAP·3HCl.^{5,8}

Previous attempts to synthesize tri-functionalized [N₃P] ligands by addition of ethylene ligands in our lab employed amines instead of amides.^{5,8} Amides were an attractive alternative because they are cost effective and easy to synthesize. Instead of initially using HIPT based ligands, the simpler to synthesize 2-chloro-*N*-phenylacetamide¹¹ ligand was explored to pre determine reactions conditions.

Chloroethylamine ligands are susceptible to the formation of aziridines when strong bases are used,⁵ so the amide was first protected. Attempts to protect the amide with a silyl group were met with mixed results. Deprotonating 2-chloro-*N*-phenylacetamide with Et₃N and adding TMSCl gave 2-chloro-*N*-phenyl-*N*-(trimethylsilyl)acetamide. The unprotected amide resonance was still observed by ¹H NMR spectroscopy at δ 8.26 ppm as 2-chloro-*N*-phenyl-*N*-(trimethylsilyl)acetamide is deprotected by trace water in the air and NMR solvents. Employing TBSCl produced similar results, despite its added steric bulk.

Since the silyl protected amide was moisture sensitive and silyl protected amines are less moisture sensitive, methods to remove the carbonyl were explored. The use of lithium aluminum hydride (LAH) produces alumina, which inhibits product isolation, especially with a phosphine present. As alternatives, sodium *bis*(2-methoxyethoxy)aluminumhydride (Red-Al[®]) and lithium triethylborohydride (LiHBEt₃) were used.

Employing 2-chloro-*N*-phenylacetamide to test reduction conditions of the amide, it was found that Red-Al[®] reduced the amide but produced many side products. The crude product was run through a plug of silica gel and 2-chloro-*N*-phenylamine was obtained in low yield (10%). Employing LAH also yielded 2-chloro-*N*-phenylamine though in low yield (25%).

There were two new resonances observed by ^1H NMR spectroscopy, δ 3.65 and 3.40 ppm integrating as two protons each, corresponding to the methylene protons rather than a single resonance at 4.30 ppm expected for the amide.

To synthesize trialkyl phosphines another proposed method was to use an alkyl Grignard and react that with a phosphite. The reaction of an alkyl Grignard with triphenyl phosphite has been shown to work for the synthesis of PMe_3 .¹² As a test reaction a THF solution of the STABASE protected 2-chloroethylamine was added to magnesium and refluxed for three hours after which the reaction mixture was cooled to 0 °C and a third of an equivalent of triphenylphosphite was added drop-wise over 15 minutes. The solution was heated to 50 °C and stirred for two hours. The color of the solution did not change over this time, and aliquots were periodically removed for ^{31}P NMR spectroscopy. Two resonances were observed by ^{31}P NMR spectroscopy: the first at δ 129.1 ppm, corresponded to triphenylphosphite, and new a second resonance at δ 146.4 ppm. With the reaction appearing incomplete by ^{31}P NMR spectroscopy, the mixture was refluxed for six hours at 100 °C. No change in the ^{31}P NMR spectrum resulted. The new product was isolated and found to be $(\text{PhO})_2\text{PCH}_2\text{CH}_2\text{N}(\text{STABASE})$ by integration of the ^1H NMR spectrum versus TMS_2O as the internal standard (Figure A.12).

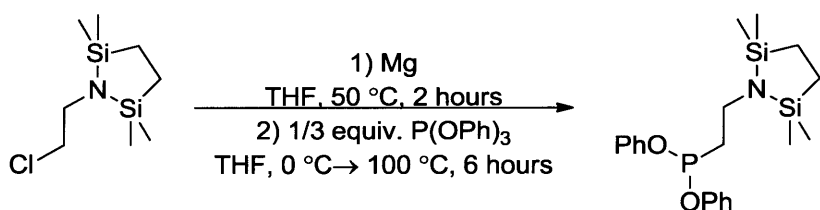


Figure A.12: Attempted Synthesis of Functionized $[\text{N}_3\text{P}]$.

Propyl Phosphine Ligands

Phosphine ligands containing three carbons in the backbone have also been explored and *tris*(cyanoethyl)phosphine was synthesized by Kolchinski.⁸ Unfortunately, the nitrile was not reduced to the amine by conventional methods.⁸ Presumably the phosphine bound to palladium on the Pd/C catalyst, preventing reduction.⁸ Instead *tris*(cyanoethyl)phosphine was hydrolyzed to the carboxylic acid (*tris*(2-carboxyethyl)phosphine = 3,3',3''-phosphinetriyltripropanoic acid = TCEP) with HCl_(aq).³

Tris(2-carboxyethyl)phosphine TCEP

While three carbon tertiary phosphine ligands were not the desired product they were easier to use for initial synthetic studies. *Tris*(2-carboxyethyl)phosphine (TCEP) was synthesized by hydrolysis of *tris*(cyanoethyl)phosphine (3,3',3''-phosphinetriyltripropanenitrile), which resulted in TCEP·HCl.⁵ Elemental analysis showed a much higher chlorine percentage suggesting a varying amount HCl. TCEP·HCl can be deprotonated by NaOH however, this was unnecessary when the ligand was oxidized with H₂O₂ to the phosphine oxide.^{5,9a} When TCEP was not oxidized to TCEP-oxide before performing the DCC reactions, separation by chromatography was problematic. Due to the high polarity of a *tris*-amide phosphine oxide that would be synthesized, it was decided to use HIPT instead of the smaller analogue previously described. The inclusion of HIPT aided in the solubility of the products in organic solvents.

DCC Coupling of TCEP with HIPT

The DCC coupling was performed in the same fashion as the prior DCC coupling of HIPTNH₂ with trinitriloacetic acid (Figure A.6). A two-fold excess of HIPTNH₂ was used with 1:1 water/THF as the solvent. DCC was added to a mixture of TCEP-oxide and HIPTNH₂ in THF and water at 5 °C and stirred overnight. DCU, (DCU = dicyclohexylurea) which precipitated out of solution overnight, was filtered off using Celite and volatiles were removed *in vacuo*. A TLC employing 50/50 ethyl acetate/hexanes elutant contained three spots. The fastest spot which eluted with an R_f of 0.99, corresponded to the HIPTNH₂. The second spot, R_f 0.3, and third spot, R_f 0.0, were presumed to be H₃[HIPTN₃P_(propyl-amide)] (H₃[HIPTN₃P_(propyl-amide)] = Tris(2-(2,4,6,2'',4'',6''-hexaisopropyl-1,1':3',1'',3'-terphenyl 5'-amide)ethyl)phosphine) and the decomposition products observed for other DCC couplings respectively.¹ The decomposition product lacked a HIPT group on at least one arm and required THF to remove it from the column.

The second spot was removed from the column using neat ethyl acetate after unreacted HIPTNH₂ was recovered. H₃[HIPTN₃P_(propyl-amide)] was then crystallized from hot chloroform in 15% yield.

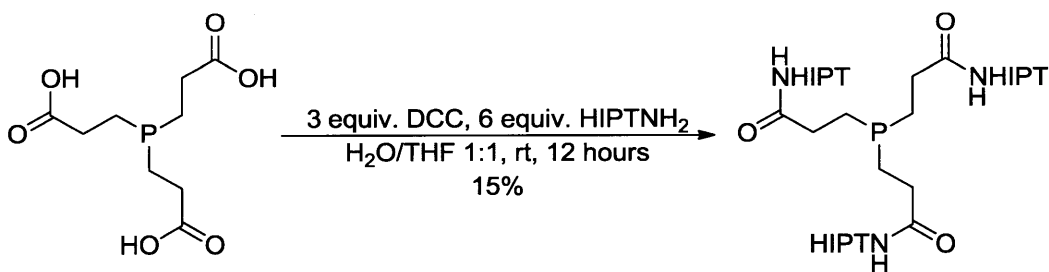


Figure A.13: Synthesis of H₃[HIPTN₃P_(propyl-amide)]

A ^1H NMR spectrum was taken with the aryl resonances and amide resonance at δ 8.39 ppm integrating to a 1:1 ratio of HIPT to each amide. The ^{31}P NMR spectrum contains a single resonance δ 51.36 ppm compared to δ 55.63 ppm for TCEP-oxide showing there is not much of an electronic influence on the phosphorus from the HIPT ligands.

A MALDI-TOF spectrum contained an observed peak of 1728 m/z and calculated $[\text{C}_{117}\text{H}_{162}\text{N}_4\text{O}_3\text{Na}]^+$ is 1728.52. The isotope distribution of the product also matches that predicted for $\text{H}_3[\text{HIPTN}_3\text{Npropyl}(\text{amide})]$. With the successful result of having a DCC coupling working for the three carbon ligand, the two carbon ligand may prove a successful route to incorporating HIPT onto TRAP.

Multiple ways can be thought of to synthesize the two carbon TCMP (TCMP = triscarboxylicmethylene phosphine, 2,2',2''-phosphinetriyltriacetic acid). The first is to use the same route as TCEP by synthesizing *tris*(cyanomethyl)phosphine, (2,2',2''-phosphinetriyltriacetonitrile, TCMP) and hydrolyzing it with $\text{HCl}_{(\text{aq})}$. *Tris*(cyanomethyl)phosphine can be synthesized by a route developed by Kolchinski using bromoacetonitrile.⁸

A published synthesis of TCMP starts from trimethylsilyl 2-chloroacetate and reacts it with $\text{P}(\text{SiMe}_3)_3$, which is commercially available to synthesize $\text{P}(\text{CH}_2\text{CO}_2\text{SiMe}_3)_3$, which is deprotected by treatment with methanol.¹³ There may be a number of ways to synthesize $\text{P}(\text{CH}_2\text{CO}_2\text{H})_3$, which would allow the synthesis of $(\text{O})\text{P}(\text{CH}_2\text{C}(\text{O})\text{NH}\text{HIPT})_3$ through methods described above. If the HIPT functionalized TRAP ligand is of interest, this may be a way to synthesize it, albeit with a considerable number of synthetic steps.

Experimentals

General. Air and moisture sensitive compounds were manipulated utilizing standard Schlenk and dry-box techniques under a dinitrogen or argon atmosphere. All glassware was oven and/or flame dried prior to use. Pentane, diethyl ether, toluene, and benzene were purged with dinitrogen and passed through activated alumina columns. Benzene was additionally passed through a column containing copper catalyst. THF, heptane and tetramethylsilane were dried over Na/benzophenone, freeze-pump-thawed three times, and vacuum transferred. Nitrobenzene and fluorobenzene were dried over CaH_2 and distilled. All dried and deoxygenated solvents were stored in a dinitrogen-filled glove box over molecular sieves or in Teflon[®] sealed glass solvent bombs. 2-chloro-N-phenylacetamide,¹¹ TRAP·HCl,⁵ TRAP,⁵ [(TMS)N₃P],⁵ and TCEP⁵ were synthesized by published methods. 2,2',2''-nitrilotriacetic acid, S₈, DCC, TMSCl, TBSCl, bromobenzene (Alfa Aesar), PH₃ (Sigma Aldrich), 2-chloroacetic acid (TCI), nBuLi, and tBuLi (Strem) were purchased and used as received unless otherwise noted. Molecular sieves (4 Å) and Celite were activated at 230 °C *in vacuo* over several days. All Mo and W complexes were stored under dinitrogen at -35 °C. ¹H, ¹³C, ¹⁹F and, ³¹P NMR spectra were recorded on a Varian Mercury 300 and Varian Inova 500 spectrometers. ¹H and ¹³C NMR Spectra are referenced to the residual protons in solvent for ¹H or solvent in ¹³C s relative to TMS (δ 0 ppm). ¹⁹F NMR spectra were referenced externally to fluorobenzene (δ -113.15 ppm upfield of CFCl₃). ³¹P NMR spectra were referenced externally to H₃PO₄ (δ 0 ppm). IR spectroscopy was performed on a FTIR spectrometer from and analyzed using IR spectroscopy software. UV-Vis spectroscopy was

performed on an agilent 8315, and analyzed using Chem Station. Elemental analyses were performed by Midwest Microlabs, Indianapolis, Indiana, U.S.A.

H₃[HIPT(N₃N)_{amide}] Tris(2-(2,4,6,2'',4'',6''-hexaisopropyl-1,1':3,1'',3''-terphenyl 5'-amide)ethyl)amine. HIPTNH₂ (3.9g, 7.83 mmol) was dissolved in 18 mL of THF and added to a 250 mL round bottom flask cooled to 0° C. 2,2',2''-nitrilotriacetic acid (234 mg, 1.22 mmol) was then dissolved in 30 mL of water and added to the round bottom. DCC (1.44 g, 6.98 mmol) dissolved in 9 mL of THF was added drop-wise over 5 minutes. The reaction was warmed to room temperature and a white precipitate formed as the reaction was allowed to stir for 12 hours. The white precipitate was removed by filtration through Celite and rinsed with THF. The volatiles in the filtrate were removed *in vacuo* and the resultant white solid was run through a silica gel column using 4:1 hexanes/ethyl acetate as the elutant. Some overlap of aniline and ligand resulted and two additional columns were run yielding a white solid, 1.1 g. (0.675 mmol, 54%): ¹H NMR (CDCl₃, 20° C): δ 8.39 (br s, 3H, NCH₂C(O)NH), 7.39 (s, 6H, 2',6'-H), 7.00 (s, 12H, 3,5-3'',5''-H) 6.76 (s, 3H, 4'-H), 3.69 (br s, 6H, NCH₂C(O)NH), 2.93 (sept, *J*_{HH} = 6.8 Hz, 6H, 4',4''-CH(CH₃)₂), 2.69 (sept, *J*_{HH} = 6.9 Hz, 12H, 2',6',2'',6''-CH(CH₃)₂), 1.31 (d, *J*_{HH} = 6.9 Hz, 36H, Ar-CH₃), 1.04 (d, *J*_{HH} = 6.8 Hz, 36H, Ar-CH₃), 1.02 (d, *J*_{HH} = 6.9 Hz, 36H, Ar-CH₃); ¹³C NMR (CDCl₃, 20° C): 168.86, 147.97, 146.49, 141.65, 137.14, 136.50, 128.02, 120.60, 119.16, 59.23, 34.49, 30.57, 24.46, 24.33. HRMS (ESI) *m/z* calcd. for C₁₁₄H₁₅₇N₄O₃⁺: 1631.2289, C₁₁₄H₁₅₆N₄O₃Na⁺: 1653.2108, found, 1631.2303, 1653.2080.

H₃[HIPT(N₃P)_{amide}] Tris(2-(2,4,6,2'',4'',6''-hexaisopropyl-1,1':3,1'',3''-terphenyl 5'-amide)ethyl)phosphine. HIPTNH₂ (6 g, 12.05 mmol) was added to TCEP (360 mg, 1.37 mmol) in 18 mL of THF and 9 mL H₂O. A 10 mL solution of DCC_(aq) (2g, 1M) was added

drop-wise to the HIPTNH₂ and TCEP solution at 5 °C. The reaction was allowed to stir for 16 hours overnight, then filtered through Celite to remove DCU. The solution was then extracted with ethyl acetate, and the organic fractions were combined, dried over MgSO₄ and volatiles were removed *in vacuo*. The resultant white solid was purified by silica gel column chromatography using 4:1 hexanes:ethyl acetate. Product was isolated from fractions containing product (second spot by TLC) by removal of volatiles *in vacuo*. A white solid was resulted in, 320 mg (0.19 mmol, 15%). ¹H NMR (CDCl₃, 20 °C): 8.22 (br s, 3H, PCH₂CH₂C(O)NH), 7.35 (s, 6H, 2',6'-H), 7.01 (s, 12H, 3,5-3'',5''-H) 6.76 (s, 3H, 4'-H), 4.08 (d, 6H, PCH₂CH₂C(O)NH), 3.48 (m, *J*_{PH} = 10.8 Hz, 6H, PCH₂CH₂C(O)NH), 2.91 (sept, *J*_{HH} = 6.76 Hz, 6H, 4',4''-CH(CH₃)₂), 2.72 (sept, *J*_{HH} = 6.9 Hz, 12H, 2',6',2'',6''-CH(CH₃)₂), 1.95 (d, *J*_{HH} = 6.9 Hz, 36H, Ar-CH₃), 1.28 (d, *J*_{HH} = 6.8 Hz, 36H, Ar-CH₃), 1.02 (d, *J*_{HH} = 6.9 Hz, 36H, Ar-CH₃); {H}³¹P NMR (C₆D₆, 20 °C): δ 51.36 P(CH₂-) MS (MALDI-TOF) m/z calcd. for C₁₁₇H₁₆₂N₄O₄PNa⁺: 1728.2234, found 1728.

References

-
1. Greco, George. *Molybdenum and Tungsten Complexes of Dinitrogen, CO, and Isocyanides that Contain Aryl-Substituted Triamidoamine Ligands* Ph. D. Thesis Mass. Inst. Tech., Cambridge, MA, 2001.
 2. a) Kurzer, F.; Douraghi-Zadeh, K. *Chem. Rev.* **1967**, *67*, 107. b) Khorana, H. G. *Chem. Rev.* **1953**, *53*, 145.
 3. a) Hartwig, J. F. *Nature* **2008**, *455*, 314. b) Surry, D. S.; Buchwald, S. L. *Angew. Chem., Int. Ed.* **2008**, *47*, 6338. Cacchi, S.; Fabrizi, G.; Goggiamani, A.; Licandro E. *Org. Lett.* **2005**, *7*, 1497.
 4. Yandulov, D. V.; Schrock, R. R., *Inorg. Chem.* **2005**, *44*, 1103.
 5. Smythe, Nathan. *Vanadium and Chromium Complexes Supported by Sterically Demanding Ligands. Studies Relevant to the Reduction of Dinitrogen to Ammonia.* Ph. D. Thesis, Thesis Mass. Inst. Tech., Cambridge, MA, 2006.
 6. Lee, S.; Jørgensen, M.; Hartwig, J. F. *Org. Lett.* **2001**, *3*, 2729.
 7. Surry, D. S.; Buchwald, S. L. *J. Am. Chem. Soc.* **2007**, *129*, 10354.
 8. Unpublished Results, Alexander Kolchinski, Post Doctoral Fellow, Schrock Group, Massachusetts Institute of Technology.
 9. a) Monkowius, U.; Nogai, S.; Schmidbaur, H. *Organometallics*, **2003**, *22*, 145. b) Field, L. D.; Wilkinson, M. P. *Tetrahedron Lett.* **1997**, *38*, 2779.
 10. Griffith, D. V.; Groombridge, H. J.; Mahoney, P. M.; Swetnam, S. P.; Walton, G. York, D. C. *Tetrahedron* **2005**, *61*, 4595.
 11. Harte, A. J.; Gunnlaugsson, T. *Tetrahedron Lett.* **2006**, *47*, 6321.

12. Luetkens Jr., M. L. *Inorg. Synth.* **1989**, 26, 7.
13. Tzchach, A.; Sieglinde, F. *Z. Chem.* **1979**, 19, 375.

Appendix B

Alterations of the Catalytic Apparatus

Appendix B. Alterations of the Catalytic Apparatus

Introduction

The original design of the catalytic reactor (standard apparatus) developed by Yandulov¹ for the reduction of dinitrogen to ammonia has proven effective for multiple years.² The set up required for a catalytic reaction with the standard apparatus is complex and problems arise that require the reaction to be abandoned or that cause the the catalyst to not reduce dinitrogen to ammonia. Through prolonged use, the apparatus wears down and must be replaced. We attempted to make improvements and modify the apparatus, as discussed below.

Syringe barrels used to manufacture the glass reactor are formed within a stringent variance allowance; however, the magnet drive that was fashioned to inject the Cp^*Cr solution from the syringe barrel into the receiving flask are not always universal for each apparatus employed in the lab. Non-uniformity between each apparatus was a common problem. The Teflon[®] plunger tips were typically bought from Hamilton, while the syringe barrels were purchased from Kloehn, because they made from the proper quality glass for manipulation and Hamilton syringe barrels were not. The higher quality glass allowed them to be manipulated to form the apparatus without deforming the syringe barrel. The Hamilton Teflon plunger tips can be purchased from Hamilton as replacement parts but must be ground uniformly, employing 600 grit sandpaper, by hundredths of a millimeter, so they could be driven using the magnets described later.

Changes to the Magnetic Drive

In an effort to alleviate the issue of using multiple brands of equipment, while employing the same reactor design, the syringe plungers provided along with the syringe barrels by Kloehn were modified by MIT's machine shop. Due to the size constraints of the syringe barrel, a 7/16" x 1/2" N52 NdFeB (NdFeB = Nd₂Fe₁₄B) axially polarized magnet was purchased, rather than the previously employed 1/2" x 1/2", which would not fit.

The plunger barrel was modified by cutting the barrel above the Teflon plunger tip, then hollowing out the interior to allow room for the magnet. The magnet was then held in place by a roll pin inserted through the top of the drive (Figure B.1, Figure B.2). The magnet's polarization must be noted before being placed into the syringe drive because the exterior magnetic belt is pre-set in a specific direction. In addition, the Teflon[®] plunger tip must be polished slightly. The friction of the Teflon on the side of the apparatus is too much for the external magnets to move the magnetic drive. The polishing can be performed using a rotary evaporator motor on 600 grit sandpaper, and only required between 5-10 rotations.

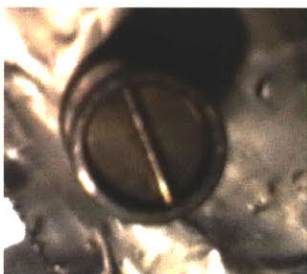


Figure B.1: Top View of Magnetic Drive.



Figure B.2: Side View of Magnetic Drive.

The second part of syringe drive system that was altered was the exterior magnetic drive unit. A bar was attached to two long threaded metal bars as described by Yandulov.¹ The

original magnetic belt that was used was not strong enough to move the new magnet drive, so a stronger and easier to use exterior magnet drive was developed (Figure B.3).

The original belt that was used consisted of six 1/4" x 1/2" NdFeB magnets (Figure B.4) that required them to be locked together with either a nut or piece of copper wire. In the new design four N52 axially polarized magnets were setup as shown in Figure B.3 so that the polarization matched the magnet drive. The magnets were then encased with metal flashing, which was attached to the metal rods and wrapped in electrical tape to protect the glassware. This set up method allowed for a shorter set-up time than previously required.¹

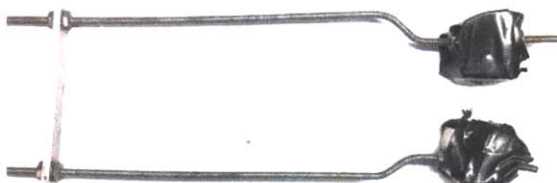


Figure B.3: New Exterior Magnet Drive



Figure B.4: Original Exterior Magnet Belt Drive

Mechanically Driven Apparatus

Other less successful set ups were also tested. In an attempt to decrease the time required to set up a reaction and to alleviate the need for a magnetically driven syringe, a new

mechanical apparatus was designed (mechanical apparatus, Figure B.5). The new mechanical apparatus would employ any standard syringe. A receiving flask was designed that contained a #15 Ace-Thred. Ace-Thred plugs can be purchased with pre-tapped NPT threads. Two side arms were also incorporated to aid the task of adding gases and analyzing ammonia.

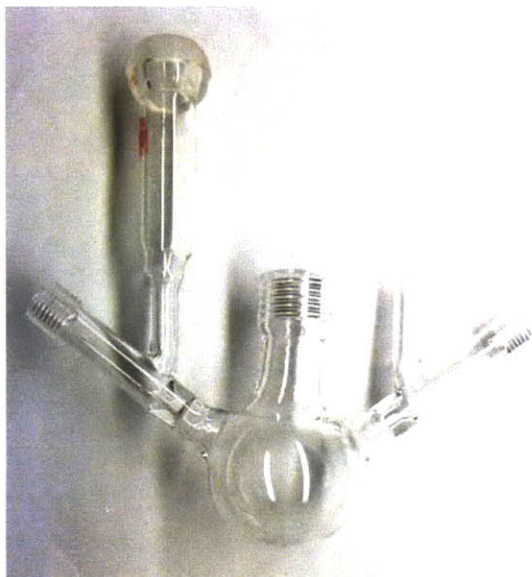


Figure B.5: Mechanically Driven Apparatus.

The entire mechanical apparatus needed to be sealed in the absence of a syringe barrel, so a Hamilton 180° two-way valve was employed between the syringe barrel and mechanical apparatus with the help of adapters. The Hamilton 180° 2-way valve contained 1/4-28 threads and the Ace-Thred #15 contained NPT threads (Figure B.6). The Kloehn syringes that we currently employ contain a female leur lock (luer lock = LL). To connect the Hamilton 180° 2-way valve to the Kloehn syringe barrel a 1/4-28 male to male LL adapter was used.

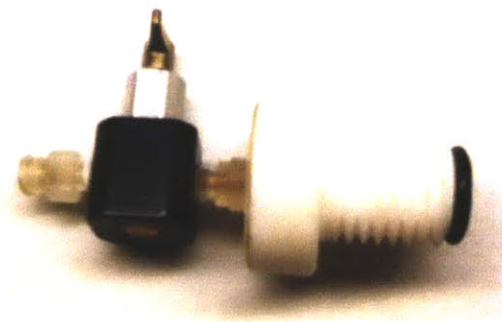


Figure B.6: Plug for Mechanically Driven Apparatus

A test of the mechanical apparatus' ability to hold ammonia showed that 90% of the added ammonia was retained after twelve hours, as determined through the indophenol method.¹ The newly designed apparatus holds vacuum as well as the standard glass apparatus, but when the system is pressurized it begins to leak. The solution of Cp_2^*Cr , ~10 mL used during a standard catalytic run, was added without the pressure equalizing arm present in the standard system so the pressure inside of the vessel was increased. The originally designed receiving flask for the mechanical apparatus was 50 mL, and a 100 mL flask was also employed to reduce the final pressure inside of the flask. Unfortunately, the apparatus only provided four equivalents of ammonia, or half of the expected amount.¹

High Pressure Apparatus

The standard apparatus originally employed in our lab was unable to be pressurized past two atmospheres so Hettterscheid investigated the development of a high pressure reactor vessel. A metal apparatus containing an internal glass reaction flask, to which a Cp_2^*Cr solution was added from a high pressure syringe proved unsuccessful.

A glass apparatus was designed as a single piece of glass which can hold up to ten atmospheres (Figure B.7). The apparatus was sealed with #18 Ace-Thred caps. A #18 Ace-Thred was used so the standard magnet drive could be added. The #18 Ace-Thred cannot be purchased pre-tapped so it was tapped to hold a 1/8" Swagelock adapter by the MIT machine shop. The adapter was connected to tubing which could pressurize the vessel and perform the indophenol work-up.

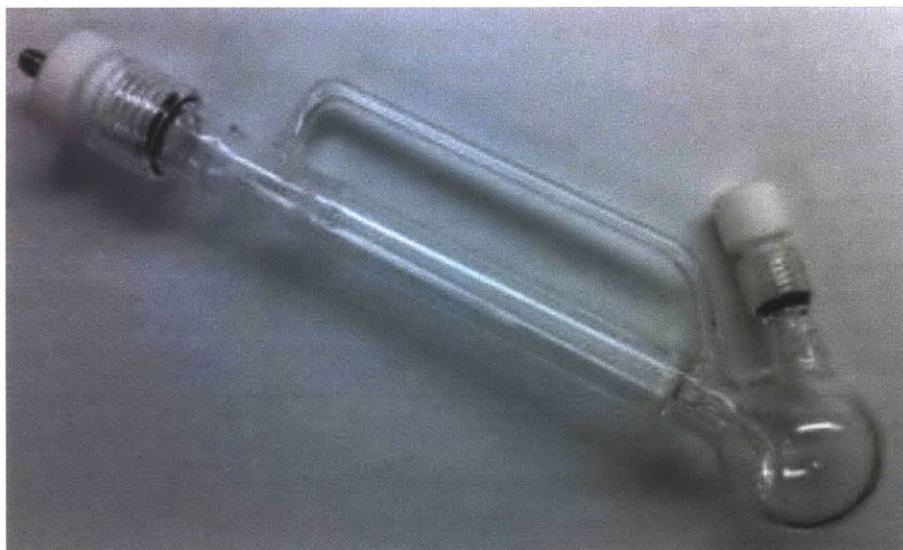


Figure B.7: High Pressure Glass Apparatus.

References

-
1. Yandulov, D. V.; Schrock, R. R. *Science* **2003**, *301*, 76.
 2. a) Ritleng, V.; Yandulov, D. V.; Weare, W. W.; Schrock, R. R.; Hock, A. S.; Davis, W. M. *J. Am. Chem. Soc.* **2004**, *126*, 6150. b) Weare, W. W.; Schrock, R. R.; Hock, A. S.; Müller P. *Inorg. Chem.* **2006**, *45*, 9185. c) Reithofer, M. R.; Schrock, R. R.; Müller, P. *J. Am. Chem. Soc.* **2010**, *132*, 8349.

Appendix C
Crystallographic Data

Appendix C. Crystallographic Data

Diffraction data were collected on a Siemens Platform three-circle diffractometer or a Bruker D8 three-circle diffractometer coupled to a Bruker-AXS Smart Apex CCD detector with graphite-monochromated Mo K α radiation (λ) 0.71073 Å performing φ and ω -scans. All structures were solved by direct methods using SHELXS and refined against F^2 on all data by full-matrix least squares with SHELXL-97.¹ All non-hydrogen atoms were refined anisotropically. Hydrogen atoms on any carbon atom that binds directly to molybdenum were taken from the difference Fourier synthesis and refined semifreely with the help of distance restraints. All other hydrogen atoms were included into the model at geometrically calculated positions and refined using a riding model unless stated otherwise. Data for the structures including CIF files are also available to the public at <http://www.reciprocalnet.org>

Table C.1: Crystal Data and Structure Refinement for [pMeOHPTN₃N]MoN

Identification code	7205	
Empirical formula	C ₁₃₉ H ₂₃₁ Mo N ₅ O ₃ Si _{5.50}	
Formula weight	2270.72	
Temperature	100(2) K	
Wavelength	0.71073 Å	
Crystal system	Monoclinic	
Space group	C2/c	
Unit cell dimensions	a = 35.472(6) Å	α = 90°.
	b = 48.984(9) Å	β = 105.748(3)°.
	c = 17.866(3) Å	γ = 90°.
Volume	29878(9) Å ³	
Z	8	
Density (calculated)	1.010 Mg/m ³	
Absorption coefficient	0.178 mm ⁻¹	
F(000)	9944	
Crystal size	0.35 x 0.35 x 0.15 mm ³	
Theta range for data collection	1.38 to 22.99°.	
Index ranges	-38 ≤ h ≤ 38, -53 ≤ k ≤ 53, -19 ≤ l ≤ 19	
Reflections collected	186968	
Independent reflections	20773 [R(int) = 0.0875]	
Completeness to theta = 22.99°	100.00%	
Absorption correction	Semi-empirical from equivalents	
Max. and min. transmission	0.9738 and 0.9404	
Refinement method	Full-matrix least-squares on F ²	
Data / restraints / parameters	20773 / 3724 / 1714	
Goodness-of-fit on F ²	1.054	
Final R indices [I > 2σ(I)]	R ₁ = 0.0758, wR ₂ = 0.1883	
R indices (all data)	R ₁ = 0.1141, wR ₂ = 0.2160	
Largest diff. peak and hole	1.136 and -0.693 e.Å ⁻³	

Table C.2: Selected Bond Length (Å) and Angles (°) for [pMeOHIPN₃N]MoN

N(4)-Mo(1)	2.433(4)	N(3)-Mo(1)-N(4)	77.41(15)
N(5)-Mo(1)	1.650(4)	N(2)-Mo(1)-N(4)	77.10(15)
Mo(1)-N(3)	1.984(4)	N(1)-Mo(1)-N(4)	76.49(15)
Mo(1)-N(2)	1.985(4)	C(4)-N(4)-C(2)	113.7(4)
Mo(1)-N(1)	1.994(4)	C(4)-N(4)-C(6)	113.3(4)
N(1)-C(115)	1.429(6)	C(2)-N(4)-C(6)	113.8(4)
N(2)-C(215)	1.429(6)	C(4)-N(4)-Mo(1)	105.1(3)
N(3)-C(315)	1.429(6)	C(2)-N(4)-Mo(1)	105.5(3)
C(1)-N(1)	1.476(7)	C(6)-N(4)-Mo(1)	104.3(3)
C(3)-N(2)	1.485(6)	N(5)-Mo(1)-N(3)	102.45(18)
C(5)-N(3)	1.486(7)	N(5)-Mo(1)-N(2)	103.42(18)
C(1)-C(2)	1.510(7)	N(5)-Mo(1)-N(1)	103.15(18)
C(3)-C(4)	1.506(8)	N(5)-Mo(1)-N(4)	179.47(19)
C(5)-C(6)	1.513(7)	N(3)-Mo(1)-N(2)	113.22(17)
N(4)-C(4)	1.466(6)	N(3)-Mo(1)-N(1)	115.47(17)
N(4)-C(2)	1.472(7)	N(2)-Mo(1)-N(1)	116.56(16)
N(4)-C(6)	1.476(7)	N(1)-C(1)-C(2)	111.0(4)
C(118)-O(1)	1.385(6)	N(2)-C(3)-C(4)	110.9(4)
C(218)-O(2)	1.383(6)	N(3)-C(5)-C(6)	110.4(5)
C(318)-O(3)	1.396(6)	N(4)-C(2)-C(1)	109.7(4)
O(1)-C(11)	1.427(6)	N(4)-C(4)-C(3)	109.4(5)
O(2)-C(21)	1.438(7)	N(4)-C(6)-C(5)	110.4(5)
O(3)-C(31)	1.409(7)	C(115)-N(1)-Mo(1)	126.0(3)
C(118)-O(1)-C(11)	111.9(4)	C(215)-N(2)-Mo(1)	126.9(3)
C(218)-O(2)-C(21)	113.9(4)	C(315)-N(3)-Mo(1)	125.6(3)
C(318)-O(3)-C(31)	114.5(5)		

Table C.3: Crystal Data and Structure Refinement for [HIPTN₃N]MoPMe₃[BPh₄]

Identification code	9327
Empirical formula	C ₁₅ H ₂₁ B Mo N ₄ P
Formula weight	2220.97
Temperature	100(2) K
Wavelength	0.71073 Å
Crystal system	Monoclinic
Space group	P2(1)/n
Unit cell dimensions	a = 19.767(2) Å α = 90°. b = 27.206(3) Å β = 94.859(2)°. c = 26.841(3) Å γ = 90°.
Volume	14382(3) Å ³
Z	4
Density (calculated)	1.026 Mg/m ³
Absorption coefficient	0.149 mm ⁻¹
F(000)	4832
Crystal size	0.20 x 0.20 x 0.10 mm ³
Theta range for data collection	1.07 to 19.98°. -19<=h<=19, -26<=k<=26, -
Index ranges	25<=l<=25
Reflections collected	154050
Independent reflections	13390 [R(int) = 0.2045]
Completeness to theta = 19.98°	100.00%
Absorption correction	Semi-empirical from equivalents
Max. and min. transmission	0.9852 and 0.9708
Refinement method	Full-matrix least-squares on F ²
Data / restraints / parameters	13390 / 122 / 1514
Goodness-of-fit on F ²	1.031
Final R indices [I>2σ(I)]	R1 = 0.0782, wR2 = 0.2081
R indices (all data)	R1 = 0.1420, wR2 = 0.2628
Largest diff. peak and hole	0.928 and -0.370 e.Å ⁻³

Table C.4: Selected Bond Length (Å) and Angles (°) for [HIPTN₃N]MoPMe₃[BPh₄]

Mo(1)-N(1)	1.946(7)	N(1)-Mo(1)-N(2)	117.2(3)
Mo(1)-N(2)	1.949(7)	N(1)-Mo(1)-N(3)	117.2(3)
Mo(1)-N(3)	1.963(7)	N(2)-Mo(1)-N(3)	116.3(3)
Mo(1)-N(4)	2.205(7)	N(1)-Mo(1)-N(4)	80.1(3)
Mo(1)-P(1)	2.569(3)	N(2)-Mo(1)-N(4)	79.9(3)
N(1)-C(115)	1.461(12)	N(3)-Mo(1)-N(4)	79.3(3)
N(2)-C(215)	1.438(11)	N(1)-Mo(1)-P(1)	100.0(2)
N(3)-C(315)	1.424(10)	N(2)-Mo(1)-P(1)	98.7(2)
N(1)-C(2)	1.490(13)	N(3)-Mo(1)-P(1)	101.9(2)
N(2)-C(4)	1.489(11)	N(4)-Mo(1)-P(1)	178.50(19)
N(3)-C(6)	1.476(12)	C(115)-N(1)-Mo(1)	131.3(6)
N(4)-C(1)	1.469(11)	C(215)-N(2)-Mo(1)	128.7(5)
N(4)-C(3)	1.471(11)	C(315)-N(3)-Mo(1)	128.1(6)
N(4)-C(5)	1.465(11)	C(2)-N(1)-Mo(1)	118.5(6)
C(1)-C(2)	1.493(13)	C(4)-N(2)-Mo(1)	118.8(6)
C(3)-C(4)	1.514(13)	C(6)-N(3)-Mo(1)	117.5(5)
C(5)-C(6)	1.506(13)	C(1)-N(4)-Mo(1)	107.6(5)
P(1)-C(3P)	1.812(9)	C(3)-N(4)-Mo(1)	107.3(5)
P(1)-C(1P)	1.815(9)	C(5)-N(4)-Mo(1)	108.4(5)
P(1)-C(2P)	1.818(9)		

Reference

-
1. Sheldrick, G. M. *Acta Crystallogr.* **2008**, *A64*, 112.

Acknowledgements

I would first like to thank Prof. Schrock, for allowing me to work for him on the dinitrogen project. Without his guidance and support, I would not be the scientist I am today. Prof. Cummins also requires a special thank you for being my committee chairman, and an excellent source of information and suggestions throughout my career. I owe Prof. Lippard, who also served on my committee, gratitude for his suggestions and helping to make improvements to the project and thesis. The remaining inorganic faculties have been great in offering their guidance throughout my career and during the oral examinations.

The Schrock lab has been a great place to work and every lab member has made the experience special in their own way. No one in the lab had a greater influence on my professional or personal success more than Dr. Keith Wampler. As a classmate, a friend, and a groomsman, I want to thank him for always being there. I do not know if I would have survived six years at MIT, without his advice and support (not to mention always being there to discuss chemistry at the Muddy). Another lab member who deserves specific mention is Dr. Jiamin Chin. As the only other graduate student on the dinitrogen project, she was an invaluable source of information and a great colleague to discuss problems and new ideas. I also owe two post docs a debt of gratitude as well, Dr. Travis Hebden and Dr. Dennis Hetterscheid. Dennis was a great friend and colleague on the dinitrogen project. I only regret we allowed him to pick the Cleveland Indians for our baseball beer bet. I owe Travis a thank you, not only for being a valuable member of the dinitrogen project, but also for his reading of my entire thesis. The document would not be what it is today without his editing skills. As classmates, I want to thank Dr. Annie King and Dr. Lindsey McQuade for the many french fry lunches on Thursday, and lab mates Dr. Brad Bailey and Dr. Adam Hock for early guidance in the lab. For the rest of the Schrock lab and inorganic students at MIT, I want to thank you, even if I did not mention you by name, especially those of you who suffered through the many versions of my thesis.

My biggest thank you has to go to my wife, Meredith, for standing by me these six years and supporting me through some of the tougher times on my project. Without her, I am sure I would not have been as successful and I am forever in her debt, especially for the last minute reading of my entire thesis. I want to also mention my parents, Meredith's parents, my brother Jeff and my sister Meg for supporting me and bringing many Yuenglings. And, to the Severo Family, Dave, and other local friends who have supported me and provided lots of fun (outside of lab) over the last few years.

There are obviously many more people I would like to thank personally and share stories about, and I want you to know you are not forgotten or any less important to me.

Thank you to everyone, your love and support means a lot to me.

Education:

August 2005-Present

Massachusetts Institute of Technology, Cambridge MA
PhD candidate in Inorganic Chemistry, expected graduation June 2011
Areas of Advanced Study: Inorganic Chemistry, Organometallic Chemistry, Physical Methods, X-ray Crystal Structure Refinement

August 2001-May 2005

University of Delaware, Newark DE
Bachelor of Science in Chemistry
Areas of Advanced Study: Instrumental and Analytical Methods
Organic Chemistry, Synthesis and Reactivity, Inorganic Chemistry, Organometallic Chemistry,

Research Experience

December 2005- Present

Massachusetts Institute of Technology, Cambridge, MA

Thesis Research was conducted under Professor Richard R. Schrock on studies relevant to the catalytic reduction of dinitrogen to ammonia using triamidoamine ligands with both molybdenum and tungsten.

- Synthesis, characterization, and catalytic studies of molybdenum triamidoamine complexes.
- Quantitative determination of ammonia and hydrogen through analytical techniques such as indophenol, UV-Vis, and Gas Chromatography.
- Kinetic and analytical investigation of the catalytic cycle using IR, NMR spectroscopy, and cyclic voltammetry.

January 2003- May 2005

University of Delaware, Newark, DE

Undergraduate Research was conducted under John Bulkowski on hexammine, di-zinc and di-copper macrocycles.

- Synthesis, and characterization, of hexamine macrocycles
- Analysis of zinc and copper incorporation through techniques such as NMR spectroscopy, UV-Vis, and IR spectroscopy.

Leadership Roles:

August 2006-Present

Group Environmental Health and Safety Representative
Massachusetts Institute of Technology, Cambridge, MA

Responsibilities:

- Weekly safety inspections for laboratory.
- Facilitating proper chemical hygiene and chemical disposal.
- Insure the laboratory complies annually with Department of Homeland Security and Scanning Analysis Response Assessment (SARA) reporting guidelines.
- Ensuring proper protection of researchers and laboratory equipment.

August 2006-Present

Laboratory Coordinator and Facilities Liaison
Massachusetts Institute of Technology, Cambridge, MA

Responsibilities:

- Coordinating between facilities and the laboratory for repairs and construction.

- Maintaining an environment in the laboratory amenable to productive research.

Teaching Experience:

August 2005- May 2006	Massachusetts Institute of Technology, Cambridge, MA Introduction to Inorganic Chemistry, General Chemistry
September 2004- July 2005	Laboratory Teaching Assistant University of Delaware, Newark, DE General Chemistry Lab, Organic Chemistry Lab
September-December 2004	Assistant Grader University of Delaware, Newark, DE Physical Chemistry
September 2004 -May 2005	Chemistry Department Tutor General Chemistry, Organic Chemistry
January-May 2005	Science and Math Tutor for underprivileged middle school students

Presentations

Studies of the effects of hydrogen on the catalytic reduction of dinitrogen to ammonia., *234th National Meeting of the ACS*, August 24, 2010.

Investigation of synthetic variations of [HIPTN₃N]Mo and direct routes to [HIPTN₃N]MoN *239th National Meeting of the ACS*, Boston, August 23, 2007

Synthesis and Reactivity of Metal Complexes of Monomacrocyclic Hexammines, *UMBC: 7th Annual Undergraduate Research Symposium*, October 16th 2004

Publications

Formation of {[HIPTN₃N]Mo(III)H}- by Heterolytic Cleavage of H₂ as Established by EPR and ENDOR Spectroscopy, *Inorganic Chemistry* **2010**, *49*, 704. **Collaboration with Hoffmann Group, Northwestern University, Evanston IL.**

Molybdenum Triamidoamine Systems. Reactions Involving Dihydrogen Relevant to Catalytic Reduction of Dinitrogen, *Inorganic chemistry* **2009**, *48*, 8569.

Technical Skills:

Nuclear Magnetic Resonance Spectroscopy and Electron Paramagnetic Resonance Spectroscopy
MALDI (Matrix Assisted Laser Desorption Ionization) Mass Spectrometry
UV-Visible, IR Spectroscopy
Gas Chromatography
Handling of Air Sensitive compounds through the use of Dry-Box and Schlenk Techniques.
Computer Skills (Microsoft Word, Excel, PowerPoint, ChemBio Draw Office, SHELXL)
Public Speaking
Laboratory Leadership

Awards:

May 2005 Frank Shaw III Undergraduate Award in Inorganic Chemistry, University of Delaware, Newark DE.